ASSESSMENT OF DROUGHT HAZARD: A CASE STUDY IN SEHOUL AREA, MOROCCO

NATSAGDORJ OTGONJARGAL
February, 2012

SUPERVISORS:
Dr. D.B. Pikha Shrestha
Dr. Ir. J. Ettema

ASSESSMENT OF DROUGHT HAZARD: A CASE STUDY IN SEHOUL AREA, MOROCCO

NATSAGDORJ OTGONJARGAL
Enschede, The Netherlands, [February, 2012]

Thesis submitted to the Faculty of Geo-Information Science and Earth Observation of the University of Twente in partial fulfilment of the requirements for the degree of Master of Science in Geo-information Science and Earth Observation.
Specialization: Applied Earth Sciences

SUPERVISORS:
Dr. D.B. Pikha Shrestha
Dr. Ir. J. Ettema

THESIS ASSESSMENT BOARD:
Prof. Dr. V.G. Jetten (Chair)
Dr. Chris Mannaerts (External Examiner)

ABSTRACT

This research deals with the assessment of drought hazard over Sehoul area of Morocco. Morocco is highly susceptible to recurrent droughts with long periods (one to six years) due to arid climate and the strengthening effect of the Azores anticyclone. The focus of this research is on increasing the understanding and applying the basic concepts, drought hazard and hazard assessment. Drought is a natural hazard originating from a deficiency of precipitation that results in a water shortage for some activities or groups. Drought hazard assessment is one of the stages of drought risk assessment. Thus it is essential for taking mitigation measures against adverse drought effects and for planning and managing water related policy.

The important aspects of drought hazard assessment such as temporal and spatial occurrence as well as vegetation response to precipitation were included for this research. Meteorological droughts where rainfall is the main parameter of interest was studied based on long term rainfall data (1950-2010) and vegetative drought was examined using SPOT NDVI data (1km) between the periods of 1998-2010 under the consideration that precipitation is a primary factor of vegetative drought. In addition, Aster image on 21 Oct 2011 was used to generate land cover map. Rainfall analysis was carried out in order to investigate the amount and timing of rainfall on vegetation. Moreover, trend analysis of extreme rainfall was conducted. The Standardized Precipitation Index (SPI) was employed to identify historical meteorological droughts and perform drought magnitude frequency analysis, applying the Joint Probability Density Function (PDF). Drought Severity Index (DSI) was used to assess spatial occurrence of vegetative drought. To examine vegetation response to variability in precipitation, time lags and vegetation phenological approach were applied. Based on the results obtained, the years of vegetative droughts were constructed during the period 1951-1997 in which SPOT NDVI data is not available and compared to the information on observed droughts found from literature. Finally, RESTREND method was employed to discriminate climate and human-induced vegetation decrease.

There are no statistically significant trend in the amount of extreme rainfall and number of extreme rainy days over time. Among the historical droughts based on SPI, the drought occurred in 1993-1995 has the longest return period, 237.7 year. Over Sehoul area, 93.6 km^2 (22.6%) of the total area (approxi. 397 km^2) is highly susceptible to droughts. The moderate and low susceptibility class covers the areas 200.5 km^2 (48.4%) and 120.3 km^2 (29.0%), respectivily. Land cover class of degraded land shows the lowest variance (0.32) and mean value (0.29) of NDVI during rainy season of the period, 1998-2010. In contrary, grass (0.54) and agriculture (0.51) class shows the higher variance in NDVI values. There is 1 month 20 days-time lag found between 10-day NDVI and 10-day rainfall. Also 48% of variance in 10-day NDVI during rainy season is explained by rainfall. In addition, it can be concluded that drought can be severe if the average fraction of total rainfall in first part of rainy season (Oct-Dec) is less than its long term mean 0.41 when the total rainfall during the whole rainy season is less than its long term mean 452.6mm except for frequent extreme rainfall or unevenly distributed rainfall events. Rainfall efficiency is dependence on two factors; unevenly distributed rainfall events in rainy season period and frequent extreme rainfall events, particularly that fall in first part of rainy season. The rainfall events that fall in first part of rainy season are more efficient on vegetation growing than the rainfall events that fall in the second part of the rainy period. Also rainfall events that are evenly distributed through time (alternately sunny and rainy periods) are more efficient than rainfall events with more frequent occurrence in a certain period. In addition, the frequent extreme rainfall events have less positive influence on growing vegetation. Under this consideration, totally 20 historical vegetative droughts were found while there are 27 dry years according to anomaly of annual rainfall. Final result reveals that 26.7km^2 (6.5%) of Sehoul area lies in high degradation class; for moderate and low classes, areas are 69.2 km^2 (16.9%) and 96.8 km^2 (23.6%), respectivily. The total degradation area is 192.7 km^2 (47.0%).

ACKNOWLEDGEMENTS

I would like to take this opportunity to thank many people who have helped me to complete this thesis.

First of all, I would like to express my gratitude to World Bank and Government of Japanese for granting me with the scholarship which allows me to study at ITC. Without this opportunity, I would not have come to ITC. Also sincere thanks to ITC for providing warm hospitality and a good environment to study. I must also thank prof, D.Chogsom, at Mongolian National University, and Dr. G.Sarantuya (director), Dr. D.Jugder, J.Tsogt and Dr. P.Gomboluudev at Institute of Meteorology and Hydrology of Mongolia for encouraging me to study for the master study and providing good recommendation letters.

Secondly, I am extremely appreciating my supervisors for their valuable support; kind advices, comments and particularly their enormous contribution to improve the quality of this thesis. Thanks to my first supervisor, Dr. D.B. Pikha Shrestha, for his patience and steady support in the most difficult times. You not only transferred your scientific knowledge, but also taught me how to write proper English. I want to extend my appreciation to my second supervisor Dr. Ir. J. Ettema for meticulously reading my MSc drafts. You commented on my drafts in a very clear, straightforward and refreshing manner. I appreciate my supervisors very much.

My deep appreciation goes to all the staff of Earth System Analysis and other ITC staffs who have shared their knowledge and expertise with us throughout one and half year; Particularly, to Prof Jetten for his valuable comments after MSc proposal and mid-term presentation; and to Dr. David Rossiter for his guidance with statistics and providing some R scripts. Also I wish to express my thanks to Dr Nanette Kingma for showing me her kindness. We talked a little about my topic but she shared her valuable experiences in MSc research and defense.

I am also grateful to Dr. Ir. C.A.J.M Kees de Bie, John Wasige and my PhD student Shruthi for providing data that supported my work. Special thanks to Ms Shruthi for her kind manner. Her modest but wise suggestions were very much appreciated throughout my research.

Many thanks to my classmates and friends for sharing knowledge and their friendship. I would like to express my heartiest thanks to my friend Beatriz Lao Ramos for being with and helping me much in many ways. Without her help, living far from my family here would not have been easier.

A big thank you to my mum and dad for your unwavering support and being healthy so far. Thank you for your love that you gave me all good things to make me what I am. I am also grateful to all my brothers and sisters, and uncle Chukhal, sister-in-low Ganbileg for their love, their support, and their confidence in me to finish the study.

I wish to thank my husband for his unconditional love and spiritual support. Thanks to you Bayarsaikhan for your patience and encouragement throughout my MSc study; Final thanks to my little daughter Enkhjin for making our life happier and wishing me "A" grades to my exams. You, my lovely two people, have given me energy to keep going and make me stronger.

A big thank you to you all!

***Хайртай аав ээж хоёртоо:** Аав таныхаа ноён нуруу, хүн чанарын ачаар үр хүүхдүүд бид чинь зөв яваа. Ээж таниасаа өвлөсөн эрч хүч, ажилч хичээнгүй чанарын ачаар бид нар сайн яваа. Миний буурал толгойтой аав минь.Тамхинаас гарчихдаг мундаг аав шүү та. Цагаан цайлган сэтгэлтэй ээж минь. Хэзээ ч зүгээр сууж чаддаггүй хүний төлөө төрчихсөн хүн шүү та минь. Та хоёр минь урт удаан наслаарай. Та хоёртоо маш их хайртай. Охин нь диплотоо тэврээд тун удахгүй яваад очино.*

Dedicated to my beloved parents, Natsagdorj and Tserendulam

TABLE OF CONTENTS

LIST OF FIGURES

LIST OF TABLES

1. INTRODUCTION

1.1. Background

As it is well known, drought hazard assessment is one important step of drought risk assessment. Therefore, the results of this study can be used for drought risk assessment in Sehoul area of Morocco. This section focuses on the understanding of the basic concepts of drought hazard and hazard assessment as well as the role of precipitation that is a key primary triggering factor of drought hazard.

1.1.1. Drought as a natural hazard

Drought is an insidious natural hazard that is generally perceived to be a prolonged period with significantly lower precipitations relative to normal levels (Wilhite et al., 1985). The reasons for the occurrence of droughts are complex because they depend not only on atmosphere, but also on the hydrologic processes (A. K. Mishra et al., 2010). Further, drought was ranked first followed by tropical cyclones, regional floods, earthquakes, and volcanoes based on most of the hazard characteristics and impacts (Tadesse et al., 2004).

Unlike many sudden hazards like flood and earthquake, impacts of drought are non-structural; however, the effect is cumulative and can spread over large geographical areas (Wilhite, 2007). Thus droughts are recognized as a widespread phenomenon (Kogan et al., 2001). In last three decades, large scale intensive droughts have been observed on all continents in Europe, Africa, Asia, Australia, and Americas (Dai, 2011). In United State, drought causes on average $6-8 billion losses per year, but in 1988 economic losses due to drought was as high as much $40 billion (Wilhite, 2007). Drought related disasters in the 1980s killed over half a million people in Africa (Hayes et al., 2003).

Another reason to call for need for drought research is that droughts are expected to become more frequent and severe due to climate change and climate variability (IPCC, 2007). A recent study (Dai, 2011) noted that many areas over most of Africa, southern Europe and the Middle East, most of Americas, Australia, and Southeast Asia could face the significant drying in the coming decades.

1.1.2. Hazard assessment

To manage the risk of drought, a thorough hazard assessment is fundamental. Any hazard assessment involves "the analysis of the physical aspects of the phenomena through the collection of historic records, the interpretation of topographical, geological, hydrological information to provide the estimation of the temporal and spatial probability of occurrence and magnitude of hazardous event" (van Westen, 2009). According to UN-ISDR (2004) "the objective of a hazard assessment is to identify the probability of occurrence of a specific hazard, in a specific future time period, as well as its intensity and area of impact.". In drought assessment, probabilistic characterization of drought events is extremely important for water resources planning and management (Cancelliere et al., 2010).

1.1.3. The relationship between NDVI and precipitation

Drought is largely driven by climate fluctuations (Rowhani et al., 2011) and vegetation is the first feature on earth surface to be affected by drought. Thus, there is a great demand for a better understanding of relationship between vegetation and climate factors. One of the important factors is precipitation. Study of NDVI relationship to rainfall would lead to a better understanding of the environmental constraints on vegetation growth. The relationship can also help to establish the climatological limits in which NDVI is a useful indicator of vegetation growth (Nicholson et al., 1990).

Many studies performed in arid and semi-arid regions of east Africa (Nicholson, et al., 1990), USA (Wang et al., 2003), Kazakhstan (Propastin et al., 2007) and China (B. Li et al., 2002; Song et al., 2011) pointed out that precipitation has the primary influence on NDVI. Also Richard et al., (1998) noted that in Mediterranean climate that is characterized by a dry summer and a wet winter season (like Sehoul area) with a small annual temperature range, photosynthetic activity follows rainfall and not temperature.

Temporal and spatial relationship between NDVI and precipitation are investigated in many research works. Particularly a good correlation in the arid regions, both temporally and spatially, is documented based on NDVI and rainfall (B. Li, et al., 2002; Richard, et al., 1998; Wang, et al., 2003; Yang et al., 1998). Studies on temporal relationship claim that NDVI responds to rainfall with certain time lag from 1 to 12 weeks (1 to 3 months), reflecting the delay in vegetation development after rain. The lag can vary depending on both climatic and non-climatic factors such as air and soil temperature, evaporation, soil or vegetation type (Nicholson, et al., 1990).

In addition, NDVI values are highly correlated with multi-month rainfall as rainfall effect on vegetation is cumulative (Wang 2003, Rahimzadeh, 2008). Results found from literatures are not consistent because of the different spatial and temporal aggregation. For example, Nicholson (1990) found the best correlation of NDVI with rainfall for the concurrent plus two antecedent months at most representative stations while Propastin (2007) obtained the highest correlation between NDVI and precipitation averaged by the whole study area by imposing time lag of approximately 2-3 10-day. Not only temporally, but also there is a good spatial agreement between NDVI and rainfall (Nicholson, et al., 1990) as the spatial distribution of the vegetation cover is strongly related to mean climatic conditions (Richard, et al., 1998). The correlation coefficients of NDVI-rainfall exhibit a clear structure in terms of spatial distribution in semi-arid area of Great Plain, USA (Wang, et al., 2003) and China (Liu et al., 2010).

Further, it was reported that change in NDVI values can be affected by the amount and timing of rainfall (Schultz et al., 1995). Nicholson (1990) demonstrates that a linear relationship between rainfall and NDVI as long as rainfall does not exceed approximately 500 mm/year or 50-100 mm /month. Above these limits, a "saturation" response occurs and NDVI increases with rainfall only very slowly. Also Yang (1998) and Propastin (2007) examined the importance of precipitation received in different periods. According to their results, Great Plains of USA is predominantly influenced by spring and summer precipitation whereas in arid region of Central Kazakhstan precipitation in June-July plays the main role in determining vegetation development.

1.2. Problem statement

Morocco is highly susceptible to recurrent droughts with long periods (one to six years) due to arid climate and the strengthening effect of the Azores anticyclone (Doukkali, 2005). Most recently, Morocco experienced severe droughts in 1980-85, 1990-95, and 1998-2000 that had adverse effects on rain fed-agriculture and the national economy since agricultural products contributes 15-20% of GDP (FAO, 2004). For instance, drought in 1995 reduced cereal production by 82% from the previous year; total agricultural output by 45%, and rural employment by 60%, resulting in the loss of 100 million work days in agricultural employment (FAO Regional Office for the Near East, 2008). Drought impacts have been exacerbated by the precipitation decrease in the southern Mediterranean region in the last decades (Karrouk, 2007) while water demand has increased due to expansion of irrigated agriculture and population growth (Taleb, 2006; Van Dijck et al., 2006).

In addition to droughts, land degradation is a serious problem in Morocco. (Van Dijck, et al., 2006). According to FAO (2004), 19 percent of land of the country (or 8.7 million hectares) is subject to severe land degradation over all Moroccan territory (excluding the Saharan provinces). Although drought is not the main cause of land degradation (Dregne, 1986), they occur frequently in the areas affected by desertification (Koohafkan, 1996; Nicholson et al., 1998). Also a recent research pointed out that the most severe annual erosion occurred in drought year, not in wet year in semi-arid region (Wei et al., 2010). In addition, precipitation is scarce and high variability in space and time. Daily storms of several hundred mm are common throughout the Mediterranean area (Romero et al., 1998). Nearing et al., (2005) stated that climatic variability will increase under global climate changes, resulting in greater frequency in intensity of extreme weather events. This could increase rates of soil loss.

Given the problems mentioned above, there is a clear demand to understand and assess historical droughts in order to develop measures for mitigating the consequences of future droughts.

1.3. The historical droughts in Morocco

Chbouki (1992) and Ouassou et al., (2005) identified the twelve drought periods in Morocco during the period of year 1896-2003: 1904-05; 1917-20; 1930-35; 1944-45; 1948-50; 1960-61; 1974-75; 1981-84; 1986-87; 1991-93; 1994-1995 and 1999-2003. Ouassou et al., (2005) also reported that the more recent droughts have resulted in even more dramatic effects. For instance, during the drought of 1981-82 in Morocco, 25% of cattle and 39% of sheep were sold or died.

1.4. Objective, research question and hypotheses

The general objective of the research is to carry out the assessment of drought hazard in Sehoul area of Morocco.

Specific objectives are the followings:

- To perform rainfall and extreme rainfall analysis
- To identify historic drought pattern based on precipitation and vegetation index
- To assess the temporal characteristics of droughts such as frequency, magnitude and duration from probabilistic point of view and generate the Drought-Severity-Duration-Frequency (SDF) curves
- To create Drought susceptibility map of Sehoul area and examine spatial variability of drought for land cover classes.
- To discriminate between the climate-induced and human-induced land degradation.

Research questions are:

No	Questions
Q1	Are there any increasing trend in the amount of extreme rainfall and number of extreme rainy days over time?
Q2	Are drought characteristics (duration, magnitude and intensity) increasing over time?
Q3	What are the return periods and the probability of severe droughts with different durations and magnitude?
Q4	Which part of this area is most prone to drought?
Q5	Can the change in vegetation cover over time (inter and intra-annual) be explained by precipitation?
Q6	How large area is affected by human-induced land degradation?

The hypotheses corresponding to the research questions are the following:

No	Hypothesis corresponding to research questions
H1	There are an increasing trend in the amount of extreme rainfall and number of extreme rainy days over time.
H2	In the Sehoul area, drought characteristics (duration, magnitude and intensity) are increasing over time.
H5	Inter-annual change in vegetation cover under drought condition can be explained by precipitation, expect for extreme rainfall condition. In a year with higher number of extreme rainfall events, vegetation can be less even if annual rainfall is high.

1.5. Novelty and benefit of this research

Annotative of this study is:

- In this study, we try to assess drought hazard including all the important aspects of drought hazard assessment such as temporal and spatial occurrence as well as vegetation response to precipitation.
- We examine vegetation response to both the amount and timing of rainfall while most studies do analysis considering only the amount of rainfall such as annual or monthly total rainfall.

The benefit of this research will be the followings:

- to local decision makers for taking mitigation measures against adverse drought effects and for planning and managing water related policy
- to risk assessment experts for evaluating the potential drought risk areas using drought susceptibility map and drought return periods.

2. DATA AND SOFTWARE USED

2.1. Study area

The study area, Sehoul, is a commune region of Morocco in Africa, covering approximately 397 km² surface area and with elevation ranging from 40 to 360m above sea level (Figure 1). It is located in Sala al Jadida province, about 30km south-east of the capital city, Rabat. The area is a part of the lower central plateau of Atlantic Meseta which is characterised rolling hill topography. The climate in this region ranges between sub-humid and semi-arid, with mean annual rainfall of 350 mm. Land use consists of rain fed wheat, barley and oats, maize and garden beans in rotation with grazing (DESIRE, 2010). The rainy season starts in October and finishes in April. During rainy season, the mean of the monthly total rainfall is 54.0-104.1mm. The rest of the year is virtually dry (less than 50mm on monthly basis). Summers are hot; winter temperature is mild (Figure 2).

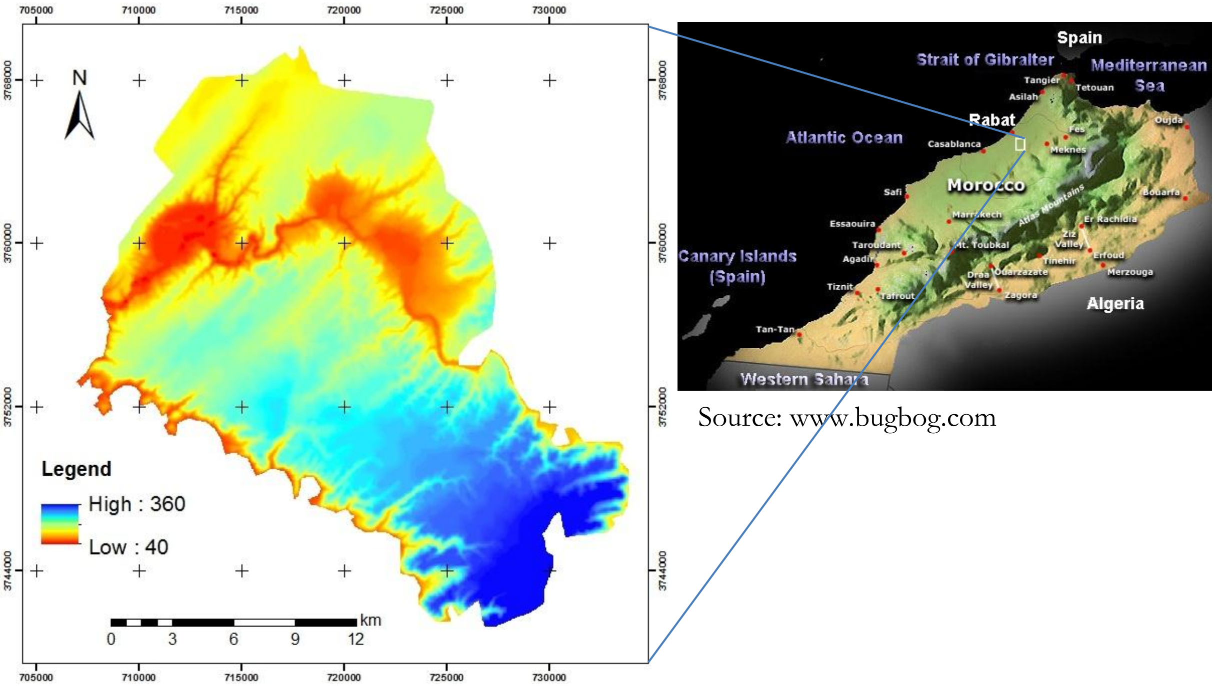

Source: www.bugbog.com

Figure 1 The elevation (m) of the study area, Sehoul area of Morocco

The study area was chosen because of two main reasons. First, the climate of the area is sub-humid and semi-arid, which can be considered to be a representative of all areas that suffer from drought. Second, this area has also serious land degradation problem like other regions of Morocco.

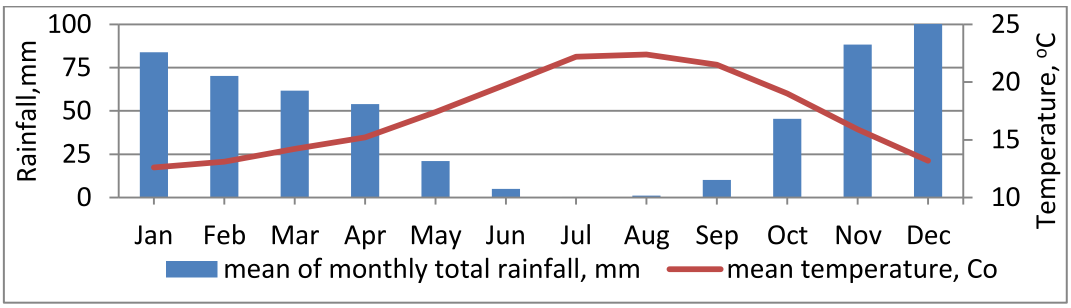

Figure 2 The mean of monthly total rainfall and daily main temperature for every month over the period 1950-2010. Temperature source: (Wikipedia, 2011).

2.2. Data description

The data for this research is presented in Table 1.

Table 1 Data description

Data available	Description	Spatial resolution	Temporal resolution
Rainfall data	The data (01 Jan 1950 to 31 Mar 2010) comes from the rainfall observation made at the Rabat meteorological station (latitude 24.05; longitude 6.77) that is approximately 30km far from the study area. (Source: Casablanca Meteorological department)	point	Daily
SPOT NDVI time series data	10-day composite (10 April 1998-30 May 2011) (Source: http://free.vgt.vito.be)	1km	10 day
Aster image	Multispectral data obtained on 21 Oct 2011	15m	-
Ikonos-2, Multi-Spectral Satellite image (MSS) and Panchromatic image	MSS and Panchromatic images with 4m and 1.0m resolution, respectively obtained on 31 Jul, 2001	4m, 1.0m	-
GEOEYE-1, MSS and Panchromatic image	MSS and Panchromatic images with 0.8m and 0.48m resolution, obtained on 20 Jul 2009	0.8m, 0.48m	-

2.3. Software used

In addition to the datasets, the following software shown in Table 2 will be used to accomplish this research.

Table 2 List of software used

Software	Purpose of usage
Microsoft Excel 2010	Rainfall data and extreme rainfall analysis Determination of onset, end and length of rainy period Regression analysis and graphic visualization
Statistical R software	Construction of the Joint Probability Density Function (PDF) Correlation analysis Statistical analysis of rainfall data
PC Raster software	Computation of phenological metrics Raster calculation
ILWIS	Image processing
Erdas 2011	Image processing Classification of NDVI map series
ENVI	Creation of map stacks from NDVI map series Land cover classification
Arc Map 10	Visualization of results Classification Area calculation

3. METHODOLOGY

This chapter contains five sections. In 3.1, methodologies to analyse rainfall data, including extreme rainfall analysis, and determination of onset and end of rainy period are explained. The section 3.2 introduces the method to evaluate drought based on the Standardized Precipitation Index (SPI). In section 3.3, the method of vegetation index based drought analysis will be discussed. The section 3.4 describes the methods to assess drought based on NDVI and rainfall data. The last section 3.5 describes the discrimination of human-induced land degradation. The general flowchart of my MSc research is presented in Figure 3 and shows how the sections are interrelated.

For all computations of total or average annual parameters for rainfall the year starts on 1st September and ends at 31st August; for 10-day composite NDVI, the year covers the period between 10th September and 31st August. These periods are chosen rather than the calendar year because the calendar year bisects the rainy season that starts in October and lasts up to April.

In order to compare point-rainfall data with pixel-based NDVI images, rainfall is assumed as homogeneous over the area as Sehoul area is relatively small (397km^2, diameter approx. 32km). Further, the elevation of the study is relatively low ranging from 40 to 360m above sea level. So it can be considered that spatial variation in rainfall caused by relief influence is less.

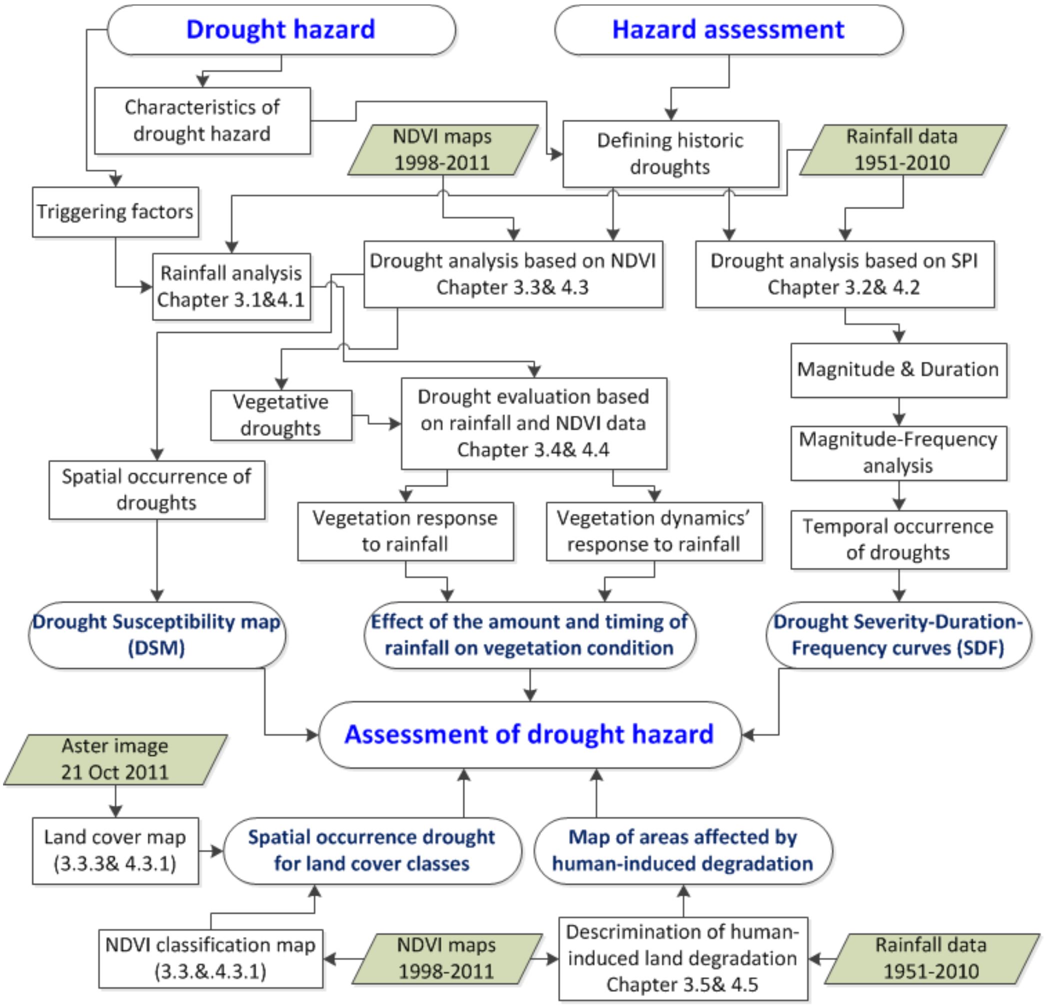

Explanation: Green boxes indicate data used.

Figure 3 Flow chart of this research

3.1. Rainfall data analysis

In this section, we describe methodologies applied to answer the research question:
Q1: Are there any increasing trend in the amount of extreme rainfall events and number of extreme rainy days over time?

These methodologies will be applied on the rainfall measurements at Rabat meteorological station (latitude 24.05; longitude 6.77) that is approximately 30km from the study area. The rainfall data which covers the period 1951-2009 is used. The year 1950/51 is eliminated as the rainfall data for this year is not complete (Jan-Aug). The rainfall analysis can be split into three parts. The first part describes a statistical approach applied for analysing the time series of rainfall data. In section 3.1.2, the method to detect changes in extreme rainfall events is described and in section 3.1.3 method to determinate the onset and end of rainy season is introduced.

The obtained results from these sections (3.1.1-3.1.3) are used for analysis of vegetation response to the amount and timing of rainfall in section 3.4.

3.1.1. Statistical analysis of rainfall

The basic statistical analysis using the statistical R software is performed based on daily, monthly and annual total precipitation. Monthly and annual total precipitations are calculated from daily rainfall data, using *"sumifs"* function in Microsoft Excel 2010. Dry and wet years are identified based on anomalies of mean annual precipitation over the period of 1951-2009.

In order to investigate vegetation response to the amount and timing of rainfall in section 3.4, the total amount of rainfall and number of rainy days (>0mm) during rainy period are taken into account. The rainy period is selected because the vegetation grows in this period. They are calculated for the entire (Oct-Mar) as well as first part (Oct-Dec) of rainy period to study the importance of rainfall received in different periods. The exceptional wet and dry years in terms of total amount of rainfall that falls during the whole as well as first part of rainy period are determined.

Additionally, the average fraction of amount of rainfall in first part of rainy period is calculated by equation (1) to examine the effect of timing of rainfall on vegetation since rainfall can fall unevenly (more frequent occurrence in a certain period and vice versa) over the period. The idea (concept) of this approach is adopted from Ling et al., (2010). Two examples are given in Table 3 to show the importance of the average fraction.

$$F_{avg} = (F_{Oct-Nov} + F_{Oct-Dec})/2 \quad (1)$$

Where F_{avg} is the average fraction of rainfall for first part of rainy season, $F_{Oct-Nov}$ is the fraction of the total rainfall between October and November. $F_{Oct-Dec}$ is the fraction of the total rainfall between October and December. They are calculated by total rainfalls for those periods (Oct-Nov or Oct-Dec) divided by the total rainfall for whole rainy period (Oct-Mar).

As seen in Table 3, the average fraction of rainfalls in first part of rainy period is appropriate to examine the effect of rainfall events that fall unevenly through the period on vegetation growing.

Table 3 An example illustration of the average fraction of rainfall in first part of rainy period (Oct-Dec)

Rainfall during rainy period, mm							Fraction of total rainfall for:		Average fraction
Oct	Nov	Dec	Jan	Feb	Mar	Total	Oct-Nov	Oct-Dec	
100	180	80	50	50	50	**510**	0.55	**0.71**	**0.63**
0	20	340	50	50	50	**510**	0.04	**0.71**	**0.37**

3.1.2. Analysis of extreme rainfall

The events which lie outside the normal range of intensity are called "extreme events" (Etkin, 1997). The extreme rainfall is quite important issue for soil moisture and vegetation growing. When the rainfall intensity is higher than the infiltration rate of the soil, water does not infiltrate into the soil and flows over the surface. This process can happen everywhere, especially in arid and semi-arid climate, like Sehoul area (Romero, et al., 1998). Therefore, detailed analysis and understanding of extreme rainfall events are crucial for drought analysis.

One of the objectives of this study is to identify whether or not the frequency and intensity of extreme rainfall have increased over time. To carry out extreme rainfall analysis, ideally, high temporal rainfall data, e.g. every 30 minute, would be used. Unfortunately, such data are not available, only at daily resolution. Hence, three extreme rainfall indices (Table 4) are used that were defined by the WMO Expert Team on Climate Change Detection Monitoring and Indices (ETCCDMI, 2009).

Table 4 Definition of indices for rainfall extremes

Index name	Definitions	Units
Very wet day precipitation	Annual total precipitation when daily precipitation > 95th percentile	mm
Heavy precipitation days	Annual count of days with daily precipitation ≥ 10 mm	Days
Very heavy precipitation days	Annual count of days with daily precipitation ≥ 30 mm	Days

Once the indicators are calculated using Microsoft Excel 2010, linear regression is utilized for testing a trend in extreme rainfall events. Linear trend analysis of time series is an standard procedure in many scientific disciplines (Bryhn et al., 2011). In order to examine if the trend is statistically significant, p value and coefficient of variation are used. The p value is used for describing the probability (from 0 to 1) in statistical significance tests in which a null hypothesis is rejected when the p value is low. The 95% confidence level ($p \leq 0.05$) has commonly been used for testing the statistical significance of a trend (Bryhn, et al., 2011). The coefficient of variation (CV) is defined as the ratio of the standard deviation to the mean of a variable. The CV for a single variable aims to describe the dispersion of the variable. The higher the CV, the greater the dispersion in the variable (Wikipedia, 2012). In this case, the trend of this variable cannot be regarded as statistically significant.

In order to investigate the influence of the amount of extreme rainfall event on vegetation growth in section 3.4, the total amount of extreme rainfall for the two extreme ranges (≥ 10 mm and ≥ 30 mm) should be calculated. But the range of precipitation ≥ 10 mm includes the precipitation ≥ 30 mm. Therefore, in order to avoid this coincidence, the total amount of extreme rainfall is computed for two extreme ranges:

- The 1st range: daily rainfall is higher or equal to 10mm and less than 30 mm (10mm≤R<30mm).
- The 2nd range: daily rainfall is higher or equal to 30mm (R≥30mm).

The calculation is done during the entire (Oct-Mar) as well as first part (Oct-Dec) of rainy period for every year as the timing of extreme rainfall has to be taken into account.

3.1.3. Determination of onset and end of rainy period

In this study, the year 2009/2010 (Sep, 2009-Aug, 2010) is eliminated as the rainfall data does not include all the months (rainfall data until 31 Mar, 2010).

The vegetation growth depends on the seasonal onset, length and termination of the rainfall. Various methods to determine the onset and end of the rainy period exist in the literature. Two methods of Stern et al. (1982) and Odekunle (2006) are adopted for the determination of onset and end of rainy season. The both methods are for the Nigerian case and use only daily rainfall data. Then the results are compared.

Stern (1982) defined the onset of rainy period as the date when rainfall accumulated over 2 consecutive days is at least 20 mm and when no dry spell within the next 30 days exceeds 10 days. Odekunle (2006) determined rainfall onset using the percentage cumulative mean rainfall. The following steps are followed for Odekunle's method:

- To derive the mean annual rainfall at each 5-day interval of the year.
- To compute the percentage of the mean annual rainfall also at each of the 5-day intervals throughout the year.
- To calculate the cumulative percentages of the 5-day periods.

When the cumulative percentage is plotted against time through the year 1951-2008, the first point of maximum positive curvature of the graph corresponds to onset of rainy period; in contrary, the last point of maximum curvature refers to end of rainy period.

In order to compare the results of these two methods, the computed onsets of Stern's method that is the daily basis are aggregated at 5-day interval as the method of Odekunle is based on 5-day interval. The length of rainy period for each year is determined by subtracting dates of onset from end of rainy season.

In addition, to check the reliability of the computation result, onset, end and length of rainy period are correlated with total amount of rainfall during the entire (Oct-Mar) and first part of rainy period (Oct-Dec) as well as the average fraction of rainfall for Oct-Dec.

3.2. Drought evaluation using Standardized Precipitation Index (SPI)

Understanding historical droughts in a region is of primary importance for drought assessment (Gebrehiwot et al., 2011; A. K. Mishra, et al., 2010). This section examines the temporal occurrence of meteorological droughts where rainfall is the main parameter of interest. To define dry and wet years, annual precipitation anomaly is commonly used. However, it cannot identify the characteristics of historic drought since it is computed on yearly basis. Therefore, the 6-month Standardized Precipitation Index (SPI) is used since it is computed on monthly basis so that drought characteristics can be identified; also it is based on long term rainfall data between 1951 and 2009. This period is enough longer to perform drought magnitude and frequency analysis. The 6-month SPI is suitable to study the characteristics of drought at medium ranges (Szalai et al., 2000) so this scale is selected for this study. In section 3.2.1 and 3.2.2, the SPI as well as the method to determine of drought characteristics are described, respectively. The joint Probability Density Function (PDF) and its estimation are discussed in section 3.2.3. In section 3.2.4, the calculation of Joint return period for drought severity and duration, and the method to construct drought Severity-Duration-Frequency (SDF) curves are introduced. The following research questions will be answered using the methodologies described in this section:

Q2: Are drought characteristics (duration, magnitude and intensity) increasing over time?
Q3: What are the return periods and the probability of severe droughts with different duration and magnitude in this area?

3.2.1. Standardized Precipitation Index (SPI)

The SPI was developed by McKee et al., (1993) for identifying and monitoring drought. The main advantage of SPI is that it can be calculated for a variety of time scales that allows its application for water recourses on all times scales. Another advantage is that SPI based on probability approach so it can be used for drought frequency analysis and forecasting (Gebrehiwot, et al., 2011; A. K. Mishra, et al., 2010). Finally, SPI is based only on rainfall data while some indices, e.g., Palmer Drought Severity Index (PDSI) requires more inputs such as soil moisture or evapotranspiration (Guttman, 1998).

In addition, the SPI is computed on weekly or monthly scale so that consistency of drought condition and drought duration can be determined according to SPI categories. Another reason to choose the SPI for this research is that it has been used in many countries including arid regions; in Turkey (Caparrini et al., 2009; Komuscu, 1999), Greece (Loukas et al., 2004), China (He et al., 2011; Wu et al., 2001), Mediterranean Italy (Bordi et al., 2001), North Africa (Gebrehiwot, et al., 2011), India (Jain et al., 2010) as well as in Spain (Lana et al., 2001) and Europe (Szalai, et al., 2000).

Mathematically, the SPI is based on the cumulative probability of a given rainfall event at a station. The historic rainfall data of the station is fitted to a gamma distribution, as the gamma distribution has been found to fit the precipitation distribution quite well. This is done through a process of maximum likelihood estimation of the gamma distribution parameters, α and β for each given month.
Since the gamma function is undefined for $x = 0$ and a rainfall distribution may contain zeros, the cumulative probability becomes:

$$H(x) = q + (1 - q)G(x) \qquad (2)$$

where q is the probability of a zero, $q = \frac{m}{n}$; m is number of zero rainfall; n is number of observations;

G(x) is the cumulative probability function. $H(x)$ is used for transformation of the inverse normal to calculate the rainfall deviation for a normally distributed probability density with a mean of zero and standard deviation of unity. This value is the SPI for the particular rainfall data (McKee et al., 1995). McKee et al. (1993) proposed 7 categories for the SPI (Table 5).

To calculate SPI values, the SPI program developed by the US National Drought Mitigation Centre (2011) is used. Also SPI values for March for the whole period of 1952-2009 are computed in MS Excel 2010 and compared with the results calculated by the SPI program. The calculation procedure in MS Excel 2010 is shown in Appendix 4.

Table 5. Drought category according to SPI value

SPI values	Drought Category	Cumulative Frequency
0 to -0.99	Mild drought	16-50%
-1.00 to -1.49	Moderate drought	6.8-15.9%
-1.50 to -1.99	Severe drought	2.3-6.7%
-2.00 or less	Extreme drought	<2.3%

3.2.2. Drought characteristics

Once defining historic droughts, drought characteristics should be identified: onset, duration, magnitude and intensity. They can be identified using the computed SPI time series based on the run theory as proposed by Yevjevich (2011) (Figure 4).

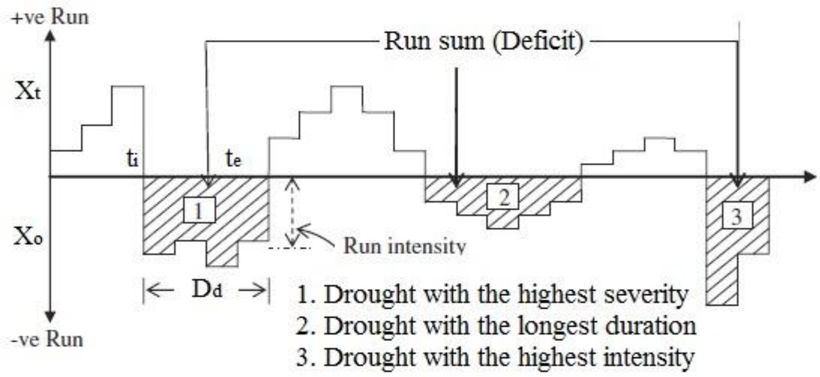

Figure 4 Drought characteristics using the run theory for a given threshold level. Source: (Mishra and Singh, 2010)

Drought onset and duration: A drought begins (onset, t_i) when the 6-month SPI value first falls below zero following a value of -1.0 or less and ends (t_e) with positive value of SPI. Drought duration is the period (D_d) between drought onset and end time. It can be expressed in years/months/weeks depending on user's desire. In this study, the monthly scale is selected since the most papers on drought analysis did use this scale (Gebrehiwot, et al., 2011; McKee, et al., 1993).

Drought magnitude: Drought magnitude (DM) is defined by the accumulated SPI during a drought event.

Drought intensity: Drought intensity (DI) is measured as drought magnitude divided by the duration.

After the historical droughts are quantified, linear regression is utilized for testing a trend to detect positive or negative trends in drought duration and intensity in order to answer the research question two.

In order to investigate whether precipitation is the reason for the increasing or decreasing trend in drought characteristics over time, total amount of rainfall for the whole year and also rainy season are plotted against the years. In addition, the intensity of dry spells during rainy season is examined. The dry spells are considered the days in which no rain days exceed 10 days. The intensity of dry spell is calculated by dividing sum of length of dry spells by the number of dry spells during rainy season in each year.

3.2.3. Joint Probability Density Function (PDF) and its estimation

From the statistical point of view, droughts are considered as multivariate events whose dimensionality depends on their characteristics such as the duration (D), severity (S) and frequency (F) (González et al., 2004). Drought events with same duration do not necessarily have the same intensity, and vice versa (Frick et al., 1990). Also the drought with higher severity for a longer duration will have more negative consequences. Therefore, several studies were proposed the Joint Probability Density Function (Joint PDF) for determining probabilistic characteristics of drought parameters (Kim et al., 2003; Mishra et al., 2009; Shiau et al., 2001). Furthermore, many studies indicate that there are not universally accepted distributions for drought related variables (Smakhtin, 2001). As the circumstances, parametric probability distributions sometimes result in strongly biased estimates (Sharma, 2000). Therefore, in this research, distribution free-nonparametric technique is employed to construct the Joint PDF for drought severity and duration.

Most nonparametric density estimation relies on a kernel density estimator which entails a weighted moving average of the empirical frequency distribution of the sample (Sharma, 2000). Given a set of observations $x_1 \ldots x_n$, a mathematical expression of a bivariate kernel probability density estimator $f_{S,D}$ is

$$f_{S,D}(s,d) = \frac{1}{n\, h_s h_d} \sum_{i=1}^{n} \left\{ K\left(\frac{s-s_i}{h_s}\right) K\left(\frac{d-d_i}{h_d}\right) \right\} \qquad (3)$$

where n is number of observations; s_i and d_i are drought severity and duration respectively; and h_s and h_d are bandwidths for the drought severity and duration, respectively. K is the kernel function. The choice of the bandwidth, h_s and h_d, is an important issue as the kernel estimator is very sensitive to bandwidth (Moon et al., 1994). The estimation of optimal bandwidth is

$$h_{di,opt} = \left[\frac{4}{n(p+2)}\right]^{1/(p+4)} \sigma_{di} \qquad (4)$$

Where $h_{di,opt}$-optimal bandwidth; σ_{di} denotes the standard deviation of the distribution in dimension d; and p-number of dimensions; p=1 for an univariate kernel estimator and p=2 for a bivariate kernel estimator.

The R script to estimate the joint PDF for drought duration and severity (magnitude) is provided in Appendix 5. The estimated joint PDF is exported into MS Excel 2010 and used to construct the joint cumulative PDFs which are required for the calculation of the joint (bivariate) return periods of droughts. The joint cumulative density function, $P(D \leq d, S \leq s)$, is constructed by summing up the Joint PDF between 0 and s for drought severity (magnitude) and between 0 and d for drought duration.

3.2.4. Drought Severity-Duration-Frequency curves (SDF)

The aim at estimating of the joint cumulative PDF is to calculate the joint return periods and to generate Severity-Duration-Frequency (SDF) curves. The steps to derive SDF are presented in Figure 5.

Based on the joint cumulative PDF, return periods, $T_{S,D}$, for drought severity and duration are calculated through the frequency analysis. Since the droughts sometimes last more than one year, $T=1/P_{Right}$ cannot be adopted. (Bonaccorso et al., 2003).

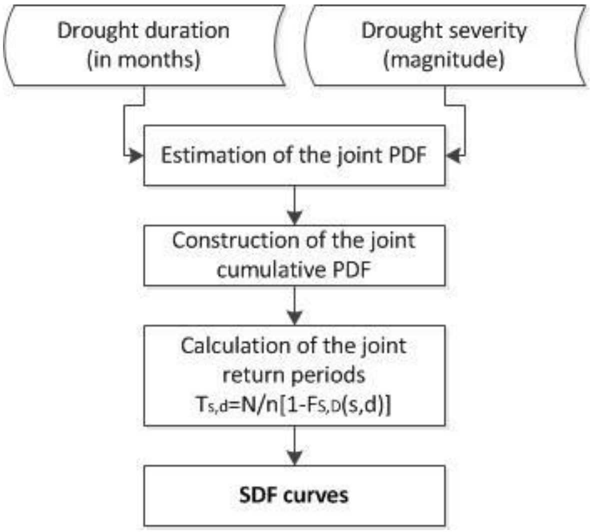

Figure 5 Flowchart to generate SDF curves

The following formula is used to define the joint return period of drought (Kim, et al., 2003):

$$T_{s,d} = \frac{N}{n[1-F_{S,D}(s,d)]} \qquad (5)$$

where $T_{s,d}$ is the joint return period, s is drought severity, d-drought duration, $F_{S,D}(s,d)=P(S\le s, D\le d)$ is the joint cumulative distribution of drought severity and duration.

Once defining the joint return periods, the Drought Severity-Duration-Frequency (SDF) curves of Sehoul area are created. Further, the bivariate return periods of historical droughts are analyzed.

3.3. Vegetation index based drought analysis

Remote sensing indices have been developed and used to monitor drought from vegetation response; among them, Normalized Difference Vegetation Index (NDVI) is most commonly used index (Tucker et al., 1986). In 3.3.1 section, Drought Severity Index (DSI) based on NDVI is introduced and the pixel based-spatial characteristic of drought is examined using DSI in section 3.3.2. In section 3.3.3 the spatial occurrence drought is studied for each land cover class. The research question 4 will be answered applying the methodology described in this section.
Q4: Which part of this area is most prone to drought?

In this study, time series of SPOT NDVI images between 10 April 1998 and 30 March 2010 with spatial resolution 1km and temporal resolution 10-days are used for the classification of these images. The ASTER image with spatial resolution 15m on 21 October 2011 is used to generate land cover map. Also Ikonos-2, Multi-Spectral Satellite image (MSS) with 4m resolution (31 Jul, 2001) and GEOEYE-1, Multi-Spectral Satellite image (MSS) with 0.8m resolution (20 Jul 2009) are used to select a representative spectral signatures of land cover classes. These two images cover a small part of the study area (184.8km^2 (46.5%) for Ikonos-2 and 55.4km^2 (13.9%) for GEOEYE-1). The rainfall data is not used since it is a point data and cannot be used for spatial analysis.

3.3.1. Drought evaluation based on Drought Severity Index (DSI)

NDVI by itself does not reflect drought or non-drought conditions. The severity of a drought can be expressed by the drought severity index (DSI). This index is defined as a measure of the deviation of the current NDVI values from their long-term mean (Amin et al., 2011). In this study the average NDVI maps during rainy season for each year are computed based on 10-day NDVI maps. From these average maps, the long-term mean of NDVI maps is also generated. Then DSI is computed for every pixel in each year.

$$\mathrm{DSI} = \mathrm{NDVI_i} - \mathrm{NDVI_{mean}} \qquad (6)$$

In the equation above, $NDVI_i$ represents the average NDVI during rainy season for year i and $NDVI_{mean}$ is the long-term NDVI mean. A negative DSI indicates below normal vegetation conditions and therefore could suggest a prevailing drought.

3.3.2. Drought susceptibility map (DSM)

In assessment of any hazard, the generation of a hazard susceptibility map is important since risk assessment experts evaluate the potential drought risk areas using drought susceptibility map and drought return periods. For the generation of drought susceptibility map (DSM), the Drought Severity Index (DSI) based on maximum NDVI (MNDVI) is used. The reason for selecting MNDVI is to avoid the effect of harvesting. The DSI is calculated as the deviation of current MNDVI values from their corresponding long-term mean MNDVI values for every pixel.

$$\mathrm{DSI_{mndvi}} = \mathrm{MNDVI_{i,j}} - \mathrm{MNDVI_{mean,j}} \qquad (7)$$

where $MNDVI_{i,j}$ is the MNDVI value for m pixel for the i year, $MNDVI_{mean,j}$ is the long-term mean MNDVI values for j pixel.

Afterwards, the formula of Loukas (2004) is used to generate DSM:

$$\mathrm{DSM} = \sum_0^n(-\mathrm{DSI_{mndvi}}) \times \frac{n}{N} \qquad (8)$$

Where $\mathrm{DSI_{mndvi}}$ is minus deviation of MNDVI; n is the number of the year in which $\mathrm{DSI_{mndvi}}$ is minus, and N is the total number of years.

DSM is generated in PCRaster software using equation 7 and 8 (see Appendix 6). The final map is classified, using Natural Breaks (Kenks) method in ArcMap 10.

3.3.3. Investigation of drought occurrence for each land cover class

First, landcover land map is created based on Aster image of 21 Oct, 2011 applying Maximum Likelihood Supervised classification approach in ENVI software. High resolution multispectal images (Ikonos-2; GEOEYE-1) and Sehoul area map in Google Earth are used select representative spectral signatures of land cover classes.

Second, a new map stack that includes only NDVI images for rainy season is created and used to create NDVI classification map using ISODATA unsupervised classification in Erdas 2010. The number of class is selected based on the statictics of classification separability.

Finally, these two maps are overlapped in ArcMap10 and NDVI classes that lie in each landcover class are defined visually. Then consistent higher and lower mean NDVI values and variations are determined for corresponding land cover class using statistics of unsupervised classification. If a landcover class correspond to consistent lower mean NDVI values or its higher variation, this landcover class could be more subject to drought.

3.4. Vegetation response to rainfall

This section discusses the methodology to examine vegetation response to variability in precipitation. Two approach, time lags and vegetation phenology, are used. Based on the results, the years of vegetative droughts are constructed during the period 1951-1997 in which SPOT NDVI data is not available and compared with the information on observed droughts found from literature.
Q5: Can the change in vegetation cover over time (intra and inter-annual) be explained by precipitation?

3.4.1. Evaluation of the relationship between NDVI and precipitation

Rainfall is assumed as homogeneous over the study area as rainfall can be considered to be homogeneous if the diameter of area is around 25km (Yang, et al., 1998). The diameter of Sehoul area is approximately 32km. In order to account for time lag between NDVI and rainfall, the time lags of 1 up to 10 10-days and its rainfall sum with preceding 10-days periods of 0 up to 7 are used. In Figure 6, an example is illustrated. If 10-day NDVI image is for 31st January, the time lag of 6 and its sum with preceding two 10-days corresponds to the sum of 10-day rainfall for 10th, 20th and 30th Nov.

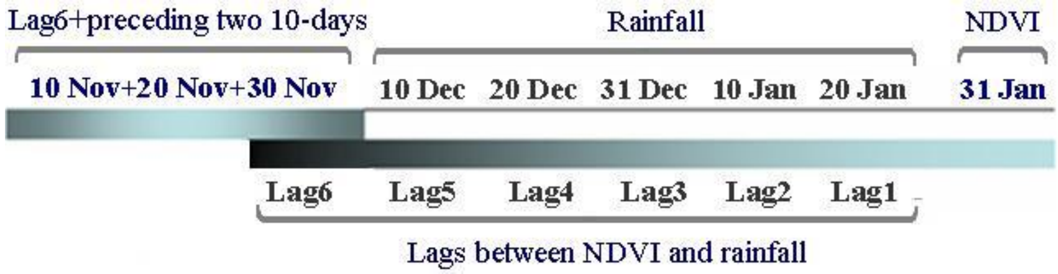

Figure 6. Time lag of 6 and its sum with preceding two 10-days rainfall for 10-day NDVI image of 31, Jan.

For the time lag analysis, 10-day rainfall amounts are computed between the years 1998-2010 in which NDVI images are available and correlated with the corresponding 10-day NDVI. Dry months (Apr-Sep) with low rainfall and poor vegetation condition can be lead to a higher correlation. So these months are eliminated from lag analysis. The correlation coefficient is computed for every pixel separately. The spatially averaged correlation maps would reveal the presence of a certain lag between NDVI and rainfall.

Further, the 6-month SPI for March is selected in this section as its computation is based on sum of rainfall between October and March that corresponds to rainy season in Sehoul area. Then the 6-month SPI for March is compared with the averages of 10-day rainfall and 10-day NDVI averaged by study area.

The obtained results are used to examine the vegetation response to rainfall. Based on the analysis, vegetative drought years over the period 1951-1997 in which SPOT NDVI data is not available are determined considering three conditions: a) total rainfall for rainy season (Oct-Mar) is two times less than its long term mean or b) the average fraction of rainfall in first part of rainy season (Oct-Dec) is two time less than long term mean or c) both is less than their long term mean.

3.4.2. Vegetation phenology and phenological metrics

Another method to examine the relation between vegetation and rainfall makes use of vegetation phenology. Vegetation phenology is the study of recurring vegetation cycles and their connection to climate commonly relying on climatological and agro-meteorological data. However, spatially and temporally continuous observations of phenology are difficult to generate from sparse ground stations (White et al., 1997). In recent years, remote sensing satellite data, particularly NDVI, have been used for monitoring vegetation phenological metrics, such as green-up, peak and offset of vegetation development (J. Li et al., 2011) as seasonal variations of NDVI are closely related to vegetation phenology (McCloy et al., 2004).

Vegetation phenology is assessed based on phenological metrics (Table 6). These metrics can be divided into three types (Lloyd, 1990; Reed et al., 1994):

- temporal (based on the timing of an event)
- NDVI-based (the NDVI value at which events occur)
- Metrics derived from time-series characteristics.

Table 6 NDVI metrics and their phenological interpretation (adopted from Reed, 1994).

Metric	Phenological interpretation	The computed metrics in this study
Temporal NDVI metrics		**P**-Period;**V**-Vegetation
Time of onset of greenness	Beginning of measurable photosynthesis Cessation of	OnP
Time of end of greenness	measurable photosynthesis Duration of photosynthesis	EndP
Duration of greenness	activity	DurP
Time of maximum NDVI	Time of maximum measurable photosynthesis	MaxP
NDVI-value metrics		
Value of onset of greenness	Level of photosynthesis activity at beginning of growing season	OnV
Value of end of greenness	Level of photosynthesis activity at end of growing season	EndV
Value of maximum NDVI	Maximum measurable level of photosynthesis activity	MaxV
Range of NDVI	Range of measurable photosynthesis activity	RanV
Derived metrics		
Time-integrated NDVI	Net primary production	TINDVI
Rate of green up	Acceleration of photosynthesis	-
Rate of senescence	Deceleration of photosynthesis	-
Modality	Periodicity of photosynthesis activity	-

3.4.3. Phenological metrics' calculation

Calculation of Onset (OnV) and end (EndV) of greenness

Vegetation phenological metrics, such as green-up (OnV, OnP), peak (MaxV, MaxP) and end (EndV, EndP) of greenness (Figure 7), can be determined by remote sensing using mainly the NDVI (Delbart et al., 2005). Different algorithms have been developed to derive the metrics related to phenology: threshold, derivative, smoothing and model fit (Beurs et al., 2010). In this study, smoothing method (Reed, et al., 1994) is employed together with the threshold approach in the study of Groten (2002).

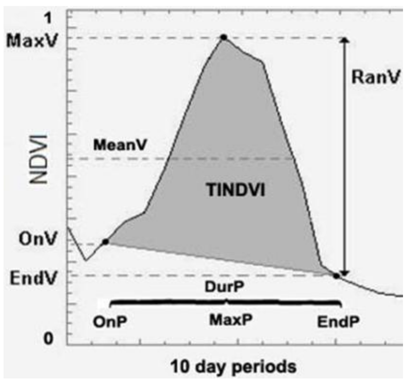

Figure 7 Derivation of phenoloigcal metrics from temporal NDVI profile. Source: (H¨opfner et al., 2011)

First, new time series maps of 10-day NDVI are created per year, starting from 10 September to 31 August. The total number of maps per a year is 36 (Table 7).

Table 7 Number of date series for new NDVI time series in each year

Number of series	1	2	3	4	…	34	35	36
date	10 Sep	20 Sep	30 Sep	10 Oct	…	10 Aug	20 Aug	31 Aug

Second, the auto-regressive moving average (ARAMA) approach is used. The calculation of the moving average for defining onset of greenness is given in equation below:

$$Y_t = (X_t + X_{t-1} + X_{t-2} + \cdots + X_{t-(w-1)})/w \qquad (9)$$

Here, Y_t is the moving average value for time t, X_t is the smoothed NDVI value for time t, and w is the moving average time interval. In our case, ten is selected as the moving average interval of 10 day composite.

The onset of greenness is defined as the point (Figure 8, pinkish circles) at which the NDVI time-series crosses the moving average in an upward direction since onset of greenness refers to a significant trend change. The end of growing season is determined in a similar manner, but the moving average is applied in reverse chronological order (Reed, et al., 1994).

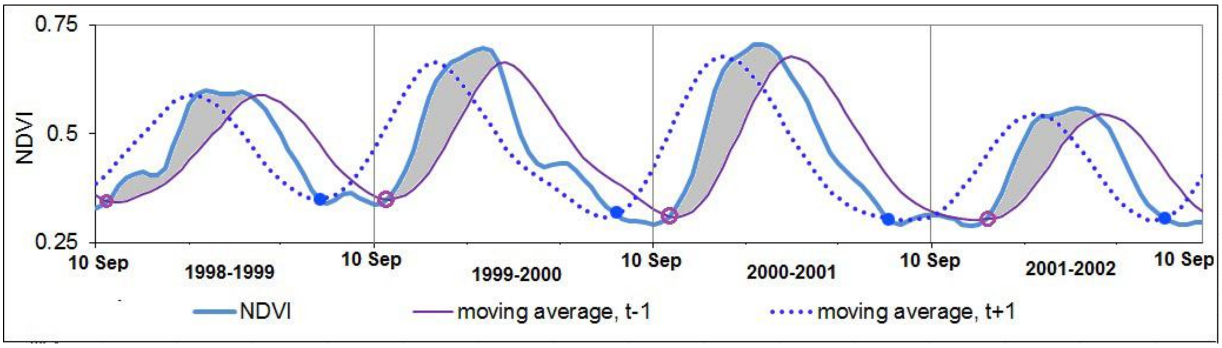

Figure 8 An example of moving average series for computing the metrics at an sampling pixel, 1998-2002. Grey colour segments are the period in which peak of greenness are calculated. Pinkish circles and blue dotes indicate onset and end of greenness, respectively (adopted from Reed et al., 1994).

Groten (2002) used the thresholds for defining onset of vegetation growth to exclude marginal positive NDVI increments that are very close to zero and to avoid "false onset" of growing season. These thresholds are adopted and should be modified for Sehoul area since they are for Burkina Faso, Africa. The threshold values modified in this research are as results of several examinations for different pixels. The NDVI increment has to satisfy the following conditions for identification of the onset:

- Two consecutive NDVI increments should be higher than 0.014 (Figure 9a). Groten (2002) used the values of 0.003, 0.016 and 0.023 for north, central and south part of Burkina Faso.
- Onset must be the point at which NDVI value should be 0.017 higher than moving average (Figure 9 b).

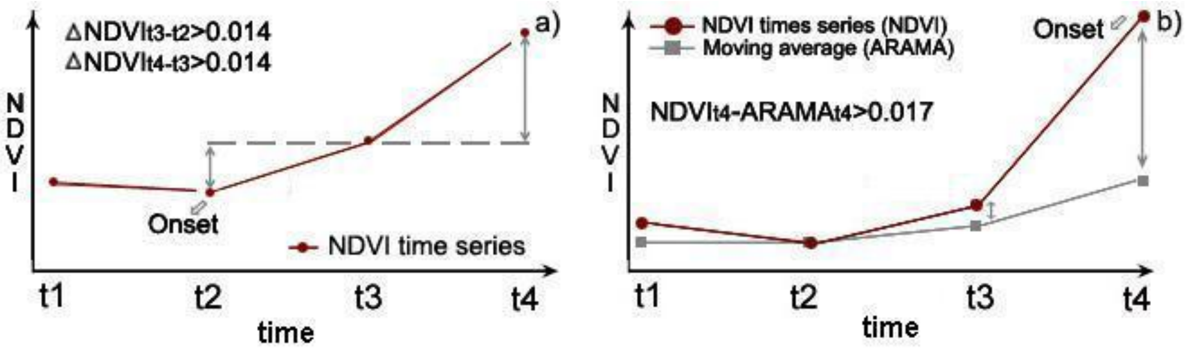

Figure 9 Thresholds used for determination of onset

In Figure 9, the two thresholds are illustrated separately. But for the real case, the two thresholds should be considered together at a pixel for a certain 10-day.

Calculation of other metrics

- Length of greenness period (DurP) is the period between the dates of onset (OnP) and end of greenness (EndP).
- Maximum NDVI value of greenness (MaxV) is defined within the period highlighted in grey colour in Figure 8. MaxV is needed to define RanV.
- Range of NDVI (RanV) is determined by the minimum value subtracted from MaxV, after the minimum of OnV and EndV is defined.
- Time integrated NDVI (TINDVI) is determined as the sum of NDVI value the during greenness period.

The script to derive phenological metrics is provided in Appendix 7.

3.4.4. Evaluation of accuracy of derived metrics

Before the computed phenological metrics are used for further analysis, the accuracy is assessed for every pixel in each year in the following way.

- ***To check values***: NDVI value of MaxV should be higher than both NDVI values for onset (OnV) and end (EndV) of greenness period.
- ***To check dates***: The date of maximum value of NDVI (MaxP) should be later than the date of onset (OnP) and earlier than the date of end of greenness (EndP).

Also the evaluation is done spatially aggregating by the entire study area for each year using “majority” function in PC Raster software in order to check any discrepancy in the dates of onset, end and maximum of greenness.

Unfortunately, in-situ phenological records from ground stations are not available for validation of computed metrics. Therefore, as a key metric, the dates of onset are compared with the total rainfall in first part of rainy season based on the assumption that delayed rainfall should cause less amount of rainfall during that period, leading to late onset in vegetation growth. The period between October and December is considered as the first part of rainy season.

3.4.5. Phenological metrics’ response to rainfall

In order to investigate the response of phenological metrics to inter-annual variability of rainfall, the metrics that are computed for every pixel are spatially averaged by the study area and correlated with total amount of rainfall for whole rainy period as well as total amount and the average fraction of rainfall in first part of rainy season. Moreover, the spatially averaged metrics and the rainfall amounts are plotted against the years (1998-2008); their peaks and pattern of curves are compared.

3.5. Human-induced land degradation

Even though drought is usually caused by climatic variance; human activity can aggravate it. That is why droughts occur more frequently in the areas affected by land degradation (Koohafkan, 1996; Nicholson, et al., 1998). Hence, human-induced land degradation is important issue that has to be taken into account for drought assessment study.

3.5.1. The discrimination of human-induced land degradation

Land degradation is a serious problem in Morocco. According to FAO (2004), 19 percent of land of the country (or 8.7 million hectares) is subject to severe land degradation over all Moroccan territory (excluding the Saharan provinces). Since in arid and semi-arid lands, the role of climate factors, especially precipitation, is so large, distinguishing the human-induced degradation from the climate signal is a difficult task (Evans et al., 2004). The most common approach to detect human-induced loss of vegetation cover is to remove the variation associated with rainfall from the NDVI time series (Evans, et al., 2004; Omuto et al., 2010; Weiss et al., 2001; Wessels et al., 2007). Elimination of climatic variations from remote sensing images requires the establishment of a relationship between climatic variations and vegetation. Recently, Wessels et al., (2007) and Bai et al., (2008) demonstrated that the differences between remotely-sensed and rainfall-predicted NDVIs are actually good indicators of human-induced loss of vegetation cover. These co-called residuals are attributed to human influence and those areas displaying a negative trend over time are considered degrading. This negative trend, if it proves to be statistically significant, would indicate an area experiencing human-induced degradation.

3.5.2. Mapping of human-induced land degradation

In this study, RESTREND (Residual trend) (Wessels, et al., 2007) technique is employed to discriminate between climate or human-induced land degradation. SPOT NDVI data and rainfall data during rainy season of 1998-2009 are used. The log transformation is applied to the rainfall values as the NDVI may not continue to increase linearly at high rainfall (Nicholson, et al., 1990). The relationships of Log-Rainfall with the average NDVI over the rainy season are characterized using least square regression analyses for every pixel. Based on this relationship, rainfall-predicted NDVIs are calculated. Then residuals are also computed by subtracting the predicted NDVIs from original NDVIs. Finally, trend analysis is performed to check if residuals are decreasing or increasing over time. The flowchart of determination of human-induced land degradation is illustrated in Figure 10 and the detailed description is given in Appendix 9.

The pixels with low R squared should be eliminated from the procedures. An R squared of 0.10 means that only 10 per cent of variance in the predicted NDVI is explained by rainfall. So the 10th Percentile of R squared is used as the threshold. Then the pixels with R squared less than the threshold are identified.

Also pixels with slope higher or equal to zero (no degradation process) are excluded from the classification procedure to create the final map. The final map is classified into high, moderate and low classes of human-induced land degradation, using Narural Breaks (Kenks) method in ArcMap 10.

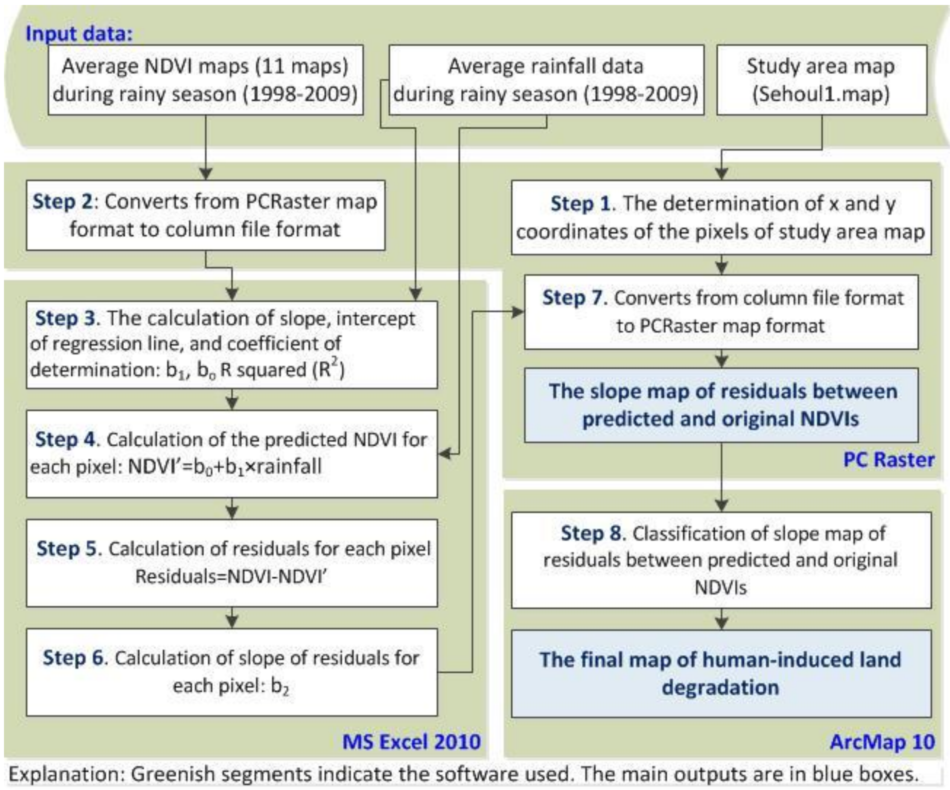

Figure 10 Flow chart of determination of human-induced land degradation

4. RESULT AND DISCUSSION

4.1. Analysis of rainfall data

The rainfall data measured at Rabat station (latitude 24.05; longitude 6.77) which covers the period 1951-2009 is used. For all computations of total or average annual parameters for rainfall the year starts on 1st September and ends at 31st August.

4.1.1. Statistics of rainfall data

The mean of daily rainfall is 1.5mm and the minimum is 0.0mm. The maximum of daily rainfall is 151.3mm that fell on 8th April 1998. The mean annual rainfall is 543.6 mm averaged over the period 1951-2009. The minimum of annual rainfall is 190.8 mm in year 1994, whereas the maximum is 927.9 mm in year 1968 (see Appendix 1).

The daily rainfall distribution is strongly right-skewed with short tail. The "tail" of the rainfall distribution is short that means the higher the rainfall amounts, the fewer the observations. The monthly total rainfall has similar distribution to daily rainfall; but with longer tail. In contrary, the distribution of annual total rainfall is almost symmetric with no tail (Figure 11).

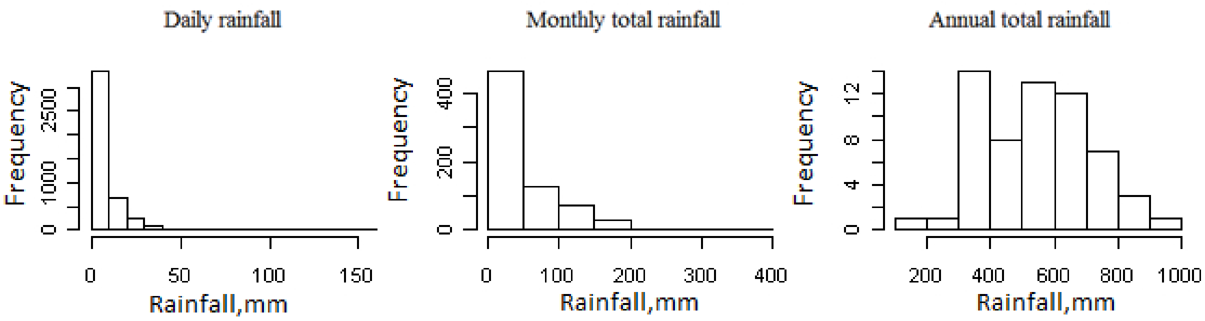

Figure 11 Histograms for daily, monthly and annual total rainfall

In Sehoul area, the rainy season starts in October and finishes in April. During rainy season, the mean of the monthly total rainfall is 54.0-104.1mm. The rest of the year is virtually dry (less than 50mm on monthly basis) (Figure 12).

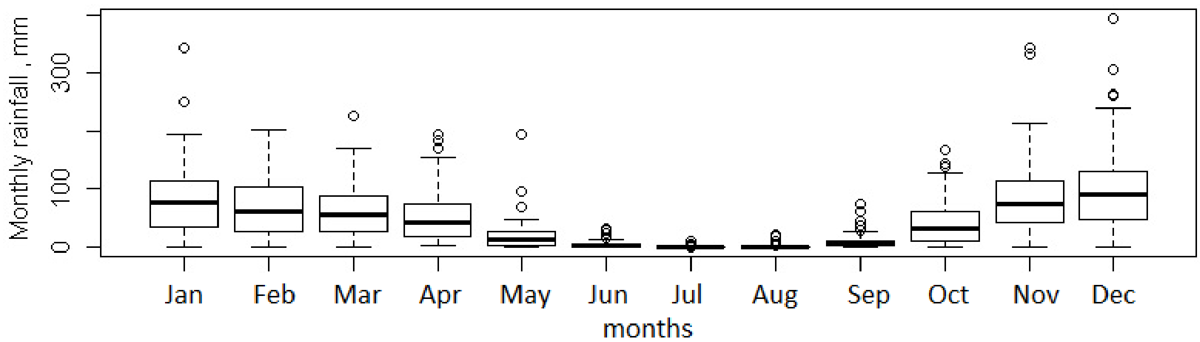

Figure 12 Boxplot for monthly total rainfall, 1951-2009. The bottom and top of the box are the 25th and 75th percentile (the lower and upper quartiles, respectively), and the band near the middle of the box is the 50th percentile (the median). Circles indicate which observations, if any, might be considered outliers.

In the past 50 years (1951-2009), there are 27 dry years (anomaly is less than 0mm) in Sehoul area. Among them, the years of 1994, 1998 and 1991 are the driest years. The mean annual precipitations are 190.8mm/-352.8mm in 1994 and 290.8mm/-253.8mm in 1998 and 305.7mm/-237.8mm in 1991 (Figure

13). On the other hand, there are 32 wet years (anomaly is higher or equals to 0mm). The years, 1968, 1995 and 2008 are the wettest years. The mean annual rainfall is 927.9mm/+384.4mm, 853.8mm/+310.2mm and 818.8mm/+275.3mm, respectively.

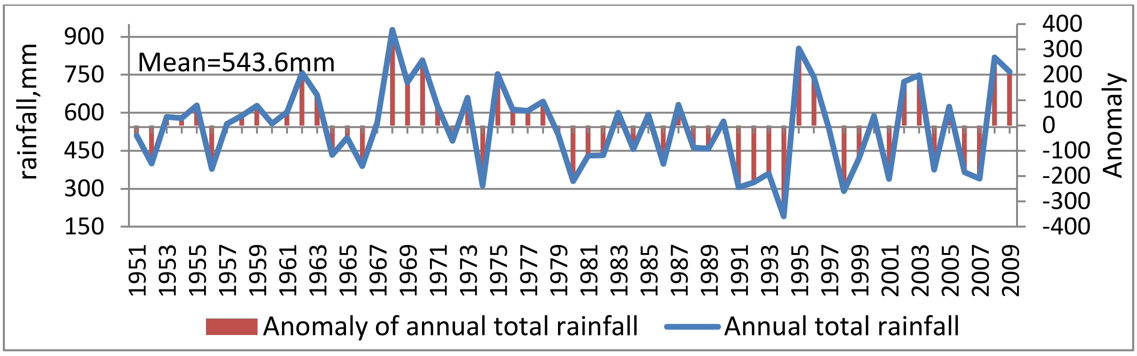

Figure 13 Annual total rainfall and its anomaly. A year starts from 1st September.

According to Table 8, long term mean of rainfall amount that falls in rainy season (Oct-Mar) is 452.6mm that accounts for 82.6% of the total amount rainfall for the entire year (543.6mm). The years 1991, 1992 and 1994 are the exceptional dry years in terms of rainfall amount that falls during rainy period (138.6-225.7mm/-314.0..-287.0mm). Conversely, in the years 1968, 1995 and 2008, the amount of rainfall that falls in rainy season is quite high (762.0-790.3mm/+310.2..+337.7mm) (see Appendix 1).

Table 8 Summary statistics of rainfall analysis

	Number of rainy days (>0mm)			Amount of rainfall, mm			Average fraction,%
	Sep-Aug	Oct-Mar	Oct-Dec	Sep-Aug	Oct-Mar	Oct-Dec	Oct-Dec
mean	74.3	55.4	26.8	543.6	452.6	237.9	0.41
Min	**43** (1994)	27 (1994)	11 (1998)	**190.8** (1994)	138.6 (1994)	29.2 (1974)	**0.11** (1974)
Max	**110** (1968)	83 (1959)	40 (2003)	**927.9** (1968)	790.3 (1968)	513.9 (2002)	**0.72** (1999)

Also the year 1974 is the year with the lowest average fraction in first part of rainy period and vice versa for 1999 (Table 8). In 1974, the rainfall events occurred more frequently in the second period of rainy season. In contrary, most rainfall amounts are concentrated in first part of rainy season in 1999 (Figure 14).

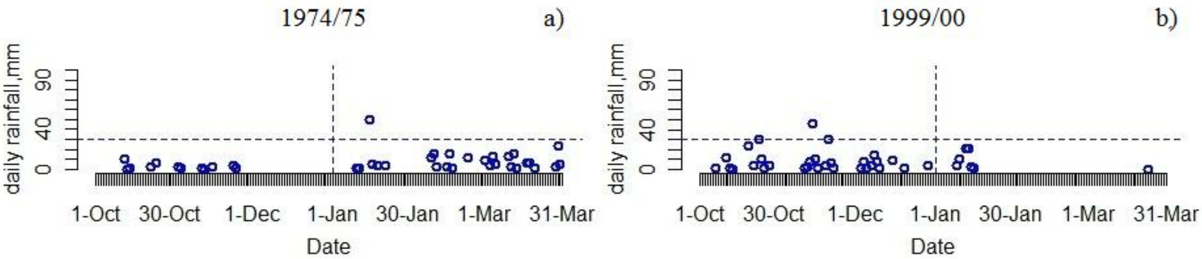

Figure 14 Temporal pattern of daily rainfall during rainy season of 1994/75 and 1999/00

As seen in Figure 15, in the years 1966, 1980 and 1999, even though the total amount of rainfall for whole rainy season is quite less (329.8-419.7mm), the average fraction of rainfalls that fell in first part of rainy period is high (0.67-0.72). So in these years vegetation condition might be not so worse. Conversely, in the year 1954, 1970, 1978, 1985, 1995 and 2009, the total amount of rainfall during whole rainy season is high (493.2-796.1mm). However, the average fraction for first part of rainy season is very low (12.8-26.1). This might influence negatively the growth of vegetation.

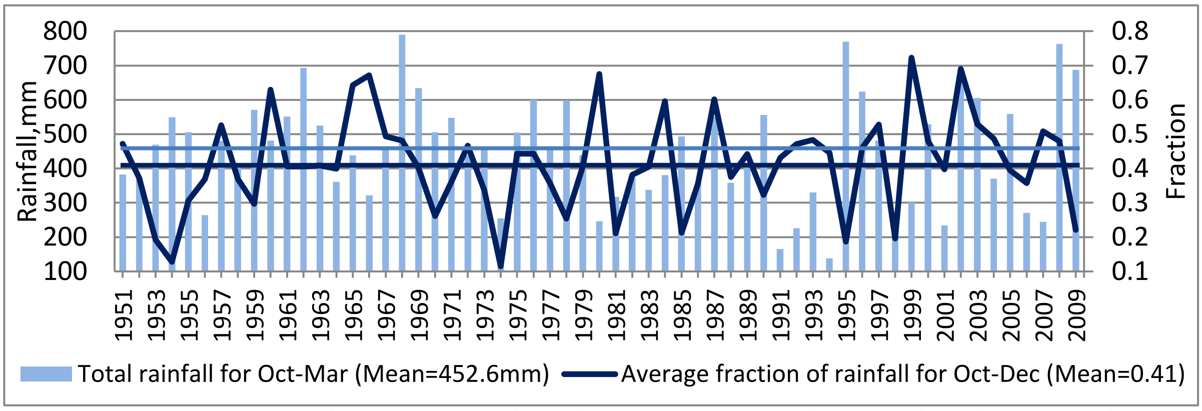

Figure 15 The comparison of total amount of rainfall with the average fraction of rainfall. Bars refer to the total amount of rainfall for entire rainy season (Oct-Mar). Solid line indicates the average fraction of total amount rainfall in first part of rainy period (Oct-Dec).

4.1.2. Extreme rainfall

Three extreme indices are used for this study: annual count of days with daily precipitation ≥ 10 mm and ≥ 30 mm and, annual total precipitation when daily precipitation > 95th percentile (in section 3.1.2).

In Table 9, the 95th percentiles of daily rainfall for each decade are presented. The mean 95th percentile averaged over the period of 1951-2010 is 9.76. The 95th percentile for the period 1951-2009 is 10.1mm.

Table 9 The 95th percentile of daily rainfall for each decade

	1951-60	1961-70	1971-80	1981-90	1991-00	2001-10	mean	**1951-2009**
95th percentile	9.82	11.1	10.5	9.1	7.6	10.4	9.76	**10.1**

Annual total precipitation when daily precipitation > 10.1mm was computed for every year plotted with other two indices in Figure 16.

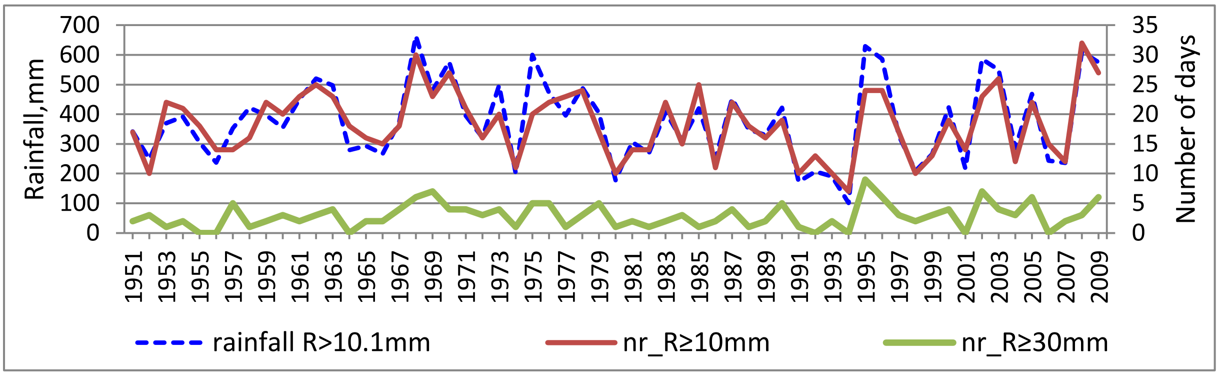

Figure 16 Computed extreme indices. The dashed line refers to annual total precipitation when daily precipitation > 95th percentile (10.1mm). Thin red and thick green lines indicate number of days with daily precipitation ≥ 10 mm and ≥ 30 mm, respectively.

Table 10 Statistics of regression analysis

		R squared	Slope	p value (p≤0.05)	Coefficient of variation
95th percentile		0.000	0.055	0.96	0.36
Number of days	R≥10mm	0.002	-0.015	0.72	0.30
	R≥30mm	0.028	0.020	0.20	0.71

For the three extreme indicators, trend analysis was carried out using linear regression. None of them displayed statistically significant trends since slopes of linear regression for three indices are close to zero (-0.015÷0.055); p values (0.20÷0.96) and coefficient of variance is very high (0.30÷0.71) (Table 10).

The statistics of the averaged indices over the period 1951-2009 are shown in Table 11. The mean of the annual total precipitation when daily precipitation > 95th percentile is 383.5mm. The minimum is 110.9mm in 1994 and the maximum is 673.2mm in 1968. The mean number of days with precipitation ≥ 10 is 18.3 days. The minimum is 7 days occurred in 1994 and the maximum is 32 in 2008. The mean number of days with precipitation ≥ 30 is 2.9 days and the maximum number, 9 days is in 1995.

Table 11 Summary of computation for extreme rainfall analysis

	Extreme indices			For rainy period (Oct-Mar)			
	Total rainfall, mm	Number of days		Number of days		Total rainfall, mm	
	R≥10.1mm	R≥10mm	R≥30mm	10mm≤R<30mm	R≥30mm	10mm≤R<30mm	R≥30mm
mean	383.5	18.3	2.9	12.9	2.6	217.8	107.3
min	110.9 (1994)	7 (1994)	0 (-)	4 (1991)	0 (-)	58.5 (1991)	0 (-)
max	673.2 (1968)	32 (2008)	9 (1995)	27 (2008)	9 (1995)	482.1 (2008)	345.0 (1995)

If we look at extreme rainfall events during rainy period, the mean number of days with rainfall 10mm≤R<30mm is 12.9 days and the corresponding amount of rainfall is 217.8 mm. This accounts for 48.1% of long term mean of rainfall amount (452.6mm) for whole rainy period. The minimum values of number of days (4 days) and amount of rainfall (58.5mm) for this range lies in 1991, vice versa for 2008 (27 days and 482.1mm). The mean of number of days with rainfall ≥ 30 is 2.6 during rainy period and the corresponding amount of rainfall is 107.3mm. This accounts for 23.8% of the total amount rainfall over the whole rainy period. The maximum number of rainy days with rainfall ≥ 30 is 9 in 1995 that accounts for 345.0mm (Table 11).

4.1.3. Onset, end and length of rainy period

The first method applied to determine the onset and end of rainy periods is Odekunle' method (section 3.1.3). This method is based on long term rainfall data (1951-2008) and determined the mean dates, which are then used to estimate the rainfall onset and retreat dates for each year. According to Figure 17, points of maximum curvature that correspond to the onset and end of rainfall are respectively at 39–40 percent and over 88 percent of the annual rainfall. The average rainfalls for 5-day interval that correspond to the first and last maximum curvature are 20.6 and 13.1mm, respectively. The onset and end of rainy period calculated for each year are shown in Figure 18 a.

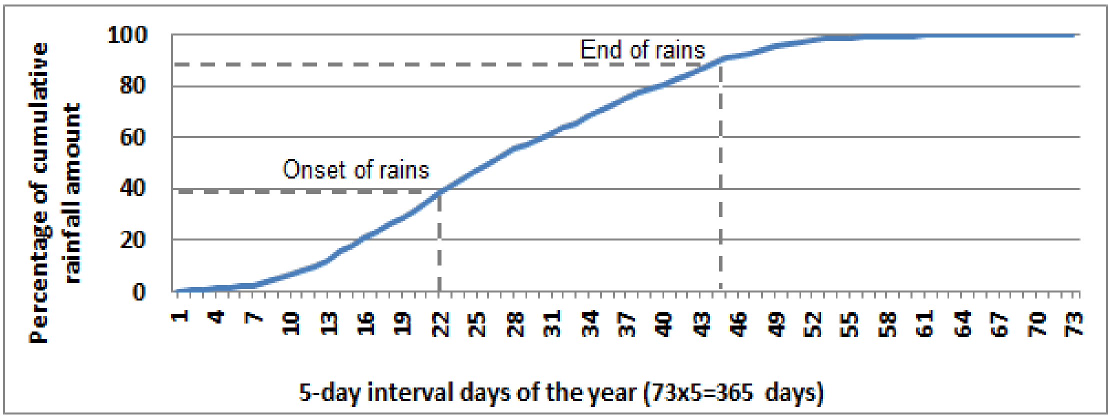

Figure 17 Mean onset and end of rainy period for the period of 1951-2008

The mean date for onset of rainy period for Odekunle's method is 28, Oct with the standard deviation 5.3 whereas for Stern's method is 10, Nov with standard deviation 8.0. The mean dates of end of rainy period for Odekunle and Stern's method are 23-24 Apr and 16-17, Feb, respectively. The corresponding standard deviations are 5.4 and 8.5 (Table 12). Stern's method reveal early end of rainy period, resulting in shorter length of rainy period (98.5 days) than Odekunle's method (178.5 days). This evidence can be seen clear in Figure 18 b).

Table 12 Statistics of onset and end of rainy period calculated for each year by the two methods

	Date of onset of rainy period		Date of end of rainy period		Length of rainy period	
Author	Odekunle	Stern et al.	Odekunle	Stern et al.	Odekunle	Stern et al.
Mean, mm (1951-2008)	12.5 (28, Oct)	15.0 (10, Nov)	48.3 (23-24, Apr)	34.7 (16-17, Feb)	178.5 days	98.5 days
Standard deviation	5.3	8.0	5.4	8.5	7.2	10.8

As shown in Figure 18 b), there are some discrepancies in which onset date is later than end of rainy period for Stern's method (e.g., 1974, 1983, 1992). Also in 2007, the date of onset could not be determined (0 date) by this method due to dissatisfaction with the onset threshold of the method.

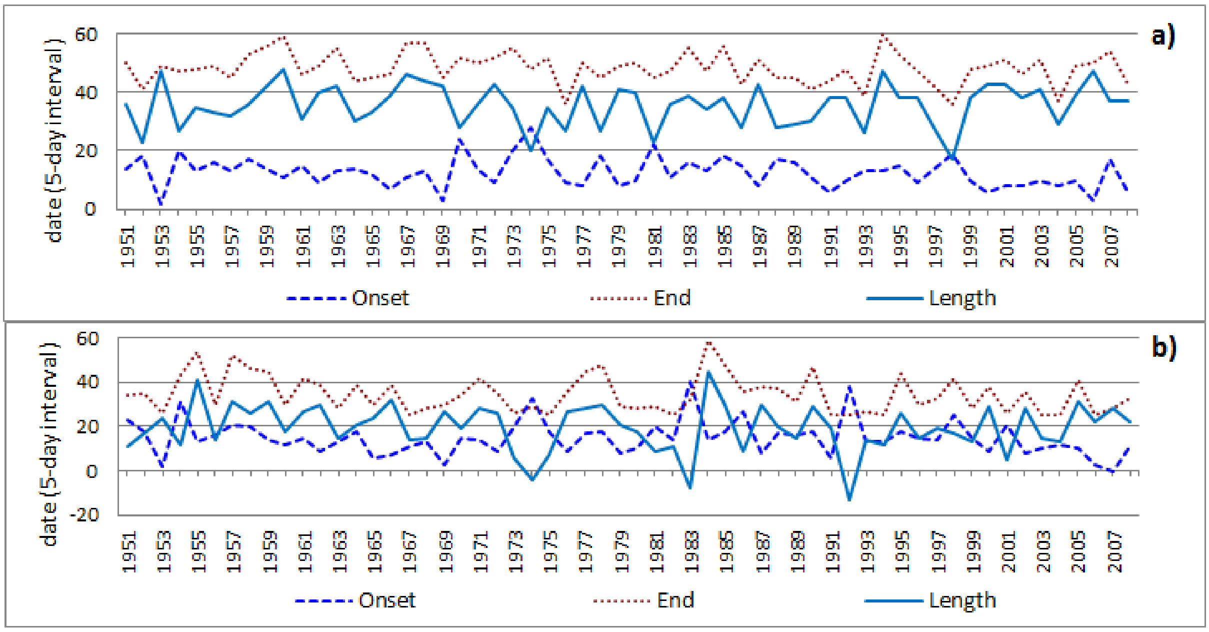

Figure 18 Temporal patterns of onset, end and length of rainy period defined by the methods of a) Odekunle b) Stern.

The correlation coefficient between onset dates defined by the two methods is 0.59; -0.13 between end dates of rainy period; 0.14 for lengths of rainy period defined by Odekunle and Stern's method (Table 13).

Table 13 Correlation coefficients between the computed dates of onset, end and length of rainy period defined by the two methods of Odekunle and Stern

		Method of Odekunle		
		Onset	End	Length
Method of Stern	Onset	0.59		
	End		-0.13	
	Length			0.14

In order to check the reliability of these two methods, computed onset, end and length of rainy period are correlated with total amount of rainfall during the entire (Oct-Mar) and first part of rainy period (Oct-Dec) as well as the average fraction of rainfall for Oct-Dec.

Table 14 Correlation coefficients between the computed onset and length of rainy period, and the amount of rainfall for different period

Methods	Method of Odekunle		Method of Stern et al.	
The amount of rainfall for different period	Onset	Length	Onset	Length
Total rainfall for Oct-Mar	-0.15	0.15	-0.21	**0.41**
Total rainfall for Oct-Dec	-0.31	0.26	-0.30	0.26
Average fraction of rainfall for Oct-Dec	**-0.42**	0.31	**-0.40**	0.34

There are a stronger negative correlations between onset dates defined by both methods (-0.42 for Odekunle's method; -0.40 for Stern's method) and average fraction of rainfall during the period of Oct-Dec. Also the onset dates reveal a stronger negative correlation (-0.31; -0.30) with the total rainfall for Oct-Dec than the total rainfall for the whole rainy period (Oct-Mar) (-0.15; -0.21). The length of rainy period defined by the method of Stern shows higher positive correlation (0.41) compared to the method of Odekunle (0.15) (Table 14).

4.1.4. Discussion

The exceptional wet and dry years are determined based on precipitation anomaly as it is a commonly used approach (in section 4.1.1). However, not all the rainfall can be efficient depending on the period in which rainfall events fall. For instance, in section 4.1.1, the different two cases were discussed (Figure 14). The rainfall events that fell at the end of rainy period of 1974/75 must be less efficient than the rainfall events that fell more frequently in first part of rainy period 1999/00. Therefore, we identified the historical dry and wet periods considering both total amount of rainfall during entire rainy period and the average fraction of rainfall between the two periods, Oct-Nov and Oct-Dec (Figure 15).

As one of the three extreme indices used in extreme rainfall analysis (section 4.1.2), the 95th percentiles of daily rainfall revealed the decreased values (9.1mm/-1.0mm and 7.6mm/-2.5mm respectively) for the decades of 1981-1990 and 1991-2000. This could be resulted from the consistent dry years between 1979-1982 and 1991-1994 (Figure 13). In Sehoul area, the mean number of days with rainfall 10mm$\leq$R<30mm during rainy season is only 12.3 days. However, this account for 48.1% (217.8 mm) of long term mean of rainfall amount (452.6mm) for whole rainy period. Moreover, the mean number of days with rainfall $\geq$ 30mm is only 2.6 during rainy period and the corresponding amount of rainfall is 107.8mm on average per year. This accounts for 23.8% of the total amount rainfall over the whole rainy period. This shows that extreme rainfall events can contribute largely to annual rainfall as well as to the amount of rainfall during rainy season. If the extreme rainfall events become more frequently over time, the rainfall efficiency for vegetation growth could be decreased (section 4.1.2). Thus, we conducted trend analysis of extreme indices. None of these extreme indices displayed statistically significant trends over the period of 1951-2008.

We also determined onset, end and length of rainy period applying two methods both based on rainfall data (in section 4.1.3). However, the method of Stern et al. (1982) for onset was found to be too strict for Morocco, resulting in years with no onset date (e.g. in 2007, Figure 18 b) or too late onset of rainy period, or too early end of rainy period due to dissatisfaction with thresholds of this method. This lead to some years in which onset date is later than end of rainy period (e.g., 1974, 1983, 1992, Figure 18 b), resulting the negative length of rainy period. The correlation coefficients between the computed onset, end and length of rainy periods defined by both methods of Odekunle and Stern is low (less than 0.42). These methods are both for Nigerian case, especially the threshold values for Stern's method. This might be the reason and some of the threshold values should be modified for Moroccan purposes. The correlation coefficients between onset dates defined by the methods and the average fraction of rainfall in first part of rainy period are higher (-0.42 and -0.40 for onset by Odekunle and Stern respectively) compared to total rainfalls for the entire and first part of rainy period. This means a delay in onset of rainy period results in less average fraction of rainfall in first part of rainy period (Oct-Dec). Therefore, the average fraction of rainfall could be a better indicator of delay in onset of rainfall. Also it can be seen that the delay in onset of rainfall results in less amount of rainfall in first part of rainy period (Oct-Dec) as there are negative correlation (-0.31 and -0.30) in Table 14.

4.2. SPI based drought analysis

In order to assess the temporal occurrence of drought, the 6-month Standardized Precipitation Index (SPI) (section 3.2.1) was employed because this scale is suitable to study the characteristics of drought at medium ranges (Szalai, et al., 2000), but also it is based on long term rainfall data between the period of 1951-2009. This period is enough for drought magnitude and frequency analysis. In addition, SPI is computed on monthly scale so that consistency of drought condition and drought duration can be determined according to SPI categories (Table 5).

4.2.1. Analysis of historic droughts defined by SPI

The calculated SPI over the period 1951-2009 is shown in . According to the graph, the values of negative SPI peaked in 1974 (-3.26), 1976 (-3.06), 1981 (-3.26), 1994 (-2.76) and 2005 (-2.66), whereas the highest value of positive SPI occurred in 1970 (2.57), 1971 (2.56), 1984 (2.52), and 1995 (2.52). The annual rainfall and its anomaly corresponding to years mentioned above are given in Table 15.

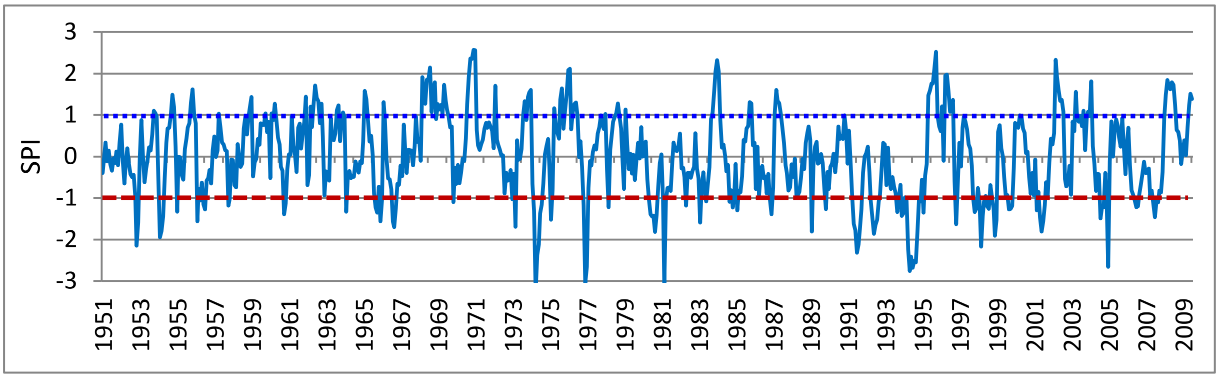

Figure 19 The 6-month SPI for every month between 1951 and 2009. The horizontal dot and dashed lines indicate the thresholds of wet and drought years respectively.

The minus peaks of the 6-month SPI coincides with the low annual rainfall expect for 1976 and 2005. Similarly, the positive peaks correspond to higher annual rainfall except for 1984.

Table 15 Peak SPI values and the corresponding annual rainfall with its anomaly

Minus peaks of SPI			Positive peaks of SPI		
Year	SPI value	Annual rainfall, mm/ its anomaly, mm	year	SPI value	Annual rainfall, mm/ its anomaly, mm
1974	-3.26	312.7mm/-230.9mm	1970	2.57	807.3mm/+263.7mm
1976	-3.06	**613.2mm/+69.6mm**	1971	2.56	627.1mm/+83.5mm
1981	-3.12	431.1mm/-112.5mm	1984	2.52	**465.7mm/-87.1mm**
1994	-2.76	190.8mm/-352.8mm	1995	2.52	853.8mm/+310.2mm
2005	-2.66	**623.7mm/+80.1mm**	2002	2.33	722.2mm/+178.6mm

Once quantifying historic droughts based on SPI, drought characteristics were identified according the method described in section 3.2.2. Among 30 droughts (SPI<-1) occurred in Sehoul area since 1950, the drought during 1993-1995 is the longest drought (25 months) with highest magnitude (32.9) (Table 16). If the intensity is considered, the drought during 1974-1975 has the highest intensity (1.61). The drought occurred in 1998-1999 and lasted for 17 months has higher magnitude (20.1) than the drought with magnitude 17.3 that lasted for 22 months in 2006-2008. This shows a good example that a longer drought is not necessarily the severer one.

Table 16 Historical droughts and their characteristics according to SPI

No	Year	Months	Duration in month	Magnitude	Intensity
1	1953	II-IX	8	6.3	0.79
2	1954-1955	IX-I	5	6.2	**1.25**
3	1955-1956	IX-I	5	2.4	0.47
4	1956-1957	X-VII	10	8.5	0.85
5	1958	VI-XI	6	3.8	0.63
6	1961	IV-VIII	5	3.4	0.68
7	1964-1965	X-VIII	11	4.7	0.43
8	1966	IV-IX	6	6.8	1.13
9	1966-1967	XII-X	11	8.5	0.77
10	1970-1971	VII-II	8	3.4	0.43
11	1973	IV-XI	8	5.9	0.74
12	1974-1975	X-V	8	12.9	**1.61**
13	1975	IX-XI	3	2.6	0.86
14	1977	VI-XII	7	8.2	1.18
15	1978	X-XI	2	1.5	0.77
16	1980-1982	XII-IV	**17**	**17.6**	1.04
17	1982-1983	X-VI	9	4.2	0.46
18	1983-1984	VIII-IV	9	6.3	0.70
19	1985-1986	III-I	11	8.2	0.75
20	1986-1987	XII-IX	10	7.1	0.71
21	1989	X-XI	2	2.0	1.01
22	1990	V-XI	7	3.8	0.54
23	1991-1992	XI-VII	9	12.3	**1.37**
24	1992-1993	XI-VII	9	10.2	1.14
25	1993-1995	XII-XII	**25**	**32.9**	**1.32**
26	1998-1999	V-IX	**17**	**20.1**	1.18
27	2000	II-VIII	7	6.4	0.92
28	2001-2002	VI-VII	14	12.7	0.91
29	2004-2005	XII-X	11	10.3	0.93
30	2006-2008	XI-VIII	**22**	**17.3**	0.78

The duration and the severity (magnitude and intensity) of historical droughts have an increasing trend over time. The slopes of linear regression are 0.2932, 0.3651 for drought duration and magnitude, respectively. But the slope for drought intensity is not so much (0.0083) (Figure 20).

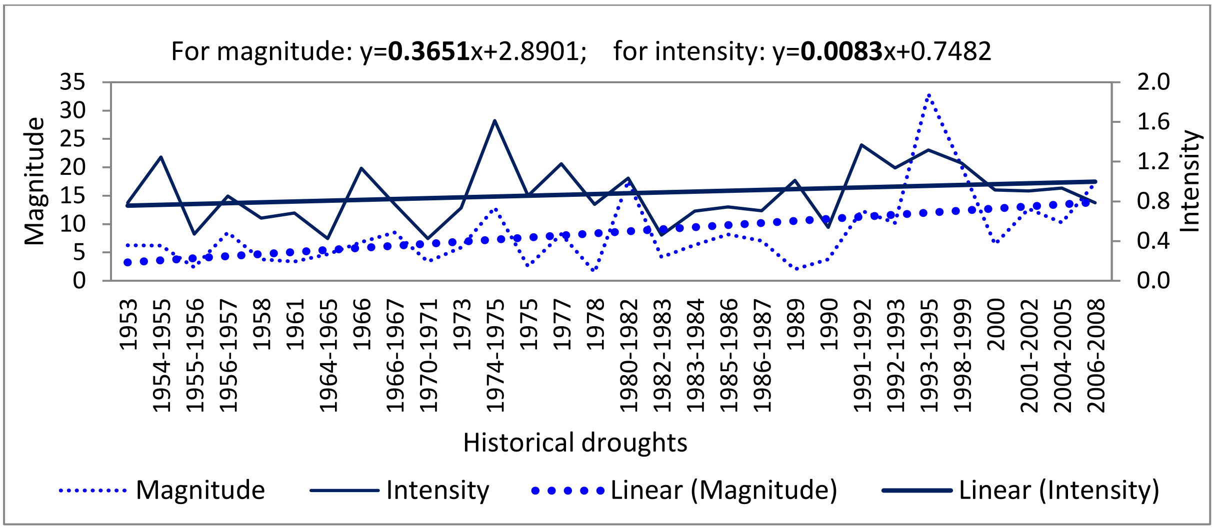

Figure 20 Characteristic of historical droughts and trend analysis.

In order to investigate the reason for the increasing trend in drought characteristics over time, total amount of rainfall for the whole year and rainy season were plotted against the years. The both have a decreasing trend over time (Figure 21). This might be one of the reasons for the increasing trend in drought characteristics. Also we see that the magnitude of droughts slightly increased, with peak of the 1993-1995 droughts coinciding with a slight decrease in total annual and total rainfall for rainy period.

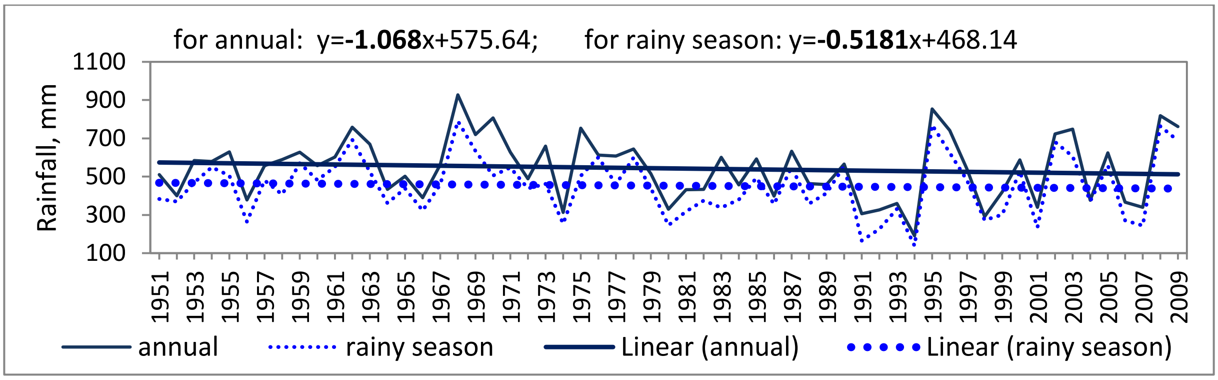

Figure 21 Trend in total rainfall for the whole year and rainy season

The second reason is that there is an increasing trend in intensity of dry spells during rainy season over time (Figure 22).

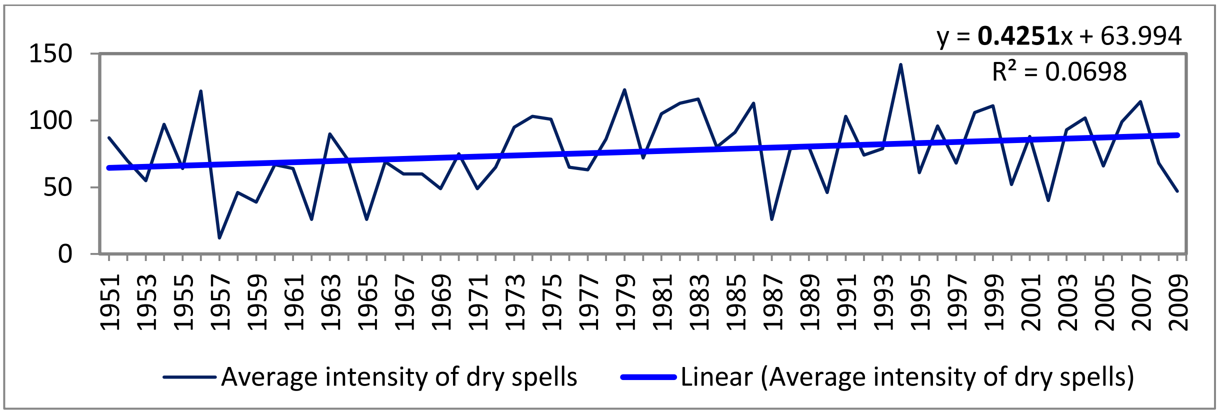

Figure 22 Trend in the average intensity of dry spells during rainy season of 1951-2009.

4.2.2. The Joint PDF and drought Severity-Duration-Frequency (SDF) curves

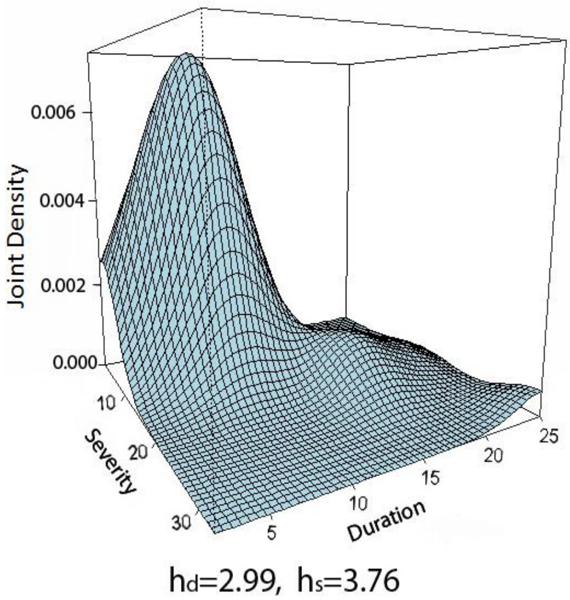

Based on the drought characteristics, duration and magnitude based on 6-month SPI (section 4.1.1), the joint PDF is estimated (Figure 23).

This joint cumulative PDF is an input for the calculation of the joint (bivariate) return periods of drought. Once return periods of droughts were calculated based on the formula (5) (section 3.2.3), the drought Severity-Duration-Frequency (SDF) curves of Sehoul area were created (Figure 24).

Figure 23 The Joint PDF for drought Duration and Severity (Magnitude)

The graph shown below reveals that bi-variate return periods increase with the increase in drought duration and severity.

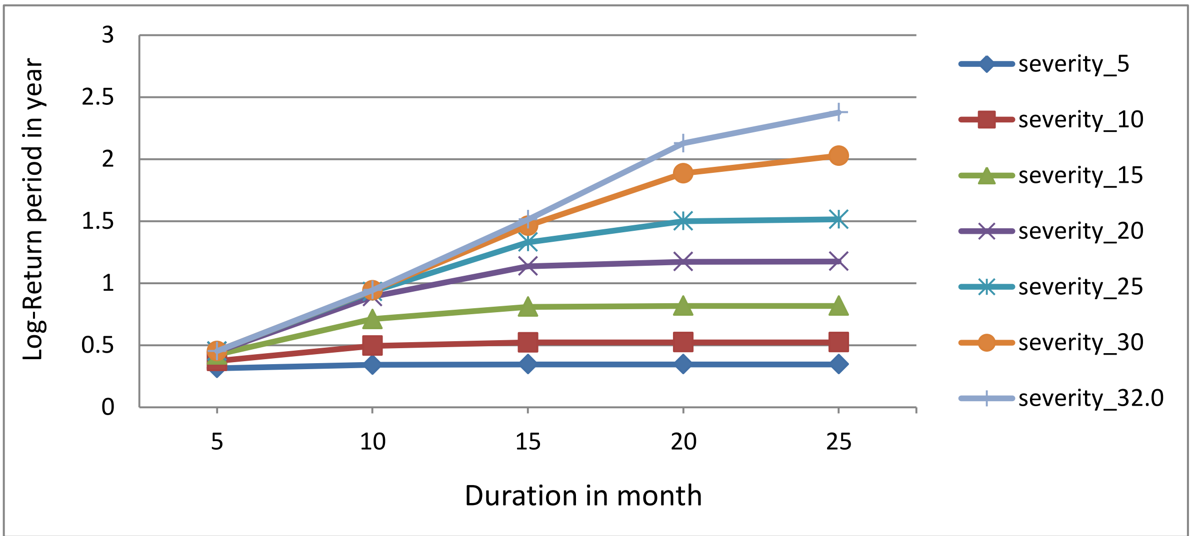

Figure 24 The joint return periods for severity (magnitude) corresponding to duration

The bivariate return periods of historical droughts in the Sehoul area are presented in Figure 25. There are four severer droughts over the period 1952-2008. The first ($T_{S,D}$=8.9 years) started in December 1980 and its duration is 17 months. The second drought is the severest drought in terms of drought duration (25 months) and magnitude (32.9). It has longest return period ($T_{S,D}$=237.7 years). The next with return period, 15.7 years started in May 1998 and lasted for 17 months. The last severe drought ($T_{S,D}$=9 years) occurred in 2006-2008 and lasted for 22 months.

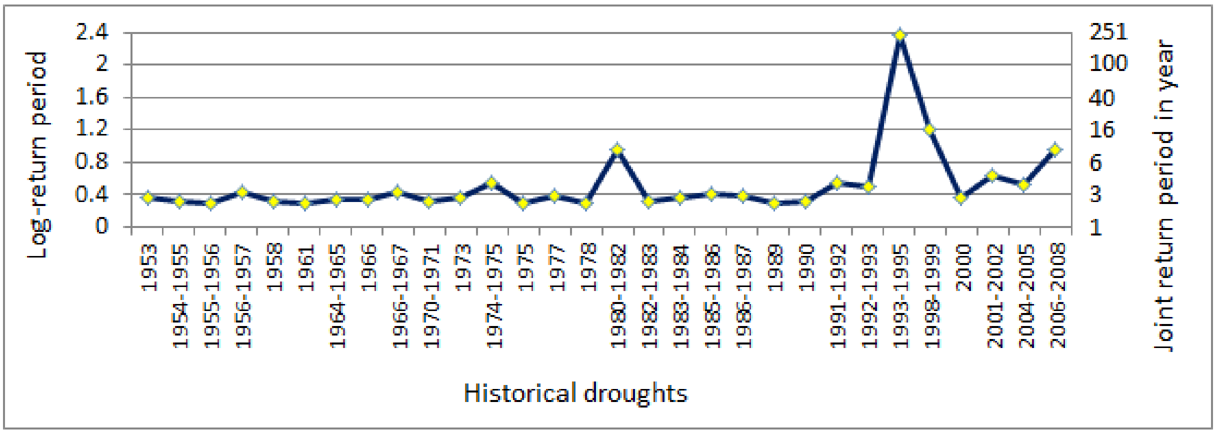

Figure 25 The joint (bivariate) return periods of observed droughts

4.2.3. Discussion

There are three mismatches between the significant peaks (both minus and positive) of SPI time series and the annual rainfall; in 1976 and 2005 for the minus peaks and in 1984 for the positive peak (Table 15). The 6-month SPI are calculated for every month based on the sum of rainfall for preceding 6 months whereas the annual rainfall are computed per year including all the months within a year. This difference in time scale might be result in these discrepancies. For instance, the negative peak (-3.06) of SPI in 1976 is observed in August that is calculated based on the sum of rainfall between March and August. This period include all the dry months. In the remaining period of this year, there must be frequent rainfall events because the annual rainfall is higher than normal (613.2mm/+69.6mm). Therefore, the 6-month SPI cannot be an appropriate index for this study. The 12-month SPI could be used. However, its scale is longer than vegetation growing period. Thus it is suggested for drought assessment at longer time scale such as ground water drought (A. K. Mishra, et al., 2010). Another way is to use the anomaly of annual and rainy season rainfall. However, the time scale is not continues (per year, not for every month) so we cannot compute drought characteristics such as duration and severity considering drought consistency period. Therefore, another better index that is computed at least on monthly scale should have been employed to assess temporal occurrence of droughts.

If the historical droughts and their characteristics are identified properly, drought magnitude-frequency analysis that is employed the Joint PDF can be a promising approach for drought hazard assessment.

4.3. Vegetation index based drought analysis

In this study, SPOT NDVI between 10 April 1998 and 30 May 2010 with spatial resolution 1km and temporal resolution 10-days, and ASTER image (15m) on 21 October 2011 are used. Also Ikonos-2, Multi-Spectral Satellite image (MSS) with 4m resolution (31 Jul, 2001) and GEOEYE-1, Multi-Spectral Satellite image (MSS) with 0.8m resolution (20 Jul 2009) are used for selection of representative spectral signatures for land cover classes. These images cover a small part the study area (184.8km^2 (46.5%) for Ikonos-2; 55.4km^2 (13.9%) for GEOEYE-1). The rainfall data is not used since it is a point data and cannot be used for spatial analysis.

4.3.1. Vegetative drought and drought prone area of Sehoul area

For the analysis of vegetative droughts, drought severity index (DSI) (section 3.3.1) was computed for every pixel (Figure 26). The mean of DSI averaged over the study area is 0.46. According to DSI and DSI anomaly averaged over study area, 1998/99 (0.39/-0.07), 2001/02 (0.34/-0.12) and 2006/07 (0.41/-0.05) years are drought years. Among them 2001/02, drought was the severest. In contrary, during growing period of 2008/09, vegetation was in the best condition (0.52/+0.07) among rainy periods between the years of 1998-2010.

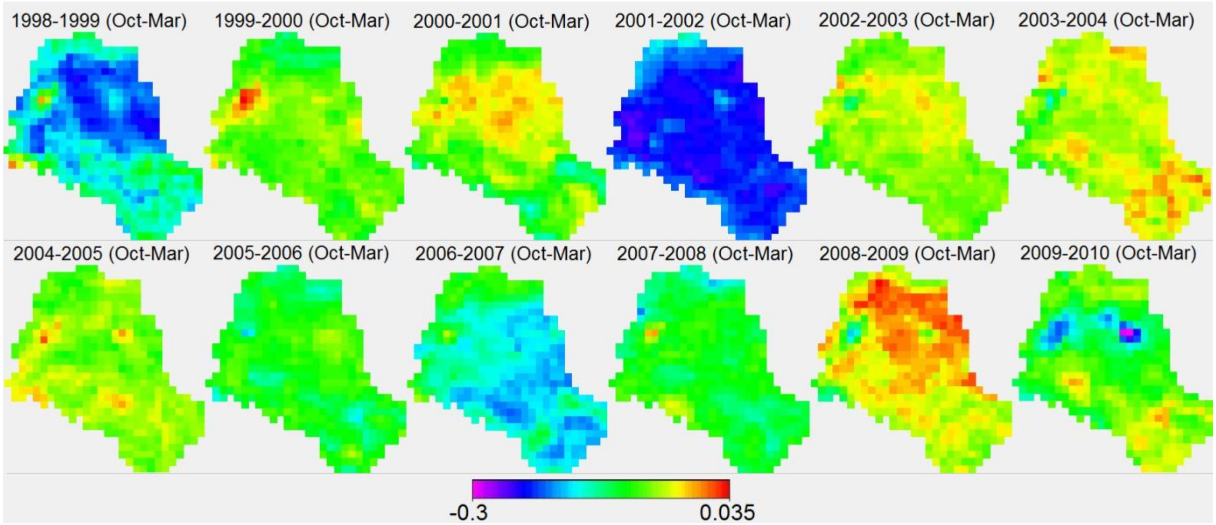

Figure 26 Drought severity maps based on the anomaly of average NDVIs during rainy season

Using the DSI maps, the pixel based Drought susceptibility map (DSM) of Sehoul area was generated (Figure 27 a) applying the method discussed in section 3.3.2 and classified into high, moderate and low susceptibility classes (Figure 27 b).

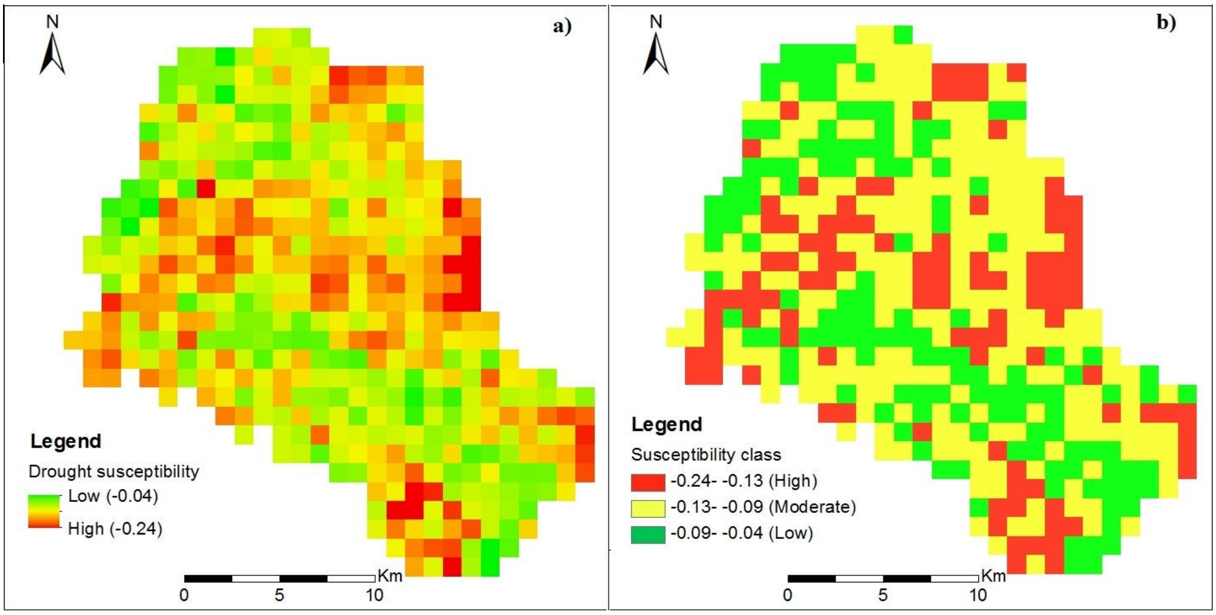

Figure 27 a) Drought Susceptibiliy map, b) The classified Drought Susceptibility map

The total area which lies in high susceptibilty class is 93.6 km² (22.6%); for moderate and low susceptibility classes, the areas are 200.5 km² (48.4%) and 120.3 km² (29.0%), respectivily.

Apart from pixel based analysis, spatial characteristics of drought were examined for different land cover classes. Land cover map was generated and shown in Figure 28. Overall Accuracy = 74.0%. Kappa Coefficient = 0.618.

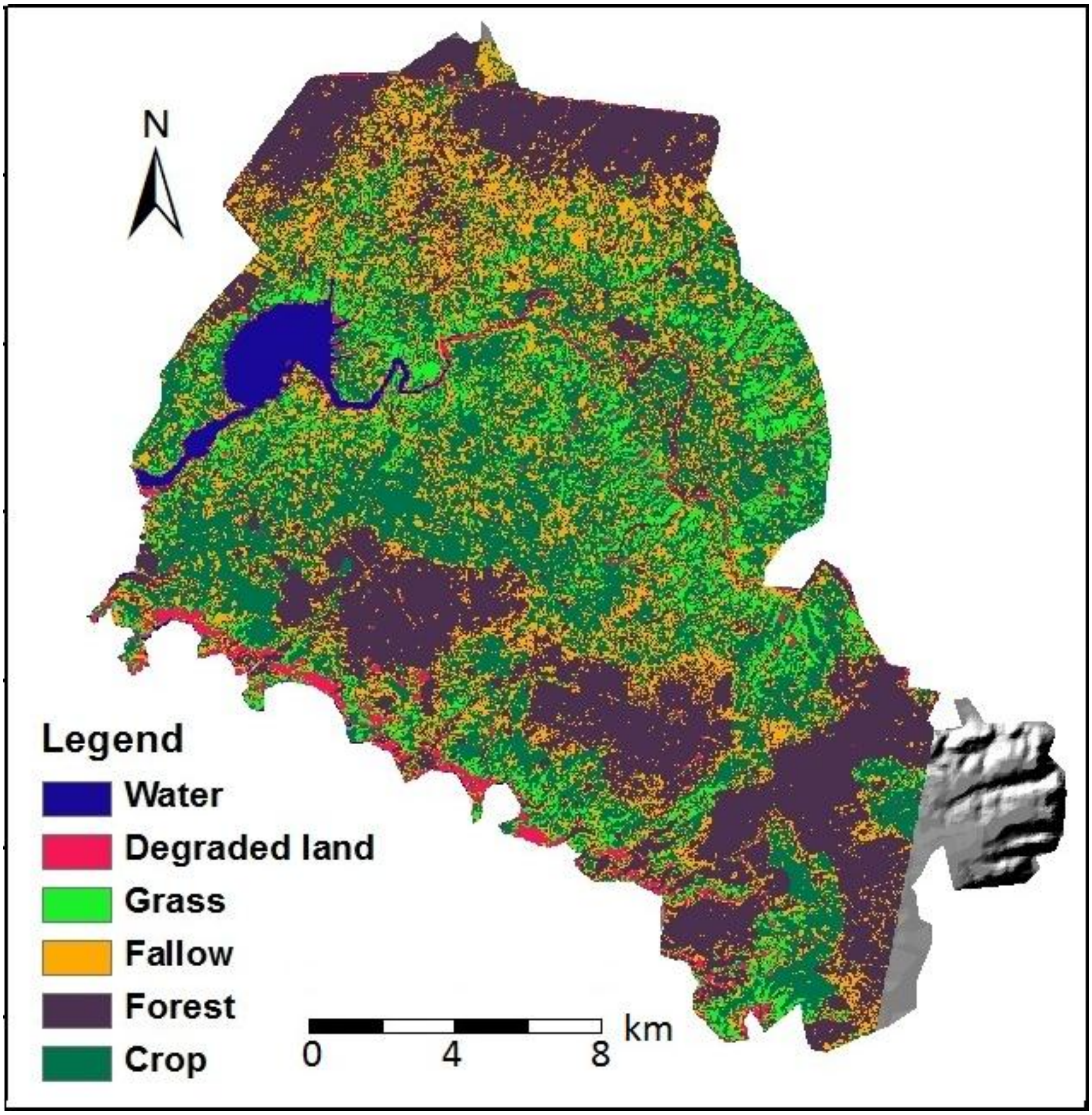

Figure 28 Land cover map of Sehoul area

In Sehoul area, forest covers 117.5km^2 area and it accounts for 31.8% of the total area. The grass, fallow and agricultural classes cover 75.1, 76.1 and 80.2km^2 areas respectively. The area that belongs to water class is 8.5 km^2, for degraded class is 12.2km^2.

Table 17 Area (km^2) for each land cover class

	Water	Degraded land	Grass	Fallow	Forest	Agriculture
area, km^2	8.5	12.2	75.1	76.1	117.5	80.2
Percentage, %	2.3	3.3	20.3	20.6	31.8	22.7

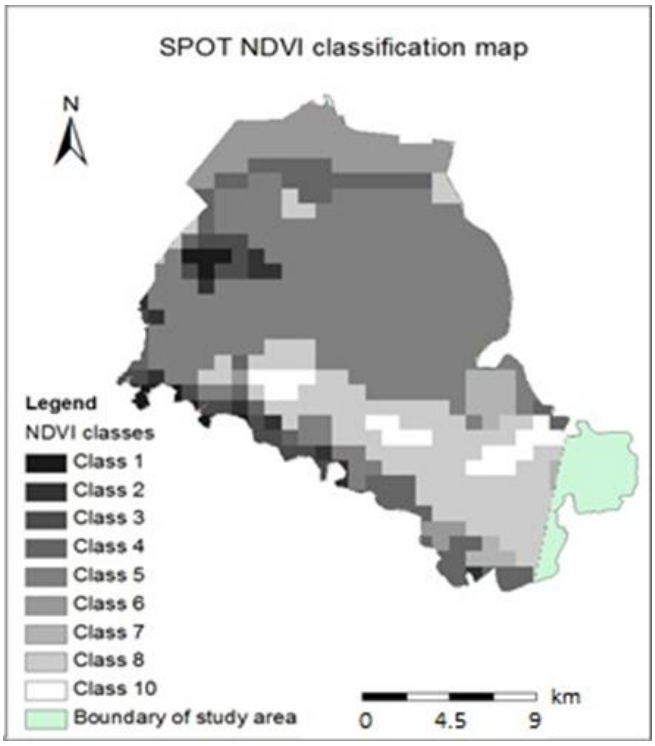

The NDVI classification map was generated based on NDVI time series images that includes only rainy season period and shown in Figure 29. The classification was done for 10 classes since average of best minimum separability of classification is 552 and minimum is 163.

Figure 29 NDVI classification map

The statistics corresponding to NDVI classes are shown in Table 18. The minimum (0.22) of mean is for class 1, vice versa (0.58) for class 10. The class with smallest (0.27) variance is class 1; the class 9 has the highest variance (0.60).

Table 18 Statistics corresponding for NDVI classes

NDVI	NDVI classes									
	1	2	3	4	5	6	7	8	9	10
minimum	0.11	0.18	0.20	0.23	0.18	0.30	0.18	0.24	0.19	0.34
maximum	0.38	0.68	0.57	0.67	0.71	0.64	0.74	0.73	0.79	0.72
variance	**0.27**	**0.50**	**0.38**	**0.44**	**0.53**	**0.34**	**0.55**	**0.49**	**0.60**	**0.38**
mean	**0.22**	**0.40**	**0.36**	**0.46**	**0.46**	**0.50**	**0.47**	**0.52**	**0.52**	**0.58**

As shown in Table 19, NDVI classes of 1,3, and 4 lie in water class of land cover. The Degraded class has 2 NDVI classes (1 and 3). Grass includes NDVI classes 5 and 7. Fallow includes 4-6 and 8 NDVI classes; Agriculture has classes 5 and 8. Degraded land class correspons to lowest variance and mean of NDVI, wheres the highest variance is for Grass (0.54) and the highest mean (0.53) of NDVI is for Forest.

Table 19 Aggregation of NDVI statistics for land cover classes

Average for land cover classes	Water			Degraded land		Grass		Fallow				Forest			Agriculture	
	1	3	4	1	3	5	7	4	5	6	8	6	8	10	5	8
Variance	0.36			0.32		0.54		0.45				0.40			0.51	
Mean	0.34			0.29		0.47		0.48				0.53			0.49	

4.3.2. Discussion

According to the result obtained the analysis done for land cover classes, the class of grass shows the highest variance (0.54) in NDVI values. This result is not in agreement with findings from other literatures (Liu, et al., 2010). This might be caused by the heterogeneity in landcover map (except forest) compared to NDVI class map. No another certain reason has not given to this fact. Also agriculture class shows higher variance (0.51). This might result from droughts; also possible caused by the difference between higher NDVI values when crop reaches its maximum stage and lower NDVI values when suddent drops occur after harvesting. Finally, forest displays the highest value of mean NDVI. This result is consistent with the statements by Liu (2010).

4.4. Drought assessment based on both vegetation and rainfall data

4.4.1. The relationship between NDVI and rainfall over Sehoul area

First, the relationship between 10-NDVI and 10-day rainfall is investigated by implying varies time lags and its rainfall sum with different preceding days (in section 4.3.1). The correlation maps for 50 combinations are shown in Figure 30.

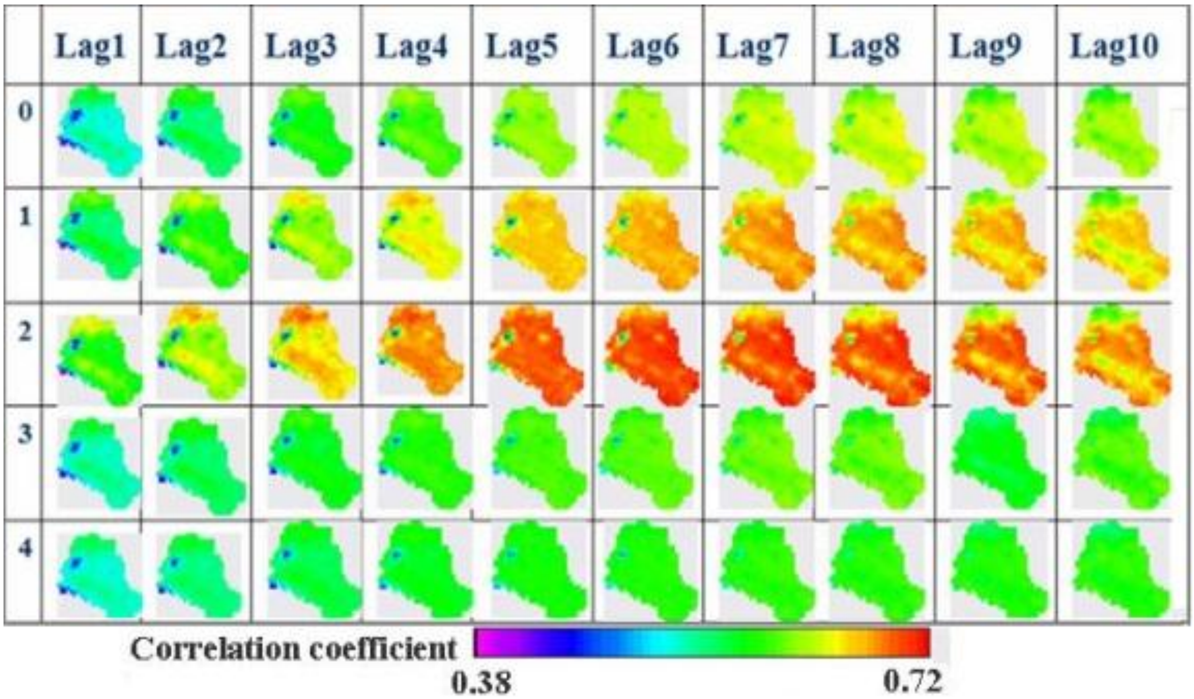

Figure 30 Correlation maps between 10-NDVI and 10-day rainfall with lags and their sum with preceding 10-days during rainy season for 60 combinations. The numbers in 1st column indicate the number of preceding 10-days.

The correlation maps are averaged over the whole study area and these results are shown in Table 20. All the maps and correlation coefficients in 3rd row (preceding two 10-days) show higher correlation compared to others. The highest correlation (0.625) between 10-day NDVI and 10-day rainfall is found for the combination of time lag of 6 (1 month and 20 days) and its sum with two preceding 10-days. This result is supported by the findings from other papers (Propastin, et al., 2007).

Table 20 Correlation coefficients averaged by the entire study area, corresponding to correlation maps in Figure 30

Preceding 10-days	lag1	lag2	lag3	lag4	lag5	lag6	lag7	lag8	lag9	lag10	Mean
0	0.110	0.191	0.271	0.328	0.385	0.418	0.431	0.438	0.417	0.399	**0.339**
1	0.202	0.306	0.393	0.462	0.514	0.539	0.550	0.542	0.520	0.490	**0.452**
2	**0.301**	**0.408**	**0.500**	**0.563**	**0.606**	**0.625**	**0.619**	**0.608**	**0.579**	**0.537**	**0.535**
3	0.132	0.199	0.252	0.295	0.325	0.341	0.357	0.352	0.335	0.327	**0.291**
4	0.112	0.168	0.213	0.248	0.276	0.293	0.305	0.299	0.290	0.293	**0.250**
5	0.098	0.147	0.186	0.218	0.244	0.259	0.269	0.267	0.267	0.269	**0.222**
6	0.088	0.131	0.167	0.197	0.221	0.234	0.246	0.250	0.250	0.257	**0.204**
7	0.080	0.120	0.154	0.181	0.203	0.217	0.233	0.238	0.241	0.250	**0.192**
Mean	**0.140**	**0.209**	**0.267**	**0.312**	**0.347**	**0.366**	**0.376**	**0.374**	**0.362**	**0.353**	**0.311**

According to Figure 31, there is a sharp increasing trend in average correlation between 10-day rainfall and 10-day NDVI up to 2 preceding 10-days for all lags, while the correlations are decreased consistently for the remaining preceding 10-days.

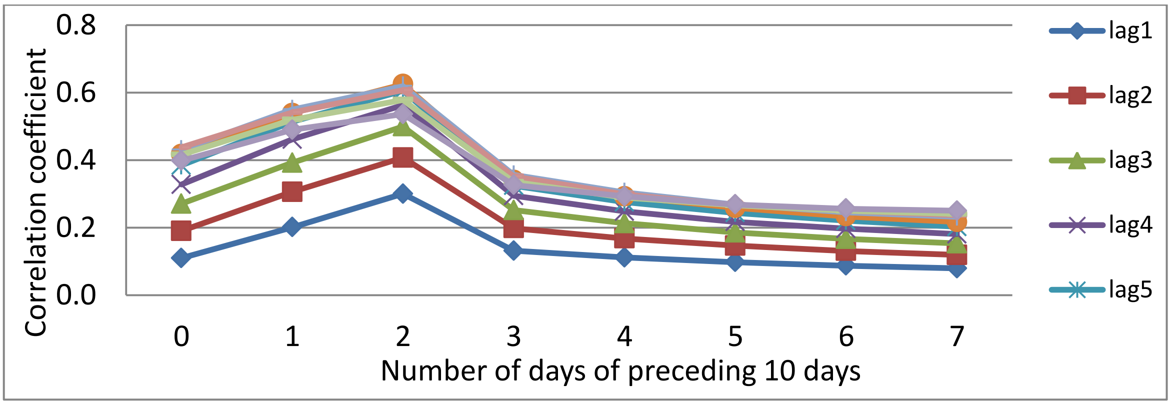

Figure 31 Correlation coefficient between of 10-day NDVI and 10-day rainfall with lags and their sum with preceding 10-days.

The relationship of the average NDVI to the average rainfall and SPI during rainy season

The 6-month SPI for March is selected in this section since its computation is based on sum of rainfall between October and March that corresponds to rainy season in Sehoul area. There is a strong relation (r^2=0.993) between SPI and rainfall. Approximately 48.0% of variance in NDVI can be explained by both SPI and rainfall during rainy season (Figure 32).

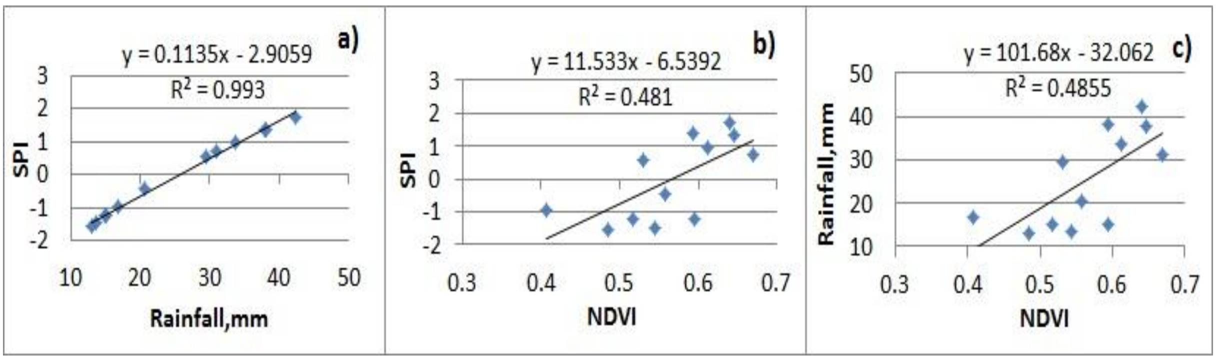

Figure 32 The 6-month SPI for March compared with averages of 10-day rainfall and NDVI during rainy. a) SPI and Rainfall, b) SPI and NDVI c) rainfall and DVI

4.4.2. The effect of amount and timing of rainfall on vegetation and Discussion

In this part, analysis was done for the rainy season of 1998-2009 periods in which both NDVI and rainfall data are available. Further, the results of rainfall analysis (section 3.1.1 and 3.1.2) and DSI maps generated in section 4.3.1 were used. DSI maps were averaged by the study area. Anomalies of these spatially averaged DSI values and the corresponding anomalies of total rainfall during rainy season are plotted against the years (Figure 33).

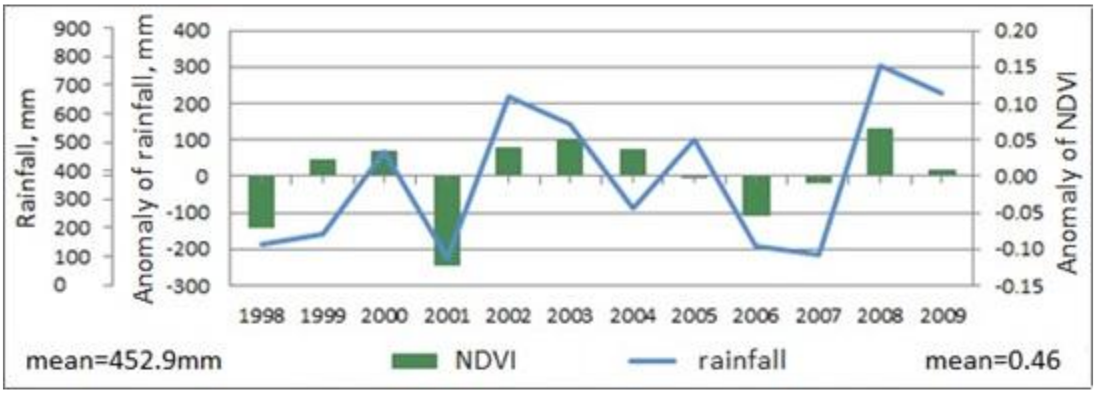

Figure 33 Anomalies of the spatially averaged NDVI and total rainfall during rainy season (1998-2009)

Based on the both anomalies of vegetation and rainfall, the years (1998-2009) can split into four categories: *Higher_Rainfall and Higher_Vegetation (HH), Higher_Rainfall and lower_Vegetation (HL), lower_Rainfall and higher_Vegetation (LH), lower_Rainfall and lower_Vegetation (LL)*. For each category, the corresponding the total rainfall (in mm) during the whole rainy season with its anomaly and the average fraction of rainfall in first part of rainy season period (Oct-Dec) in percentage (%) are shown; Also spatially averaged NDVI values that is also temporally averaged for rainy season and their anomalies (Table 21).

There are 4 years (1998, 2001, 2006 and 2007) in which both vegetation and rainfall are lower than normal condition (LL). In contrary, the years of 2000, 2002, 2003 and 2008 are the years in which both vegetation and rainfall are higher than normal condition (HH) (Table 21).

Table 21 Four categories of years according to anomalies of rainfall and NDVI. For each category, the corresponding the total rainfall (in mm) with its anomaly during the whole rainy season (Oct-Mar) and the average fraction of rainfall in first part of rainy period (Oct-Dec) in percentage (%); Also spatially averaged NDVI values that is also temporally averaged for rainy season and their anomalies.

<table>
<tr><td colspan="2" rowspan="2"></td><td colspan="2">The average NDVI (V)</td></tr>
<tr><td>Higher than normal</td><td>Lower than normal</td></tr>
<tr><td rowspan="2">Total rainfall (R)</td><td>Higher than normal</td><td>HH:
2000 R:529.0mm/ + 76.4, 47.9%; V:0.49/+0.03
2002 R:680.9mm/+228.3, 69.0%; V:0.50/+0.04
2003 R:605.3mm/+152.7, 52.9%; V:0.51/+0.05
2008 R:762.8mm/+310.2, 48.0%; V:0.52/+0.07</td><td>HL:
2005 R:558.9mm/+106.3, 39.5%;V: 0.46/+0.00
2009 R:687.4mm/+234.8, 22.1%;V:0.47/ +0.01</td></tr>
<tr><td>Lower than normal</td><td>LH:
1999 R:301.6mm/-151.0, 72.3%; V:0.48/+0.02
2004 R:370.7mm/ - 81.9, 48.7%; V:0.50/+0.04</td><td>LL:
1998 R:272.6mm/-180.0, 19.6%; V:0.39/-0.07
2001 R:234.5mm/-218.1, 39.7%; V:0.34/-0.12
2006 R:270.3mm/-182.3, 35.8%; V:0.41/-0.05
2007 R:244.3mm/-208.3, 50.8%; V:0.45/-0.01</td></tr>
</table>

In 1999 and 2004, even if the total rainfall during the entire rainy season is quite low (301.6-370.7mm), the vegetation condition is good (LH) in terms of anomaly of DSI values (0.48/+0.02 in 1999; 0.50/+0.04 in

2004). If we look at the timing of rainfall events during rainy season in these years, most rainfall (48.7-72.3%) fell in first part of rainy period. This might lead to a good vegetation condition. The opposite situation can be seen in 2005 and 2009 (HL). In these years, the rainfall is quite high (558.9mm/+106.3mm; 687.4mm/+234.8mm), but vegetation condition is just near to or a slight higher than normal because relatively less rainfall (22.1-39.5%) fell in first part of growing season (Table 21).

Further, in 2007 the vegetation condition could have been worse because of the extreme low rainfall (244.3mm/-208.3) almost close to 2001 (234.5mm/-218.3) that is an example of extreme case; but the average NDVI is a slight lower than the long-term mean (0.45-0.01). In 2007, there are no longer dry spells and alternately sunny and rainy periods (see Appendix 3). This situation might influence positively growing vegetation.

In contrary, in 2002, the vegetation condition could have been better than 2003 because of higher rainfall (680.9mm/+228.3) compared to 2003 (605.3mm/+152.7) (Table 21). However, it is opposite; vegetation condition is not better (0.50/+0.04) in 2002 than 2003 (0.51/+0.05). The year 2002 is the year with the most frequent rainfall events (7 times) for the range R≥30mm that fell in first part of growing period (see Appendix 3). These heavy rainfalls account for 50.3% of the total rainfall during rainy season; however, less efficient on vegetation growing. Also the number of heavy rainfall is 6 in 2005; three of them fell in first part rainy period (see Appendix 3). In this year vegetation condition is in normal condition (0.46/0.00) even if the total rainfall is higher (558.9mm) than its long-term mean (452.9mm).

Based on the analysis of vegetation response to rainfall done for the period of 1998-2010, vegetative drought years over the period 1951-1997 in which SPOT NDVI data is not available were determined considering three conditions: a) total rainfall for rainy season is two times less than its long term mean 452.6 or b) the average fraction of rainfall for Oct-Dec is two time less than long term mean 0.41 or c) the both are less than their long term mean. Under this consideration, totally 20 years in which vegetation is in drought condition found while there are 27 dry years according to anomaly of annual rainfall. Among them, 15 years are coincidence with dry years defined by annual precipitation anomaly. There are 5 years (1953, 1954, 1958, 1983, 1995) in drought condition if the average fraction of rainfall is considered while these years are normal years according to anomaly of annual rainfall. In contrary, the years 1959, 1984, 1989, 1997, 2004 and 2007 reveal non-drought years according to three conditions used whereas these years have minus anomaly of annual rainfall (Appendix 8). Among the constructed droughts, 8 droughts are coincided with the historical droughts found from literature that occurred over the period of 1951-2003 in Sehoul area.

4.4.3. The evaluation of accuracy of derived metrics

A method to examine vegetation dynamics' response to variability in precipitation is the vegetation phenological approach. Vegetation dynamics are assessed based on phenological metrics. These metrics were computed using the methods described in section 3.4.3. The accuracy of computed metrics should be assessed.

Examination of accuracy of computed metrics

Before the computed phenological metrics are used for further analysis, the evaluation whether they are properly calculated is necessary. The following investigation was done for every pixel in each year.

- ***check values***: NDVI value of MaxV should be higher than both NDVI values of onset (OnV) and end of vegetation (EndV).
- ***check dates***: The date of maximum value of NDVI (MaxP) of greenness should be later than the date of onset of vegetation (OnP) and earlier than the date of end of greenness (EndP).

The checking result for greenness period of 1998-1999 is shown in Figure 34 as an example. The percentages of the pixels with error in date and value are 2.6% and 1.9% (red pixels compared with total study area) respectively in greenness period of 1998-1999. The most remaining years (not shown here) also have no error and some has error no more than 1.5%.

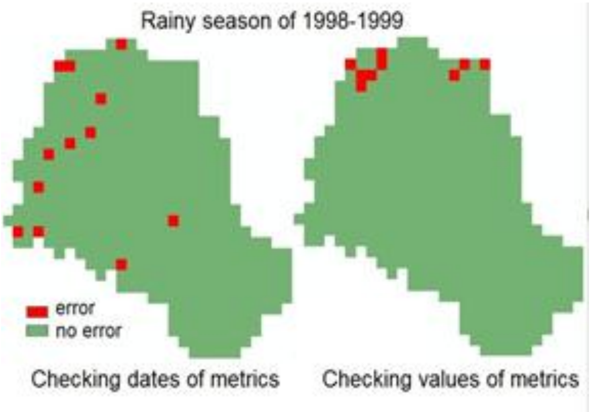

Figure 34 Results of checking the dates and values of main metrics. Red color indicates incorrect of calculation and green refers to correct results.

Also the evaluation was done spatially aggregating by the entire study area for each year and plotted against years, 1998-2009 (Figure 35). According to the plot presented in Figure 35 a)**,** the dates of OnV (blue bar) are earlier than both dates of MaxV (red bar) and EndV (green bar) for all year and vice versa for the dates of EndV. In Figure 35 b), the MaxV values are higher than both the values of OnV and EndV for all year. Thus, it can be viewed that the derived phenological metrics were calculated properly. The pixels with error in both values and dates of metrics are excluded for further analysis.

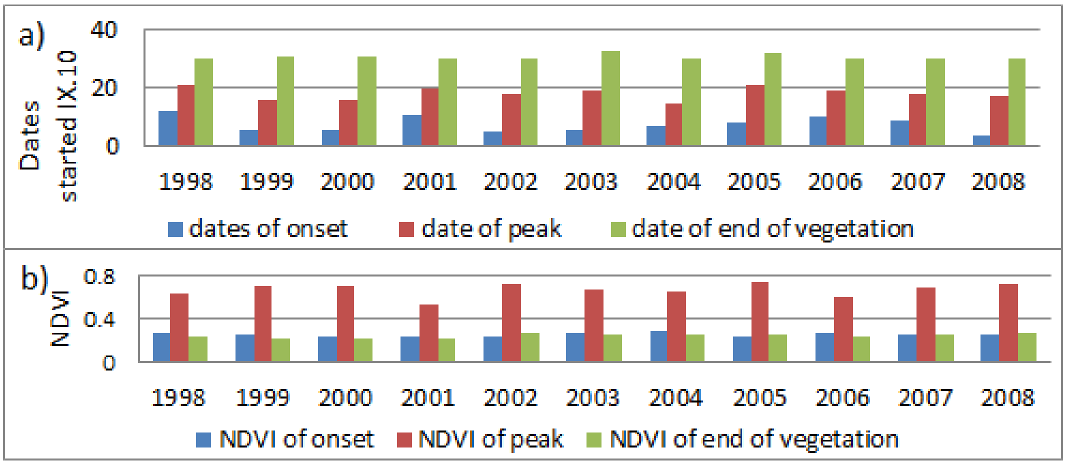

Figure 35 Date and average NDVI value of onset, peak and end of vegetation growing, 1998-2008

Validation of computed onset of greenness

The phenological parameters derived from NDVI time series are usually compared with in-situ phenological records from ground stations (Delbart 2005). However, this kind of data was not available for this research. Thus, as a key metric, the date of onset was validated with the total rainfall in first part of rainy period based on the assumption; the delayed rainfall should result in less amount of rainfall during that period. The period between October and December is considered as first part of rainy season.

The correlation coefficient between dates of onset and the total rainfall for Oct-Dec is -0.84, showing a good agreement with the assumption above. For instance, the delay in onset of vegetation in 1998 and 2001 corresponds to less amount of rainfall in first part of rainy season in those years (Figure 36).

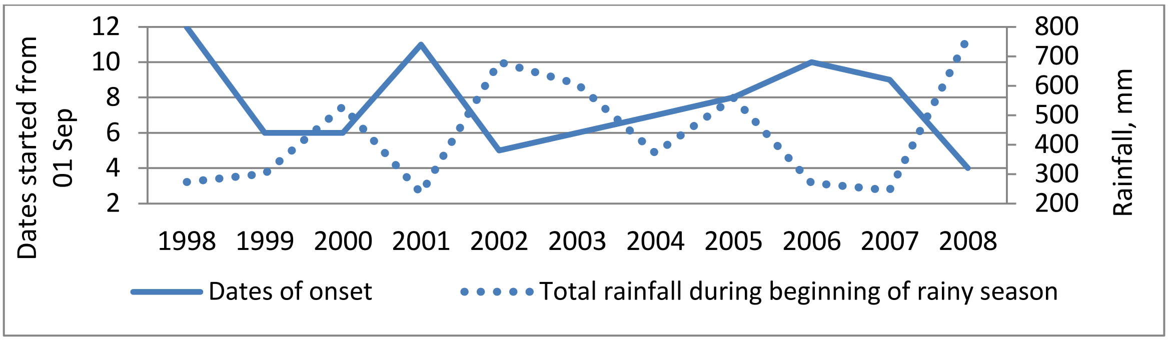

Figure 36 Onset of vegetation growth compared with the total rainfall fell in first part of rainy period (Oct-Dec).

4.4.4. The vegetation dynamics' response to rainfall and Discussion

Totally nine phenological metrics were calculated for every pixel (Table 22). Those metrics were spatially averaged over study area and correlated with the total rainfall for entire and first part of rainy season as well as the average fraction of rainfall in first past of rainy season obtained from rainfall analysis in section 4.1.1. There is a good negative correlation (-0.84) between OnP and the total rainfall at beginning of rainy season, suggesting that onset of greenness (OnP) can be earlier if enough rains fall at the beginning of rainy season. This then leads to a good vegetation condition, showing higher positive correlation (0.88) with TINDV (Table 22).

Table 22 The correlation of the derived metrics with the amount of rainfall for different periods

Total rainfall in mm	The derived metrics								
	OnP	OnV	EndP	EndV	MaxP	MaxV	RanV	DurP	TINDVI
whole rainy season	-0.75	-0.37	0.52	**0.66**	-0.08	0.69	0.62	0.79	0.87
Beginning of rainy season	**-0.84**	-0.42	0.52	0.53	-0.31	0.61	0.57	0.87	**0.88**
Rainfall fraction of rainfall for Oct-Dec	-0.76	-0.52	0.27	0.06	**-0.67**	0.48	0.56	0.68	0.59

Further, there is also a good negative correlation (-0.67) between the average fraction of rainfall in first part of rainy period and the dates of maximum NDVI values (MaxP). The rainfall events that fall unevenly through that period can result in the delay in occurrence of maximum vegetation (MaxP).

The derived phenological metrics were also compared with onset and length of rainfall (Table 23) determined by the methods of Stern (1982) and Odekunle (2006) in section 4.1.3. As seen in Table 23, the correlation of the metrics is stronger with onset and length defined by Stern's method than that by Odekunle's method. The correlation between onset of rainy period defined by Stern method and OnP is 0.49 (for Odekunle is 0.30), suggesting that the earlier onset of rainy period causes the earlier of onset of vegetation growth. Also the early onset of rainy period can lead to higher TINDVI (R^2=-0.53). In addition, there are good correlations of length of rainy season defined by Stern with MaxV (0.63) and RanV (0.68). Those metrics can be higher when the length of rainy period is longer. However, there is not a good correlation (0.37) between the length of rainy period and the duration of greenness (DurP). Also the correlation between onset of rainy period and MaxP is just 0.38.

Table 23 Correlation of the derived metrics with the onset and length of rainy period

Total rainfall in mm	The derived metrics								
	OnP	OnV	EndP	EndV	MaxP	MaxV	RanV	DurP	TINDVI
Onset defined by Stern	**0.49**	0.22	-0.47	-0.21	**0.38**	-0.40	-0.39	-0.56	**-0.53**
Length of rainy period by Stern	-0.31	-0.42	0.34	0.29	-0.02	**0.63**	**0.68**	**0.37**	0.42
Onset defined by Odekunle	0.30	0.22	-0.22	0.13	0.21	0.06	0.00	-0.32	-0.24
Length of rainy period by Odekunle	-0.15	-0.52	0.49	-0.25	-0.15	-0.10	0.00	0.32	0.18

In Figure 37, the inter-annual variability of the main derived metrics (Figure 37 a) is compared with the amount of rainfalls for different periods between the years, 1998-2009 (Figure 37 b).

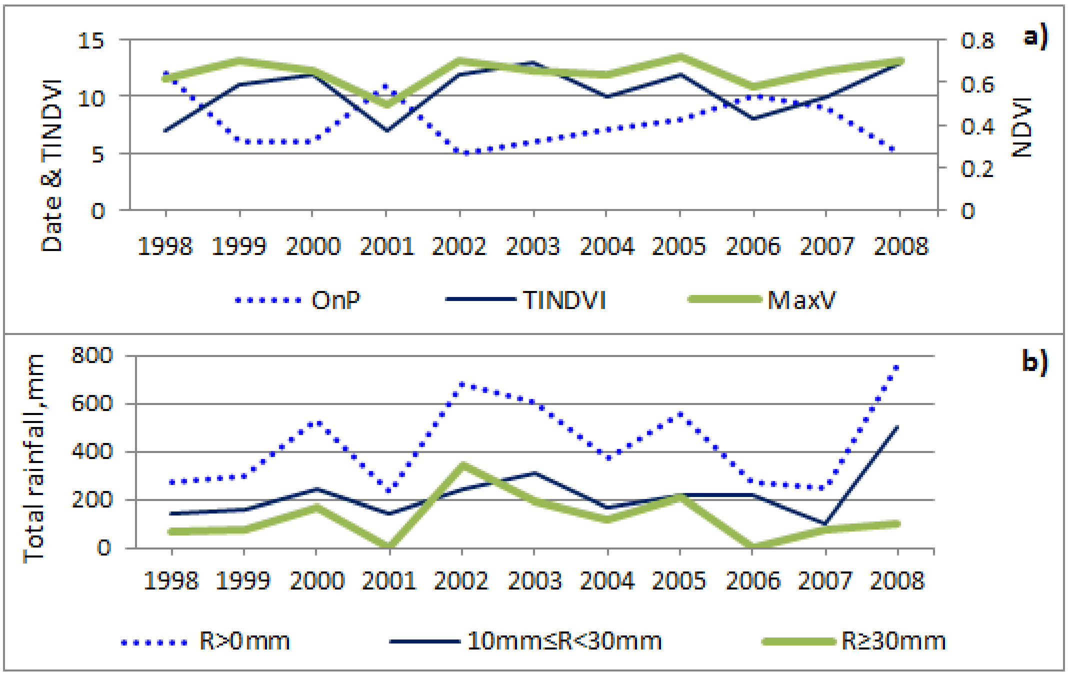

Figure 37 Main derived metrics compared with the total amount of rainfall for different ranges

There are six significant peaks (1999, 2000, 2002, 2003, 2005 and 2008) in TINDVI (thin solid line). Those peaks correspond to the peaks in the total rainfall for the 10mm≤R<30mm range, except for 1999 and 2002. According to the previous result in section 4.1.1, even if the total rainfall during rainy period is quite low (301.6mm) in 1999, most rains (72.3%) fell in first part of rainy period. That might result in higher TINDVI in 1999. In 2002, a significant peak can be seen in the total amount of rainfall for the R≥30mm range (thick yellow line) for 2002 (Figure 37 b). This peak must be result in the relatively less TINDV in 2002, demonstrating that the extreme rainfall events with rainfall amount ≥30mm is less efficient on vegetation growing. Also among the peaks in TINDVI, the peak in 2003 is quite higher (13) that is equal to the peak in 2008 while the total rainfall in 2003 (605.3mm) is less than that in 2008 (762.8mm). This peak can be explained by the corresponding peak in the amount of rainfall for the 10mm≤R<30mm range in 2003 (Figure 37 b).

In addition, there are three peaks in OnP (delay in greenness) for 1998, 2001 and 2006, leading to a sharp drop in both TINDVI and MaxV. As studied in section 4.1.1, in these years, the total rainfall for the whole rainy period (Oct-Mar) and the average fraction of rainfall in first part of rainy season (Oct-Dec) are both quite low. This situation could result in the worse vegetation condition in these yeas.

The last interesting finding from Figure 37 a) is that TINDVI dropped in 2004 while MaxV is enough higher. If we look at timing of daily rainfall in 2004, there is long dry spells that started on 30 Dec, lasting for 27 days (see Appendix 3). This might cause the decrease in TINDVI for 2004. Also even if in 2006, there is no extreme rainfall with rainfall amount ≥30mm and the total amount of rainfall for the 10mm≤R<30mm range that accounts for 79.6% of the total rainfall during rainy season, the TINDVI is relatively less (8). The dry spells lasted from 9 Dec 2005 until 21 January 2006 should have contributed to this less TINDVI.

4.5. Human-induced land degradation in Sehoul area

The first step to detect human-induced loss of vegetation cover was to establish the relationship between rainfall variations and vegetation, using least square regression analyses for every pixel. The statistics for R squared of the predicted NDVI by rainfall is shown in Table 24. The mean R squared of the predicted NDVI by rainfall over the study area is 0.4026. However, minimum R squared is 0.000212.

Table 24 Summary statistics for R squared of NDVI predicted by rainfall

	Min.	1st Qu.	Median	Mean	3rd Qu.	Max.
R squared	0.000212	0.372600	0.433500	0.402600	0.471900	0.564300

So the pixels with low R squared should be eliminated from the further analysis. R squared of 0.10 (0.26045) was used as the threshold since only 10 per cent of variance in the predicted NDVI is explained by rainfall.

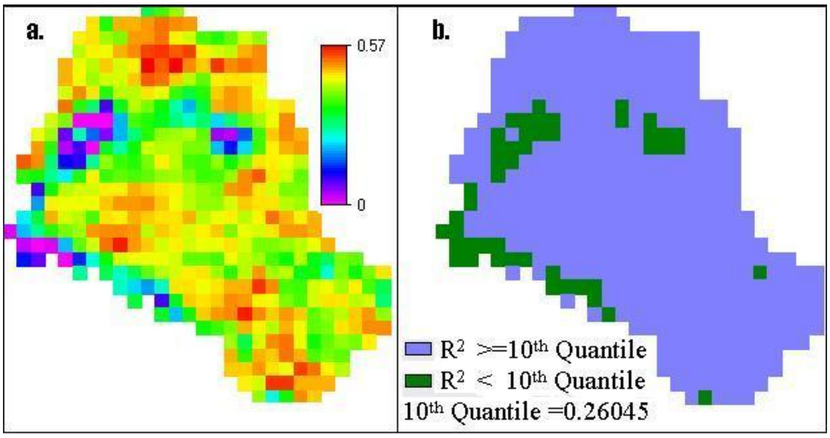

Figure 38 a) R squared of the NDVI predicted by rainfall, b) The illustration of the pixels with R squared less than 10th Percentile.

The pixels with R squared less than the threshold were identified. Most of those pixels are the water body or the edge pixels of water bodies (Figure 38 b).

In Table 25, the statistic of slope of residuals between predicted and original NDVI values is shown. Here, not only the pixels with R squared less than its 10th Percentile, but also the pixels with slope that is higher or equal to zero were also excluded. The remaining pixels were used for the classification procedures.

Table 25 Summary statistics for slope of residual between predicted and original NDVI

	Min.	1st Qu.	Median	Mean	3rd Qu.	Max.
R squared	-6.00E-03	-1.89E-03	-1.10E-03	-1.35E-03	-5.35E-04	-1.41E-05

The final map was classified into high, moderate and low classes using Natural Breaks (Kenks) method in ArcMap 10 and shown in (Figure 39). The area which lies in high degradation class is 26.7km² (6.5%); for moderate and low classes, areas are 69.2 km² (16.9%) and 96.8 km² (23.6%), respectivily. The total degradation area is 47.0% (Table 26).

Table 26 Area (km²) for each degradation class

Class	High	Moderate	Low	Total
Area (km^2)	26.7	69.2	96.8	192.7
Percent (%)	6.5	16.9	23.6	47.0

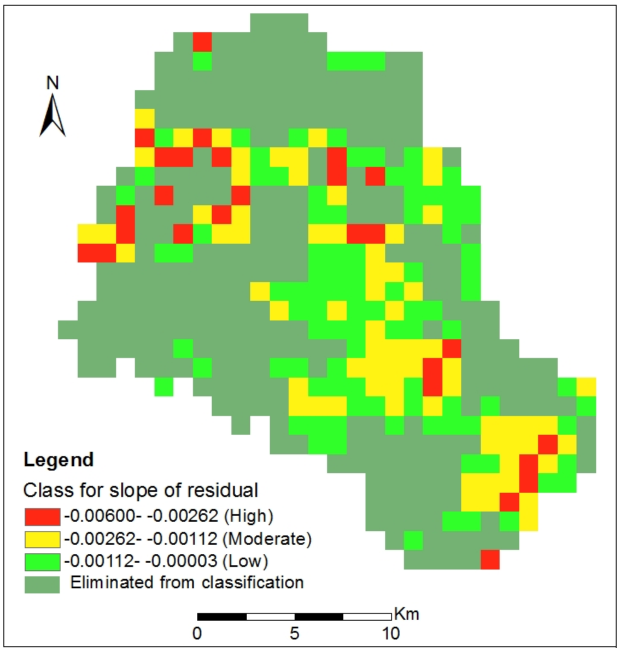

The remaining areas belong to the pixels at which the trend of residuals is positive (no degradation) or R squared of regression line between NDVI and rainfall is less than its 10th Percentile (the construction of the relationship between NDVI and rainfall is not sufficient).

Figure 39 The areas affected by human-induced land degradation

4.5.1. Discussion

There are four points to discuss the methods used (in section 3.5) and the result obtained from section 4.5. First, RESTREND method can only detect on-going degradation; does not identify already degraded areas (e.g., occurring in the past century) since slope of regression line does not reveal minus. That is why the most pixels over eastern edges of Sehoul area in which most gullies lie do not belong to any of degradation class. Second, the trend of linear regression was not tested whether it is statistically significant or not since the issue to do significance test at 465 pixels simultaneously has not been be solved during this MSc research. Finally, due to lack of data, the important driving factors of human-induced land degradation such as number of livestock and route system were not considered.

5. CONCLUSION AND RECOMMENDATION

5.1. Conclusion

The main conclusions are summarized here by answering the research questions.

Q1: Are there any increasing trend in the amount of extreme rainfall and number of extreme rainy days over time?

The first extreme index used for extreme rainfall analysis is annual total precipitation when daily precipitation > 95th percentile (10.1mm). Its long term mean is 383.5mm. The minimum is 110.9mm in 1994 and the maximum is 673.2mm in 1968. The second index is number of days with precipitation ≥ 10mm and its long term mean is 18.3 days. The minimum is 7 days occurred in 1994 and the maximum is 32 in 2008. The third index is number of days with precipitation ≥ 30mm and its long term mean is 2.9 days and the maximum number, 9 days is in 1995. None of these indices displayed statistically significant trend over time. So the hypothesis 1 (H1) (in section 1.4) is rejected.

Q2: Are drought characteristics (duration, magnitude and intensity) increasing over time?

The duration and the magnitude of historical droughts have an increasing trend over the period of years 1951-2009. Slope of regression line are 0.2932 and 0.3651 for drought duration and magnitude, respectively. However, there is not significant trend in drought intensity. Thus the hypothesis 2 (H2) (in section 1.4) is generally proved.

Q3: What are the return periods and the probability of severe droughts with different duration and magnitude in this area?

Drought Severity-Duration-Frequency (SDF) curves constructed for Sehoul area reveals that bi-variate return period increases with the increase in drought duration and magnitude. Among the historical droughts observed during the period of year 1951-2009, the drought with magnitude 32.9 that started in December 1993 and lasted for 25 months has the longest return period, 237.7 years. The next is the drought with magnitude 20.1 and duration 17 months occurred in 1998-1999 that reveals the return period of 15.7 years. The drought occurred in 1980-1982 (magnitude 17.6 and duration 17 months) and 2006-2008 (magnitude 17.3 and duration 22 months) have 8.9 and 9.0 years return periods. Another better index that is computed at least on monthly scale should have been employed to assess temporal occurrence of drought as SPI might be not accurate for this region.

Q4: *Which part of this area is most prone to drought?*

According to pixel based analysis, 93.6 km² (22.6%) of the total area (approxi. 397 km²) of Sehoul is highly susceptible to droughts. The moderate and low susceptibility class covers the areas 200.5 km² (48.4%) and 120.3 km² (29.0%), respectivily. In addition, the result obtained the analysis done for land cover classes reveal that the land cover class of degraded land shows the lowest variance (0.32) and the smallest mean value (0.29) of NDVI over the period of year 1951-2009. In contrary, grass class shows the highest variance (0.54) in NDVI values. However, this result is not in agreement with findings from other literatures (Liu, et al., 2010). A certain reason has not given to this fact. Also agriculture class shows higher variance (0.51). This might be resulted from droughts or from havestting effect which causes the difference between higher NDVI values when crop reaches its maximum stage and lower NDVI values when suddent drops occur after harvesting. Finally, forest displays the highest value of mean NDVI. This result is consistent with the statements by Liu (2010).

Q5: Can the change in vegetation cover over time (intra and inter-annual) be explained by precipitation?

In Sehoul, the highest correlation (0.625) between 10-day NDVI and 10-day rainfall during rainy season is found implying the time lag of 6 (1 month and 20 days) and it' sum with two preceding 10-days. This result is supported by the findings from other papers (Propastin, et al., 2007). Approximately 48.0% variance in NDVI can be explained by both SPI and rainfall during rainy season.

Furthermore, it can be concluded that vegetative drought can be severe if the average fraction in first part of rainy season (Oct-Dec) is less than its long term mean 0.41 when the total rainfall during the whole rainy season is also less than its long term mean 452.6mm except for frequent extreme or unevenly distributed rainfall events over time.

Rainfall efficiency is dependence on two factors; unevenly distributed rainfall events in rainy season period and frequent extreme rainfall events, particularly that fall in first part of rainy season. The rainfall events that fall in first part of rainy season are more efficient on vegetation growing than the rainfall events that fall in the second part. Also rainfall events that are evenly distributed through time (alternately sunny and rainy periods) are more efficient than rainfall events with more frequent occurrence in a certain period. In addition, the frequent extreme rainfall events have less positive influence on growing vegetation.

As a key phenological metric, date of NDVI (OnP) for vegetation onset is more dependence on the total amount of rainfall during first part of rainy season, resulting a less time integrated NDVI (TINDVI). Date of maximum NDVI (MaxP) is more influenced by the average fraction of rainfall amount that falls in first part of rainy season. However, the longer dry spell (consistent more than 10 days without rainfall) occurred in first part of rainy period could cause a delay in MaxP, also leading to a less TNDVI. Moreover, TINDVI decreases with the increase in number of extreme rainfall events.

Under the consideration of these results, the hypothesis 5 is generally proved (accepted).

Q6: How large area is affected by human-induced land degradation.

26.7km² (6.5%) of Sehoul area lies in high degradation class; for moderate and low classes, areas are 69.2 km² (16.9%) and 96.8 km² (23.6%), respectivily. The total degradation area is 192.7 km² (47.0%).

5.2. Limitation of this research

- The main limitation of this study is data availability. Climatic driving factors of drought such as temperature, evapotranspiration; also other factors such as soil type were not available.
- In-situ phenological records from ground stations were not available for validation of computed metrics.
- We determined the areas affected by land degradation. However, the driving factors such as number of livestock and route system were not investigated due to data absence.

5.3. Recommendation

- Apart from rainfall, another driving factors such as temperature, evapotranspiration and as well as soil type should be used.
- An appropriate index should be used to identify the characteristics of historic droughts that is computed at least on monthly basis.
- Land degradation methods gave limited results, and could be substituted by other methods or calibrated to get better results based on the available data.
- Local decision makers should rely on not only the amount of rainfall (e.g, annual total rainfall) but also consider timing of rainfall to make a decision. Also the return period of historical droughts obtained from this research could be taken into account when making policies.
- The average of fraction of rainfall for Oct-Dec that is less than 0.41 could lead to worse vegetation condition.

LIST OF REFERENCES

Amin, M. O., Jan, A., Mehrdad, R., Ali, M., & Reza, A. S. (2011). A statistical analysis of the relationship between climatic factors and the Normalized Difference Vegetation Index in China. *Journal of Water Resource and protection, 3*, 325-334.

Bai, Z. G., Dent, D. L., Olsson, L., & Schaepman, M. E. (2008). Proxy global assessment of land degradation. *Soil Use and Management, 24*(3), 223-234.

Beurs, K. M., & Henebry, G. M. (2010). Spatio-Temporal Statistical Methods for Modelling Land Surface Phenology

Phenological Research. In I. L. Hudson & M. R. Keatley (Eds.), (pp. 177-208): Springer Netherlands.

Bonaccorso, B., Cancelliere, A., & Rossi, G. (2003). An analytical formulation of return period of drought severity. *Stochastic Environmental Research and Risk Assessment, 17*(3), 157-174.

Bordi, I., Frigio, S., Parenti, P., Speranza, A., & Sutera, A. (2001). *The analysis of the Standardized Precipitation Index in the Mediterranean area: regional patterns* (Vol. 44).

Bryhn, A. C., & Dimberg, P. H. (2011). An Operational Definition of a Statistically Meaningful Trend. *PLoS ONE, 6*(4), e19241.

Cancelliere, A., & Salas, J. D. (2010). Drought probabilities and return period for annual streamflows series. *Journal of Hydrology, 391*(1-2), 77-89.

Caparrini, F., & Manzella, F. (2009). Hydrometeorological and vegetation indices for the drought monitoring system in Tuscany Region, Italy. *Adv. Geosci., 17*, 105-110.

Chbouki, N. (1992). *Spatio-temporal characteristics of drought as inferred from tree-ring data in Morocco.* Arizona.

Dai, A. (2011). Drought under global warming: a review. *Wiley Interdisciplinary Reviews: Climate Change, 2*(1), 45-65.

Delbart, N., Kergoat, L., Le Toan, T., Lhermitte, J., & Picard, G. (2005). Determination of phenological dates in boreal regions using normalized difference water index. *Remote Sensing of Environment, 97*(1), 26-38.

DESIRE. (2010). Marmora, Morocco. Retrieved 10 August, 2011, from http://www.desire-his.eu/en/marmora-morocco

Doukkali, M. R. (2005). Water institutional reforms in Morocco. *Water Policy, 7*, 71-88.

Dregne, H. E. (1986). *Desertification in arid lands*. Dordrecht, Holland: Kluwer Academic Publishers.

ETCCDMI. (2009). ETCCDI/CRD Climate Change Indices. Retrieved 15 August, 2011, from http://cccma.seos.uvic.ca/ETCCDMI/

Etkin, D. (1997). *Climate change and extreme events*. Toronto: Environmental Adaptation Research Group, University of Toronto.

Evans, J., & Geerken, R. (2004). Discrimination between climate and human-induced dryland degradation. *Journal of Arid Environments, 57*(4), 535-554.

FAO. (2004). Morocco. Retrieved August 2, 2011, from http://www.fao.org/ag/AGP/agpc/doc/Counprof/Morocco/Morocco.htm

FAO Regional Office for the Near East. (2008). *The Near East Drought Planning Manual: Guidelines for Drought Mitigation and Preparedness Planning*: FAO.

Frick, D. M., Bode, D., & Salas, J. D. (1990). Effect of drought on urban water supplies. I: Drought analysis. *J. Hydrologic Eng 116*, 733-753.

Gebrehiwot, T., van der Veen, A., & Maathuis, B. (2011). Spatial and temporal assessment of drought in the Northern highlands of Ethiopia. [Article]. *International Journal of Applied Earth Observation and Geoinformation, 13*(3), 309-321.

González, J., & Valdés, J. B. (2004). The mean frequency of recurrence of in-time-multidimensional events for drought analyses. *Nat. Hazards Earth Syst. Sci., 4*, 17-28.

Groten, S. M. E., & Ocatre, R. (2002). Monitoring the length of the growing season with NOAA. *International Journal of Remote Sensing, 23*(14), 2797-2815.

Guttman, N. B. (1998). COMPARING THE PALMER DROUGHT INDEX AND THE STANDARDIZED PRECIPITATION INDEX1. *JAWRA Journal of the American Water Resources Association, 34*(1), 113-121.

H¨opfner, C., & Scherer, D. (2011). Analysis of vegetation and land cover dynamics in north-western Morocco during the last decade using MODIS NDVI time series data. [Copernicus Publications]. *Biogeosciences, 8*(11), 3359-3373.

Hayes, M. J., & Wilhite, D. A. (2003). Drought Management. *Encyclopedia of Water Science*, 170 - 172.

He, B., Lu, A. F., Wu, J. J., Zhao, L., & Liu, M. (2011). Drought hazard assessment and spatial characteristics analysis in China. *Journal of Geographical Sciences, 21*(2), 235-249.

IPCC. (2007). *Climate change 2007: The fouth assessment report.* Cambridge, United Kingdom and New York, NY, USA.: Cambridge University Press.

Jain, S. K., Keshri, R., Goswami, A., & Sarkar, A. (2010). Application of meteorological and vegetation indices for evaluation of drought impact: a case study for Rajasthan, India. [Article]. *Natural Hazards, 54*(3), 643-656.

Karrouk, M.-S. (2007). Climate Change and its Impacts in Morocco. In A. Mellouki & A. Ravishankara (Eds.), *Regional Climate Variability and its Impacts in The Mediterranean Area* (Vol. 79, pp. 253-267): Springer Netherlands.

Kim, T., Valdes, J. B., & Yoo, C. (2003). Nonparametric Approach for Estimating Return Periods of Droughts in Arid Regions. *American Society of Civil Engineers, 8*(5), 237-247.

Kogan, F. N., & Zhu, X. (2001). Evolution of long-term errors in NDVI time series: 1985-1999. *Advances in Space Research, 28*(1), 149-153.

Komuscu, A. U. (1999). Using the SPI to Analyze Spatial and Temporal Patterns of Drought in Turkey. *Drought Network News,* pp. 7-13.

Koohafkan, A. P. (1996). Desertification, drought and their consequences. *2011*(01 August). doi:http://www.fao.org/sd/EPdirect/EPan0005.htm

Lana, X., Serra, C., & Burgueño, A. (2001). Patterns of monthly rainfall shortage and excess in terms of the standardized precipitation index for Catalonia (NE Spain). *International Journal of Climatology, 21*(13), 1669-1691.

Li, B., Tao, S., & Dawson, R. W. (2002). Relations between AVHRR NDVI and ecoclimatic parameters in China. *International Journal of Remote Sensing, 23*(5), 989-999.

Li, J., Sheng, Y., Wu, J., Wang, J., Zhang, B., Ye, B., et al. (2011). Modeling regional and local-scale permafrost distribution in Qinghai-Tibet Plateau using equivalent-elevation method. *Chinese Geographical Science, 1*, 1-10.

Ling, F., Du, Y., Xiao, F., Xue, H., & Wu, S. (2010). Super-resolution land-cover mapping using multiple sub-pixel shifted remotely sensed images. *International Journal of Remote Sensing, 31*(19), 5023-5040.

Liu, C. S., Shi, R. H., Gao, W., & Gao, Z. Q. (2010). Application of MODIS time series data for drought assessment in the East China. In W. Gao, T. J. Jackson & J. Wang (Eds.), *Remote Sensing and Modeling of Ecosystems for Sustainability Vii* (Vol. 7809).

Lloyd, D. (1990). A phenological classification of terrestrial vegetation cover using shortwave vegetation index imagery. *International Journal of Remote Sensing, 11*(12), 2269-2279.

Loukas, A., & Vasiliades, L. (2004). Probabilistic analysis of drought spatiotemporal characteristics inThessaly region, Greece. *Nat. Hazards Earth Syst. Sci., 4*(5/6), 719-731.

McCloy, K. R., & Lucht, W. (2004). Comparative evaluation of seasonal patterns in long time series of satellite image data and simulations of a global vegetation model. *IEEE Transactions on Geoscience and Remote Sensing, 42*, 140-153.

McKee, T. B., Doesken, N. J., & Kleist, J. (1993). The relationship of drought frequency and duration to time scales. *In: Proceedings of Eighth Conference on Applied Climatology, Anaheim,CA*, 179-184.

McKee, T. B., Doesken, N. J., & Kleist, J. (1995). *Drought Monitoring with multiple Time Scales.* Paper presented at the 9th AMS Conference on Applied Climatology, Dallas, TX.

Mishra, Singh, V., & Desai, V. (2009). Drought characterization: a probabilistic approach. *Stochastic Environmental Research and Risk Assessment, 23*(1), 41-55.

Mishra, A. K., & Singh, V. P. (2010). A review of drought concepts. *Journal of Hydrology, 391*(1-2), 202-216.

Moon, Y.-I., & Lall, U. (1994). Kernel quantite function estimator for flood frequency analysis. *Water Resour. Res., 30*(11), 3095-3103.

Nearing, M. A., Jetten, V., Baffaut, C., Cerdan, O., Couturier, A., Hernandez, M., et al. (2005). Modeling response of soil erosion and runoff to changes in precipitation and cover. *CATENA, 61*(2-3), 131-154.

Nicholson, S. E., Davenport, M. L., & Malo, A. R. (1990). A comparison of the vegetation response to rainfall in the Sahel and East Africa, using normalized difference vegetation index from NOAA AVHRR. *Climatic Change, 17*(2), 209-241.

Nicholson, S. E., Tucker, C. J., & Ba, M. B. (1998). Desertification, Drought, and Surface Vegetation: An Example from the West African Sahel. *Bulletin of the American Meteorological Society, 79*(5), 815-829.

Odekunle, T. O. (2006). Determining rainy season onset and retreat over Nigeria from precipitation amount and number of rainy days. *Theoretical and Applied Climatology, 83*(1), 193-201.

Omuto, C. T., Vargas, R. R., Alim, M. S., & Paron, P. (2010). Mixed-effects modelling of time series NDVI-rainfall relationship for detecting human-induced loss of vegetation cover in drylands. *Journal of Arid Environments, 74*(11), 1552-1563.
Ouassou, A., Ameziane, T., Ziyad, A., & Belghiti, M. (2005). Application of the Drought Management Guidelines in Morocco. *International Information System for the Agricultural Science and Technology, 58*, 343-1228.
Propastin, P. A., Kappas, M., Erasmi, S., & Muratova, N. R. (2007). Remote Sensing based study on intra-annual dynamics of vegetation and climate in drylands of Kazakhstan. *Basic and Applied Dryland Research, 1*(2), 138-154.
Reed, B. C., Brown, J. F., VanderZee, D., Loveland, T. R., Merchant, J. W., & Ohlen, D. O. (1994). Measuring phenological variability from satellite imagery. *Journal of Vegetation Science, 5*(5), 703-714.
Richard, Y., & Poccard, I. (1998). A statistical study of NDVI sensitivity to seasonal and interannual rainfall variations in Southern Africa. *International Journal of Remote Sensing, 19*(15), 2907-2920.
Romero, R., Guijarro, J. A., Ramis, C., & Alonso, S. (1998). A 30-year (1964–1993) daily rainfall data base for the Spanish Mediterranean regions: first exploratory study. *International Journal of Climatology, 18*(5), 541-560.
Rowhani, P., Linderman, M., & Lambin, E. F. (2011). Global interannual variability in terrestrial ecosystems: sources and spatial distribution using MODIS-derived vegetation indices, social and biophysical factors. *International Journal of Remote Sensing, 32*(19), 5393-5411.
Schultz, P. A., & Halpert, M. S. (1995). Global analysis of the relationships among a vegetation index, precipitation and land surface temperature. *International Journal of Remote Sensing, 16*(15), 2755-2777.
Sharma, A. (2000). Seasonal to interannual rainfall probabilistic forecasts for improved water supply management: Part 3 -- A nonparametric probabilistic forecast model. *Journal of Hydrology, 239*(1-4), 249-258.
Shiau, J. T., & Shen, H. W. (2001). Recurrence analysis of hydrologic droughts of differing severity. *J Water Resour Plan Manage ASCE 127*(1), 30-40.
Smakhtin, V. U. (2001). Low flow hydrology: a review. *Journal of Hydrology, 240*(3–4), 147-186.
Song, Y., & Ma, M. (2011). A statistical analysis of the relationship between climatic factors and the Normalized Difference Vegetation Index in China. *International Journal of Remote Sensing, 32*(14), 3947-3965.
Stern, R. D., Dennett, M. D., & Dale, I. C. (1982). Analysing Daily Rainfall Measurements to Give Agronomically Useful Results. I. Direct Methods. *Experimental Agriculture, 18*(03), 223-236.
Szalai, S., Szinell, C., & Zoboki, J. (2000) Drought monitoring in Hungary. *Early Warning Systems for Drought Preparedness and Drought Management* (pp. 161-176). Geneva: WMO.
Tadesse, T., Wilhite, D., Harms, S., Hayes, M., & Goddard, S. (2004). Drought Monitoring Using Data Mining Techniques: A Case Study for Nebraska, USA. *Natural Hazards, 33*(1), 137-159.
Taleb, H. (2006). WATER MANAGEMENT IN MOROCCO. In G. Dura, V. Kambourova & F. Simeonova (Eds.), *Management of Intentional and Accidental Water Pollution* (Vol. 11, pp. 177-180): Springer Netherlands.
Tucker, C. J., & Sellers, P. J. (1986). Satellite remote sensing of primary production. *International Journal of Remote Sensing, 7*(11), 1395-1416.
UN-ISDR. (2004). Living with Risk. Retrieved 02 August, 2011, from http://www.unisdr.org/eng/about_isdr/bd-lwr-2004-eng.htm
US National Drought Mitigation Center. (2011). The Standardized precipitation index. Retrieved July 13, 2011, from http://www.drought.unl.edu/monitor/spi/program/SPI_Zimbabwe.doc
Van Dijck, S., Laouina, A., Carvalho, A., Loos, S., Schipper, A., Van der Kwast, H., et al. (2006). DESERTIFICATION IN NORTHERN MOROCCO DUE TO EFFECTS OF CLIMATE CHANGE ON GROUNDWATER RECHARGE. In W. Kepner, J. Rubio, D. Mouat & F. Pedrazzini (Eds.), *Desertification in the Mediterranean Region. A Security Issue* (Vol. 3, pp. 549-577): Springer Netherlands.
van Westen, C. J. (2009). *Multi-hazard assessment*: UNU-ITC School for Disaster Geo-Information Management.
Wang, J., Rich, P. M., & Price, K. P. (2003). Temporal responses of NDVI to precipitation and temperature in the central Great Plains, USA. *International Journal of Remote Sensing, 24*(11), 2345-2364.
Wei, W., Chen, L. D., Fu, B. J., & Chen, J. (2010). Water erosion response to rainfall and land use in different drought-level years in a loess hilly area of China. *CATENA, 81*(1), 24-31.

Weiss, E., Marsh, S. E., & Pfirman, E. S. (2001). Application of NOAA-AVHRR NDVI time-series data to assess changes in Saudi Arabia's rangelands. *International Journal of Remote Sensing, 22*(6), 1005-1027.

Wessels, K. J., Prince, S. D., Malherbe, J., Small, J., Frost, P. E., & VanZyl, D. (2007). Can human-induced land degradation be distinguished from the effects of rainfall variability? A case study in South Africa. *Journal of Arid Environments, 68*(2), 271-297.

White, M. A., Thornton, P. E., & Running, S. W. (1997). A continental phenology model for monitoring vegetation responses to interannual climatic variability. *Global Biogeochem. Cycles, 11*(2), 217-234.

Wikipedia. (2011). Rabat. Retrieved 13 July, 2011, from http://en.wikipedia.org/wiki/Rabat

Wikipedia. (2012, 07 Feb 2012). Coefficient of variation. Retrieved 08 Feb, 2012, from http://en.wikipedia.org/wiki/Coefficient_of_variation

Wilhite, D. A. (2007). Drought. In J. Lidstone, L. M. Dechano & J. P. Stoltman (Eds.), *International Perspectives on Natural Disasters: Occurrence, Mitigation, and Consequences* (Vol. 21, pp. 147-162): Springer Netherlands.

Wilhite, D. A., & Glantz, M. H. (1985). Understanding the drought phenomenon: the role of definitions. *Water International, 10*(GEOBASE), 111-120.

Wu, H., Hayes, M. J., Weiss, A., & Hu, Q. (2001). An evaluation of the Standardized Precipitation Index, the China-Z Index and the statistical Z-Score. *International Journal of Climatology, 21*(6), 745-758.

Yang, L., Wylie, B. K., Tieszen, L. L., & Reed, B. C. (1998). An Analysis of Relationships among Climate Forcing and Time-Integrated NDVI of Grasslands over the U.S. Northern and Central Great Plains. *Remote Sensing of Environment, 65*(1), 25-37.

APPENDICES

Appendix 1. The computation result for rainfall data analysis.

Year	Number of rainy days (>0mm)			Amount of rainfall, mm			Average fraction for Oct-Dec
	Sep-Aug	Oct-Mar	Oct-Dec	Sep-Aug	Oct-Mar	Oct-Dec	%
1951	69	47	25	510.8	382.8	208.8	47.2
1952	67	52	22	399.5	370.2	200.8	37.3
1953	91	71	27	584.4	468.8	109.7	19.2
1954	76	64	17	578.3	549.3	105.7	12.8
1955	103	78	32	628.7	505.7	185.8	30.7
1956	58	37	13	378.2	264.2	126.7	36.9
1957	82	64	35	556.5	480.1	364.3	52.6
1958	73	58	32	588.9	407.3	244.8	36.9
1959	102	**83**	39	627.5	571.0	221.1	29.7
1960	74	57	36	557.1	481.3	402.5	62.9
1961	78	65	35	602.7	550.9	256.1	40.6
1962	102	83	40	757.5	693.0	315.0	40.5
1963	69	56	32	669.9	525.3	346.3	40.8
1964	69	56	27	433.5	361.5	195.5	39.9
1965	82	63	40	501.5	438.1	314.9	64.3
1966	68	42	22	389.1	322.3	222.3	67.2
1967	83	65	28	562.6	457.8	250.9	49.3
1968	**110**	78	32	**927.9**	**790.3**	424.7	48.1
1969	94	65	34	719.7	634.6	321.7	40.3
1970	95	64	28	807.3	505.6	191.2	26.1
1971	92	74	29	627.1	547.2	249.7	36.1
1972	74	58	31	488.7	438.9	252.6	46.6
1973	72	51	25	659.0	461.9	275.0	33.6
1974	53	39	12	312.7	254.6	**29.2**	**11.5**
…	…	…	…	…	…	…	…
1986	59	49	14	397.5	357.0	137.4	35.6
1987	87	69	40	632.3	550.5	383.5	60.2
1988	59	39	18	462.7	358.4	140.8	37.5
1989	64	49	33	458.9	413.2	254.3	44.3
1990	74	65	31	566.4	555.9	239.4	32.3
1991	61	39	22	305.7	165.6	80.3	43.1
1992	65	44	23	325.4	225.7	127.5	47.1
1993	71	51	32	360.1	330.5	170.7	48.3
1994	**43**	**27**	**11**	**190.8**	**138.6**	61.8	44.6
1995	100	76	22	853.8	769.1	206.9	18.6
1996	75	50	33	741.4	623.6	484.1	46.0
1997	86	57	37	538.8	480.9	335.6	52.8
1998	46	36	11	290.4	272.6	100.1	19.6
1999	61	37	30	419.7	301.6	242.9	**72.3**
2000	64	55	28	587.1	529.0	333.5	47.9
2001	69	46	24	338.8	234.5	142.3	39.7
2002	70	60	32	722.2	680.9	**513.9**	69.0
2003	83	62	**40**	748.1	605.3	449.8	52.9
2004	47	42	27	375.7	370.7	209.1	48.7
2005	74	59	26	623.7	558.9	230.2	39.5
2006	56	34	13	365.5	270.3	116.3	35.8
2007	52	34	14	340.2	244.3	139.6	50.8
2008	95	76	38	818.8	762.8	428.5	48.0
2009	81	74	25	762.1	687.4	243.1	22.1
mean	74.3	55.4	26.8	543.6	452.6	237.9	41.5
Min	43	27	11	190.8	138.6	29.2	11.5
Max	110	83	40	927.9	790.3	513.9	72.3

Appendix 2. The computation result for extreme rainfall analysis

year	Extreme indices			For rainy period (Oct-Mar)			
	Total rainfall, mm	Number of days		Number of days		Total rainfall, mm	
	R>10.1mm	R≥10mm	R≥30mm	10mm≤R<30mm	R≥30mm	10mm≤R<30mm	R≥30mm
1951	352.5	17	2	10	2	174.0	106.4
1952	259.3	10	3	7	3	127.0	122.5
1953	369.5	22	1	17	1	261.3	34.5
1954	401.4	21	2	18	2	318.1	68.3
1955	304.7	18	0	14	0	235.4	0.0
1956	257.3	14	0	10	0	177.7	0.0
1957	362.7	14	5	7	5	131.2	183.9
1958	421.8	16	1	15	0	270.5	0.0
1959	396.5	22	2	18	2	278.0	94.6
1960	374.4	20	3	15	3	224.8	109.5
1961	461.0	23	2	20	2	359.6	78.1
1962	550.2	25	3	20	3	365.9	148.4
1963	517.7	23	4	13	4	228.6	152.3
1964	279.3	18	0	15	0	229.1	0.0
1965	313.5	16	2	13	2	209.1	81.6
1966	266.5	15	2	12	2	164.9	82.4
1967	372.8	18	4	11	3	188.9	112.2
1968	**673.2**	30	6	17	6	319.4	273.4
….	…	…	…	…	…	…	…
1981	306.3	14	2	12	1	205.6	34.0
1982	278.8	14	1	13	1	235.2	33.8
1983	407.8	22	2	11	0	190.2	0.0
1984	311.2	15	3	10	3	170.0	112.6
1985	419.2	25	1	21	1	333.8	30.0
1986	261.8	11	2	7	2	118.8	117.1
1987	463.5	22	4	16	4	261.7	156.8
1988	348.3	18	1	14	1	245.7	33.8
1989	330.2	16	2	12	2	221.8	79.8
1990	421.6	19	5	14	5	222.9	198.7
1991	182.5	10	1	**4**	0	**58.5**	0.0
1992	217.3	13	0	8	0	137.7	0.0
1993	200.7	10	2	8	2	134.0	66.7
1994	**110.9**	**7**	0	6	0	97.5	0.0
1995	638.9	24	**9**	13	**9**	251.0	**345.0**
1996	586.5	24	6	14	6	273.7	229.5
1997	338.3	17	3	13	3	210.1	112.7
1998	209.2	10	2	8	2	143.1	66.1
1999	275.8	13	3	8	2	141.7	76.8
2000	432.8	19	4	13	4	226.2	170.0
2001	217.1	14	0	9	0	146.3	0.0
2002	586.4	23	7	15	7	234.0	342.2
2003	569.2	26	4	17	4	283.1	188.9
2004	285.6	12	3	9	3	164.1	121.5
2005	468.4	22	6	13	6	206.9	211.9
2006	263.8	15	0	11	0	195.8	0.0
2007	235.9	12	2	6	2	94.8	78.2
2008	620.8	**32**	3	**27**	3	**482.1**	103.0
2009	595.4	27	6	20	5	351.8	174.3
mean	**383.5**	**18.3**	**2.9**	**12.9**	**2.6**	**217.8**	**107.3**
min	**110.9**	**7**	**0**	**4**	**0**	**58.5**	**0**
max	**673.2**	**32**	**9**	**27**	**9**	**482.1**	**345.0**

Appendix 3. The temporal pattern of daily rainfall during rainy season of the period of 1998-2009 in which NDVI data is available.

The horizontal dashed line indicate the 30mm rainfall amounts. The vertical dashed line corresponds to 31 December.

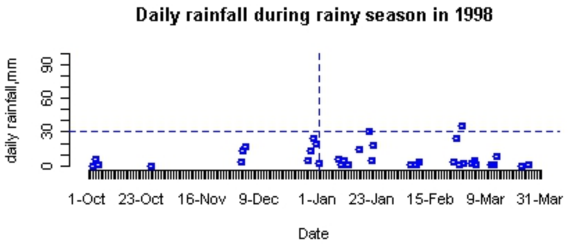

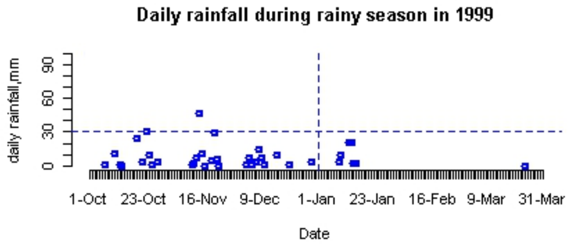

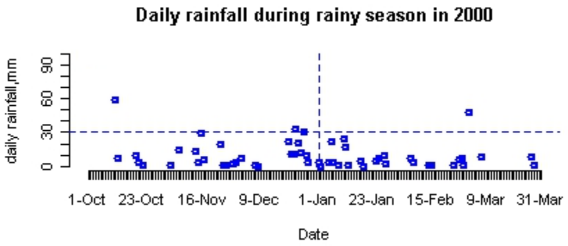

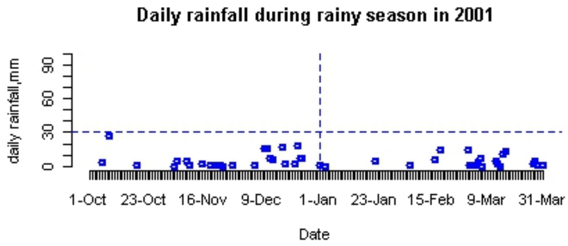

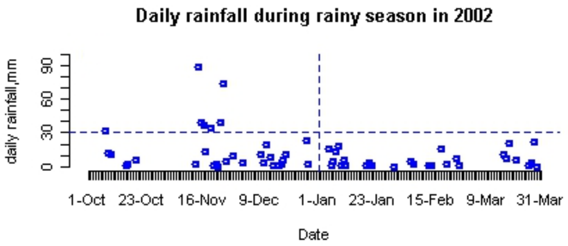

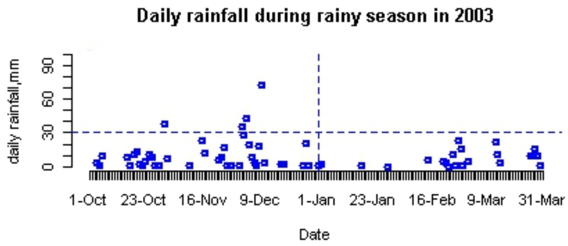

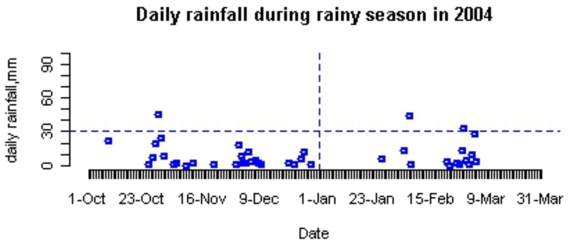

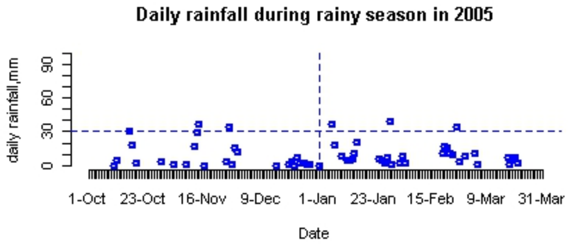

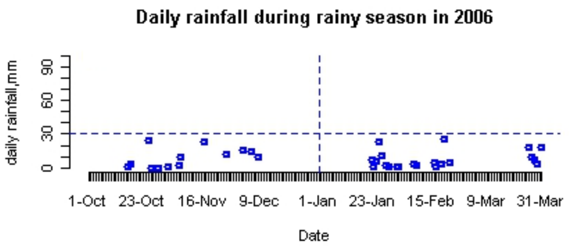

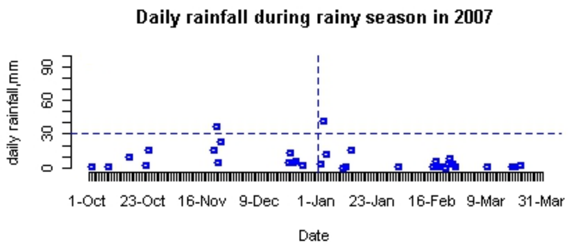

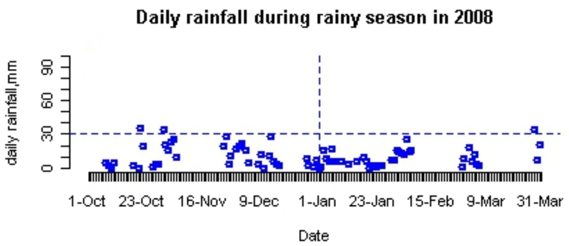

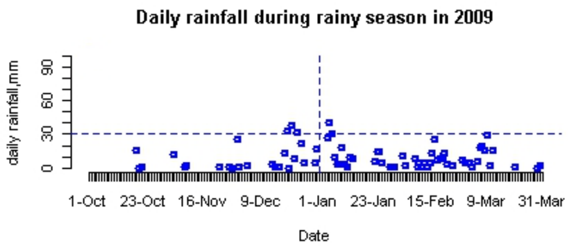

Appendix 4. The calculation of the 6-month SPI for March in Microsoft Excel 2010.

Here the 6-month SPI for March is based on the total rainfall for October, November, December, January, February, and March.

A. Estimation of gamma distribution parameters α and β for March

	mean	ln(mean)	U	α	β
March	448.55	6.04	0.06	8.13	55.14

$$\mathrm{U} = \ln(\overline{X}) - \frac{\sum \ln(X)}{n} \qquad \alpha = \frac{1}{4\mathrm{U}}\left(1 + \sqrt{1 + \frac{4\mathrm{U}}{3}}\right) \qquad \beta = \frac{\overline{\mathrm{X}}}{\alpha}$$

Where X- total rainfall for Oct-March in each year, n=58 year (1952-2009), $\overline{X} = 448.55$mm

B. The 6-month SPI for March

Year	Total rainfall for March	ln of Rainfall	GAMMA transform	H transform	t transform	SPI	SPI calculated by SPI program
1952	382.8	5.95	0.37	0.37	1.40	-0.32	-0.34
1953	370.2	5.91	0.34	0.34	1.47	-0.41	-0.43
1954	468.8	6.15	0.60	0.60	1.35	0.24	0.22
1955	549.3	6.31	0.76	0.76	1.69	0.71	0.68
2006	558.9	6.33	0.78	0.78	1.74	0.77	0.74
2007	270.3	5.60	0.11	0.11	2.09	-1.21	-1.22
2008	244.3	5.50	0.07	0.07	2.29	-1.45	-1.46
2009	762.8	6.637	0.96	0.96	2.56	1.77	1.73

Since the gamma function is undefined for $x = 0$ and a rainfall distribution may contain zeros, the cumulative probability becomes: $H(x) = q1 + (1-q)G(x)$ where q is the probability of a zero, $q = \frac{m}{n}$; m −number of zero rainfall.

$$t = \sqrt{\ln\left[\frac{1}{x_H^2}\right]} \quad where\ x_H^2 \leq 0.5\ \ or \qquad t = \sqrt{\ln\left[\frac{1}{(1-x_H)^2}\right]} \quad where\ \ x_H^2 < 1.0$$

$$SPI = -\left[t - \frac{c_0 + c_1 t + c_2 t^2}{1 + d_1 t + d_2 t^2 + d_3 t^3}\right] \qquad x_H \leq 0.5\ \ or$$

$$SPI = +\left[t - \frac{c_0 + c_1 t + c_2 t^2}{1 + d_1 t + d_2 t^2 + d_3 t^3}\right] \qquad x_H < 1.0$$

where c_o=2.515517 c_1=0.802853 c_2=0.010328 d_1=1.432788 d_2=0.189269 d_3=0.001308

Appendix 5. The R script used for this thesis

```
#####   Histograms of daily, monthly and anuual total rainfall (Figure 11)
ds <- read.csv("Daily_remove_0.csv"); par(mfrow = c(1, 3)); str(ds)
hist(ds$Rainfall,main="Daily rainfall",cex.main=1.0,xlab="Rainfall, mm",ylab="Frequency")
month <- read.csv("monthly.csv")
hist(month$monthly,main="Monthly total rainfall",cex.main=1.0,xlab="Rainfall,mm",ylab="Frequency")
year.sum <- tapply(ds$Rainfall, ds$yyyy, sum)
hist(year.sum,main="Annual total rainfall",cex.main=1.0, xlab="Rainfall, mm",ylab="Frequency");

##### Boxplot for monthly total rainfall, 1951-2009 (Figure 12)
month.yr.sum <- tapply(ds$Rainfall, ds[,1:2], sum, simplify=T)
month.sum <- data.frame(month.yr.sum)
boxplot(month.yr.sum)
str(month.sum)
##### The calculation of 95th percentile of daily rainfall for decades of 1951-2010 (Table 9)
dt<-read.csv("daily_rain.csv"); head(dt); quantile(dt$rain,c(.95),na.rm=TRUE) #10.1
dt1961<-subset(dt,dt$yyyy<"1962"); quantile(dt1961$rain,c(.95),na.rm=TRUE) # 9.82
..........................................................................
dt2010<-subset(dt,((dt$yyyy>"2000") & (dt$yyyy<"2011"))); quantile(dt2010$rain,c(.95),na.rm=TRUE)
# 10.9
##### Temporal pattern of daily rainfalls during crop season of 1998-1999 (Oct-Mar)
## This script was run for the remaining year, 1999-2009. The results are shown in Appendix 3.
ds1 <- read.csv("heavy_rainfall_crop_season.csv"); head(ds1);tail(ds1); par(mfrow = c(3, 2))
dt.1998<-ds1[ds1$year=="1998",]; tail(dt.1998); dt.1998    # Subset
 plot(dt.1998$rainfall, lwd=2.0, col="blue", type="p",main="Daily rainfall during rainy season in 1998",
ylab="daily rainfall,mm",xlab="Date",axes=FALSE)
plot.axes = { axis(2, seq(0.0, 100, by = 10))}
date12<-dt.1998[ ,4]; head(date12); axis(1, 1:182,date12)
abline(h=30, lty=2,col="blue")    # In order to highlight the rainfalls higher than 30mm.
abline(v=93, lty=2,col="blue")   # drawing the vertical line that corresponds to 1 Jan to see whether
                                 # the rainfalls higher than 30mm fall before 1 Jan.

#### Chapter 3.2 and 4.2 The Joint Probability Density Function (PDF)
######## Reading data
dt<-read.csv("1 drought SPI6.csv"); dt
#### Create The Joint Probability Density Functin (PDF) (Figure 22)
library(sm)   # load package
x<-cbind(dt$duration,dt$spi06); x
h<-h.select(x) ;h
f1<-sm.density(x, h, method = "cv", weights = NA, group=NA,xlab="Duration",ylab="Magnitude",
panel=TRUE); f1
```

Appendix 6. The PC Raster script used for generation of Drought Susceptibility Map.

The methodology described in section 3.3.2 and final result is shown in 4.3.1.

```
################ 1: Maximum NDVI (MNDVI) in each year
max_1998.map=max(ndvi0000.016,ndvi0000.017,.....,ndvi0000.050,ndvi0000.051);
max_1999.map=max(ndvi0000.052,ndvi0000.053,.....,ndvi0000.061,ndvi0000.062);
………………………………………………………………………………………..
max_2007.map=max(ndvi0000.340,ndvi0000.341,.....,ndvi0000.374,ndvi0000.375);
max_2008.map=max(ndvi0000.376,ndvi0000.377,…..,ndvi0000.410,ndvi0000.411),

################ 2: Average of MNDVI maps
avg_MNDVI.map=(max_1998.map+max_1999.map…..max_2007.map+max_2008.map)/11;

################ 3: To create time series of (MNDVI-avg_MDVI)
deviatio.001=max_1998.map-avg_MNDVI.map;
deviatio.002=max_1999.map-avg_MNDVI.map;
……………………………………………………
deviatio.010=max_2007.map-avg_MNDVI.map;
deviatio.011=max_2008.map-avg_MNDVI.map;

################ 4:  Calculation of n and sum of minus deviation for each pixel
```

The following formula used to create drought susceptibility map:

$$\mathrm{DSM} = \sum_{0}^{n} (-\mathrm{DSI}_{\mathrm{mndvi}}) \times \frac{n}{N}$$

```
binding
clone=sehoul1.map;     # Input map
nr=DS_nr.map;          # Output map 1
sum=DS_sum.map;        # Output map 2
areamap
clone;
timer
 1 11 1;
initial
 nr=0;  sum=0;
dynamic
 deviation= timeinput(deviatio);
 report nr=if(deviation <0,nr+1,nr);
 report sum=if(deviation < 0,sum+ds,sum);

 ################ 5: To generate Drought Susceptibility Map
 DSeverity.map=DS_nr.map*DS_sum.map/11;    # (Figure 27 a)
```

Appendix 7. The PC Raster Script used to derive phonological metrics for 1998 as an example.

The methodology described in section 3.4.3 and final result is shown in 4.4.3.

A. Onset of greenness related metrics for 1998

```
binding
#INPUTS:
mask=clone_ndvi.map; stations=station.map;  date1=date_sep_aug.tss;
  s_1998=sep_1998;   # NDVI: 10 Sep, 1998- 31 Aug, 1999
  sm_1998=t_1_1998;   #smoothed NDVI by ARAMA: 10 Sep, 1998- 31 Aug, 1999
  s_1998_0=se0_1998;    #10-day lag (t-1) NDVI : 31 Aug, 1998- 20 Aug, 1999
  s_1998_1=se1_1998;   #10-day lag (t+1) NDVI: 20 Sep, 1998- 10 Sep, 1999
  #OUTPUTS
  onv_98=onv_1998;  min98=onv_1998.map;  min98_day=onv_1998_day.map;
  min98_day_ch=onv_1998_day_check.map;
areamap
  mask;
timer:  1 36 1;
initial:
 t=0;  nrCells = maptotal(mask); min98=2;    # Possible high value
 min98_day=0;  min98_day_ch=0;   min99=2;
dynamic
   t=t+1*mask;
  ## Read date from table
  d98 = timeinputscalar(date1, nominal(stations));  idp = 2;
  dd98 = inversedistance(mask gt 0, d98, idp, 0, 0); # Inverse distance interpolation with power 2
  date = dd98*mask;   # restrict to area mask
############Onset related metrics for 1998
  n_98 = timeinput(s_1998)*0.004-0.1;
 n_sm_98=timeinput(sm_1998)*0.004-0.1;
 n_98_0=timeinput(s_1998_0)*0.004-0.1;
 n_98_1=timeinput(s_1998_1)*0.004-0.1;
 report onv_98=if((n_98-n_sm_98 >=0.018 and n_98-n_98_0>=0.015 and n_98_1-
n_98>=0.015),n_98,2);
 report min98_day=if(onv_98<min98,date,min98_day);
 report min98_day_ch=if(onv_98<min98,t,min98_day_ch);
 report min98=if(onv_98<min98,onv_98,min98);
```

B. End of greenness related metrics for 1998

```
binding
#INPUTS:
mask=clone_ndvi.map; stations=station.map;  date1=date_sep_aug.tss;
  s_1998=sep_1998;   # NDVI: 10 Sep, 1998- 31 Aug, 1999
  sm_1998=t_1_1998;   #smoothed NDVI by ARAMA: 10 Sep, 1998- 31 Aug, 1999
  s_1998_0=se0_1998;    #10-day lag (t-1) NDVI : 31 Aug, 1998- 20 Aug, 1999
  s_1998_1=se1_1998;   #10-day lag (t+1) NDVI: 20 Sep, 1998- 10 Sep, 1999
#OUTPUTS
enV_1998=env_1998; min1998=endv_1998.map;
min1998_day=env_1998_day.map;  min1998_day_ch=env_1998_day_check.map;
```

```
areamap
 mask;
timer
1 36 1;
initial
 nrCells = maptotal(mask);  t=0;   min1998=2;    # Possible high value
 min1998_day=0;  min1998_day_ch=0;
dynamic
  t=t+1*mask;
  d98 = timeinputscalar(date, nominal(stations));  ## Read date data from table
  idp = 2;
  dd98 = inversedistance(mask gt 0, d98, idp, 0, 0);  # inverse distance interpolation with power 2
  date1 = dd98*mask;   # restrict to area mask

################## enV 1998
 n_1998 = timeinput(s_1998)*0.004-0.1;
 n_sm_1998=timeinput(sm_1998)*0.004-0.1;
 n_1998_0=timeinput(s_1998_0)*0.004-0.1;

 report enV_1998=if((n_1998>n_sm_1998 and abs(n_1998-n_1998_0)>=0.015),n_1998,2);
 report min1998_day=if(enV_1998<min1998,date1,min1998_day);
 report min1998_day_ch=if(enV_1998<min1998,t,min1998_day_ch);
 report min1998=if(enV_1998<min1998,enV_1998,min1998);
```

C. Duration of greenness (DurP) and TINDVI for 1998

```
binding
  #INPUTS
  mask=sehoul1.map;  stations=station.map;  date0=date_sep_aug.tss;
  s_1998=sep_1998;                                  # NDVI: 10 Sep, 1998- 31 Aug, 1999
onvday1998=onv_1998_day_check.map; envday1998=env_1998_day_check.map;
   #OUTPUTS
    cropday1998=cropday_1998.map;   # Duration of greenness (DurP)
  sum1998=sum_1998.map;                # The sum of 10-day NDVIs during greenness period (TINDVI)
areamap
 mask;
timer
 1 36 1;
initial
 nrCells = maptotal(mask);  t=0;  cropday1998=0;  sum1998=0;
dynamic
  t=t+1*mask;

 ########### 1998
 n_1998 = timeinput(s_1998)*0.004-0.1;
 report cropday1998=if((t>=onvday1998 and t<=envday1998),cropday1998+1,cropday1998+0);
 report sum1998=if((t>=onvday1998 and t<=envday1998),sum1998+n_1998,sum1998+0);
```

D. MaxV, MaxP and RanV for 1998

```
binding
  #INPUTS
  mask=clone_ndvi.map;   stations=station.map;   date0=date_sep_aug.tss;
  s_1998=sep_1998;        # NDVI: 10 Sep, 1998- 31 Aug, 1999
  onV_1998=onv_1998;    #If growing period, ndvi value, othervise 2.
  enV_1998=env_1998;   t1_1998=t_1_1998;
```

```
  #OUTPUTS
 cropday1998=cropday_1998.map;
 cr1_1998=cr1_1998;
 cr2_1998=cr2_1998;
 sum1998=sum_1998.map;
 peak1998=peak_1998.map;
 peak1998_day=peak_1998_day.map;
 peak1998_day_ch=peak_1998_day_ch.map;
 min1998=min_1998.map;
 ranV1998=ranv_1998.map;
areamap
 mask;
timer
 1 36 1;
initial
 nrCells = maptotal(mask);  t=0;
  min1998=2;    # Possible high value
 cropday1998=0; peak1998=-1;  peak1998_day=0;  peak1998_day_ch=0;  sum1998=0;
dynamic
  t=t+1*mask;
 ## Read date data from table
  d98 = timeinputscalar(date0, nominal(stations));
  idp = 2;
  #dt1_inter = inversedistance(dt1 > 5, dt1, idp, 0, 0);
  dd98 = inversedistance(mask gt 0, d98, idp, 0, 0);
  # inverse distance interpolation with power 2

  date = dd98*mask;   # restrict to area mask

########## 1998
 n_1998 = timeinput(s_1998)*0.004-0.1;
 t_1_1998=timeinput(t1_1998)*0.004-0.1;
 onV_1998=timeinput(onv_1998);
 enV_1998=timeinput(env_1998);

 cr1_1998=if(n_1998>t_1_1998,n_1998,-1);
 cr2_1998=if((onV_1998!=2 or enV_1998!=2),n_1998,2);

 report peak1998_day=if(cr1_1998>peak1998,date,peak1998_day);
 report peak1998_day_ch=if(cr1_1998>peak1998,t,peak1998_day_ch);
 report peak1998=if(cr1_1998>peak1998,cr1_1998,peak1998);
 report min1998=if(cr2_1998<min1998,cr2_1998,min1998);
```

Appendix 8. The vegetative drought based on the result of analysis of vegetation response to rainfall in section 4.4.2

Three condition were used to construct vegetative drought years over the period 1951-1997 in which SPOT NDVI data is not available: a) total rainfall for rainy season is two times less than its long term mean (452.6mm) or b) the average fraction of rainfall for Oct-Dec is two time less than long term mean (0.41) or c) both is less than their long term mean. Some non-drought years according to these 3 conditions were excluded. Minus anomaly of annual rainfall with rainfall fraction are highlighted in red colour for comparison purpose. In addition, the years are highlighted in yellow colour which are coincided with the historical droughts observed in Sehoul area.

Year	Rainfall amount, mm			Anomaly			Drought years considering rainfall fraction
	Annual Sep-Aug	Rainy season Oct-Mar	Average fraction Oct-Dec	Annual Sep-Aug	Rainy season Oct-Mar	Average fraction Oct-Dec	
1951	510.8	382.8	0.47	**-32.8**	-69.8	5.7	0
1952	399.5	370.2	0.37	**-144.1**	-82.4	-4.2	**1**
1953	584.4	468.8	0.19	40.8	16.2	-22.3	**1**
1954	578.3	549.3	0.13	34.7	96.7	-28.7	**1**
1955	628.7	505.7	0.31	85.1	53.1	-10.8	0
1956	378.2	264.2	0.37	**-165.4**	-188.4	-4.6	**1**
1957	556.5	480.1	0.53	12.9	27.5	11.1	0
1958	588.9	407.3	0.37	45.3	-45.3	-4.6	**1**
1964	433.5	361.5	0.40	**-110.1**	-91.1	-1.5	**1**
1965	501.5	438.1	0.64	**-42.1**	-14.5	22.8	0
1966	389.1	322.3	0.67	**-154.5**	-130.3	25.7	0
1972	488.7	438.9	0.47	**-54.9**	-13.7	5.2	0
1973	659.0	461.9	0.34	115.4	9.3	-7.9	0
1974	312.7	254.6	0.11	**-230.9**	-198.0	-30.0	**1**
1979	515.3	439.8	0.41	**-28.3**	-12.8	-0.7	**1**
1980	329.8	246.2	0.68	**-213.8**	-206.4	26.1	0
1981	431.1	317.0	0.21	**-112.5**	-135.6	-20.3	**1**
1982	432.5	375.1	0.38	**-111.1**	-77.5	-3.3	**1**
1983	600.7	337.9	0.41	57.1	-114.7	-1.0	**1**
1984	456.5	380.2	0.60	**-87.1**	-72.4	18.2	0
1985	592.1	493.2	0.21	48.5	40.6	-20.2	0
1986	397.5	357.0	0.36	**-146.1**	-95.6	-5.9	**1**
1987	632.3	550.5	0.60	88.7	97.9	18.7	0
1988	462.7	358.4	0.38	**-80.9**	-94.2	-3.9	**1**
1989	458.9	413.2	0.44	**-84.7**	-39.4	2.8	0
1990	566.4	555.9	0.32	22.8	103.3	-9.2	0
1991	305.7	165.6	0.43	**-237.9**	-287.0	1.6	**1**
1992	325.4	225.7	0.47	**-218.2**	-226.9	5.7	**1**
1993	360.1	330.5	0.48	**-183.5**	-122.1	6.8	0
1994	190.8	138.6	0.45	**-352.8**	-314.0	3.1	**1**
1995	853.8	769.1	0.19	310.2	316.5	-22.8	**1**
1996	741.4	623.6	0.46	197.8	171.0	4.6	0
1997	538.8	480.9	0.53	**-4.8**	28.3	11.4	0
1998	290.4	272.6	0.20	**-253.2**	-180.0	-21.9	**1**
1999	419.7	301.6	0.72	**-123.9**	-151.0	30.9	0
2000	587.1	529.0	0.48	43.5	76.4	6.4	0
2001	338.8	234.5	0.40	**-204.8**	-218.1	-1.7	**1**
2002	722.2	680.9	0.69	178.6	228.3	27.5	0
2003	748.1	605.3	0.53	204.5	152.7	11.4	0
2004	375.7	370.7	0.49	**-167.9**	-81.9	7.2	0
2005	623.7	558.9	0.39	80.1	106.3	-2.0	0
2006	365.5	270.3	0.36	**-178.1**	-182.3	-5.7	**1**
2007	340.2	244.3	0.51	**-203.4**	-208.3	9.3	0
2008	818.8	762.8	0.48	275.2	310.2	6.5	0
2009	762.1	687.4	0.22	218.5	234.8	-19.3	0
mean	**543.6**	**452.6**	**0.41**	**27**	**28**	**32**	**20**

Appendix 9. The steps of determination of human-induced land degradation described in section 3.5.2.

The methodology described in section 3.5.2 and final result is shown in 4.5.

The steps of 1,2 and 7 was done in PCRaster software. After the average NDVI maps converted to column file format, the remaining steps (3,4,5 and 6) was performed in MS Excel 2010 for every pixel during rainy seasons 1998-2009.

Step 1. The determination of x and y coordinates of the pixels of clone map
pcrcalc x_sehoul.map=xcoordinate(boolean(sehoul1.map))
pcrcalc y_sehoul.map=ycoordinate(boolean(sehoul1.map))
map2col --coorul x_sehoul.map x_sehoul.txt;   map2col --coorul y_sehoul.map y_sehoul.txt

Step 2. Converts from PCRaster map format to column file format
map2col --coorul avgX_III.001 avgX_III_1998.txt
map2col --coorul avgX_III.002 avgX_III_1999.txt
……………………………………………………
map2col --coorul avgX_III.011 avgX_III_2008.txt
map2col --coorul avgX_III.012 avgX_III_2009.txt

Step 3. The slope and intercept of regression lone and coefficient of determination

$$b_1 = \frac{\sum[(x_i - \bar{x})(y_i - \bar{y})]}{\sum[(x_i - \bar{x})^2]} \quad \text{or} \quad b_1 = r\frac{\sigma_y}{\sigma_x}; \qquad b_0 = \bar{y} - b_1 \times \bar{x}$$

$$R^2 = \left[(1/N) * \sum [(x_i - \bar{x})(y_i - \bar{y})]/(\sigma_x \sigma_y)\right]^2$$

Where $\mathbf{b_o}$ is y intercept of the regression line, $\mathbf{b_1}$ is the slope of regression line, **r** is the correlation between x and y, $\mathbf{x_i}$ and $\mathbf{y_i}$ are the average rainfall and the average NDVI respectively during rainy season in i year (1998-2009), $\bar{\mathbf{x}}$ is the mean of x, $\bar{\mathbf{y}}$ is the mean of y, $\boldsymbol{\sigma_x}$ is the standard deviation of x, and $\boldsymbol{\sigma_y}$ is the standard deviation of y, $\mathbf{R^2}$ is the coefficient of determination. **N** (N=11) is number of years.

Step 4. Calculation of the predicted NDVI for each pixel (1998-2009)

$NDVI' = b_0 + b_1 \times x_i$;   where $NDVI'$ is the predicted NDVI in i year,

Step 5. Calculation of residuals for each pixel (1998-2009)

$$\text{Residuals}_{i,j} = \text{NDVI}_{i,j} - \text{NDVI}'_{i,j}$$

where $NDVI_{i,j}$ is the original NDVI (average NDVI during rainy season)

Step 6. Calculation of slope of residuals for each pixel
The same formula in Step 3 was used. But $\mathbf{x_i}$ is the years, from 1998 to 2009. $\mathbf{y_i}$ is the residuals determined in Step 5.

Step 7. Converts from column file format to PCRaster map format
col2map --clone sehoul1.map residual_slope.txt residual_slope.map

Step 8. Classification procedure
Excluded pixels: a) R^2 is less or equal to its 10^{th} Qu; b) Slope of residual is higher or equal to zero:

class1.map=nominal(if(r2.map<=0.26045,1,if(residual_slope.map>=0,2,3)));
mask.mpr=iff(class1=3,class1,?)   # In ILWIS 3.31
residual_slope1.map   # residual_slope.map masked by mask.mpr in ArcMap10
Degradation.map   # The final map classified in ArcMap10.
 # Final map is shown in Figure 39